INDUSTRIAL APPLICATIONS OF MÖSSBAUER SPECTROSCOPY

Massimo Carbucicchio
Physics Department, University of Parma, Parco Area delle Scienze 7/A, 43124 Parma, Italy

In the last few years great attention has been devoted to the study and engineering of innovative functional materials useful for industrial applications (metallurgy, catalysis, biotechnology, mineralogy, electrochemistry and tribology) as well as to the development of low dimensional systems for the microelectromechanical and information/energy storage devices (MRAM, ion battery, nanotechnology, nuclear and renewal energy). The analysis and optimization of the material properties in view of their particular field of application require a number of complementary and finalized techniques which in many cases are not sufficiently locally sensitive and selective.

In this regard, the Mössbauer Spectroscopy is a very powerful tool allowing a lot of industrial applications thanks to the possibility to obtain, simultaneously, information on composition, crystallographic phases and magnetic properties with a very high local sensitivity. This technique can be performed in different geometry, varying the measurement temperature, and selecting the resonant particle and his energy allowing depth-selective analyses and the study of interface phenomena in low dimensional systems. Moreover, the non-destructive character of the Mössbauer spectroscopy makes this technique suitable also for applications in the field cultural heritage.

The present lecture will evidence the great versatility and high capability of the Mössbauer Spectroscopy and a few examples will be presented pointing out its actual usefulness in the industrial Research and Development, as well as its suitability for applications in fields of technological interest.

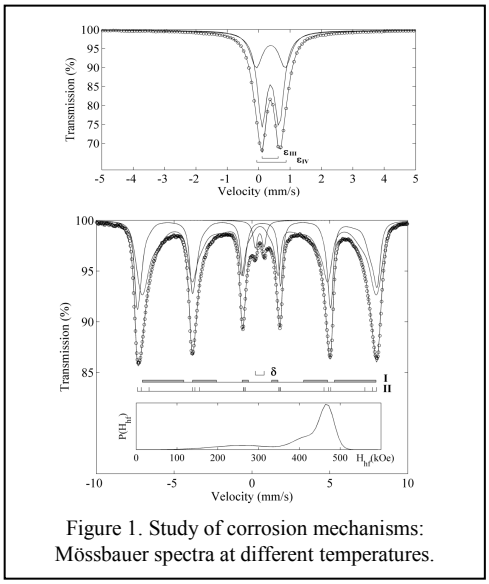

Figure 1. Study of corrosion mechanisms: Mössbauer spectra at different temperatures.

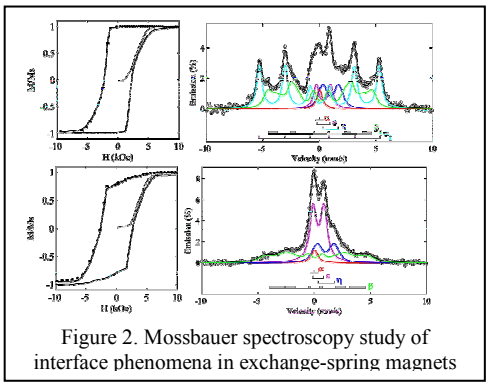

Figure 2. Mossbauer spectroscopy study of interface phenomena in exchange-spring magnets

Session 1(T3) I-1 In Memoriam Rudolf L. Mößbauer

INDUSTRIAL APPLICATIONS OF GREEN RUSTS RELATED COMPOUNDS AND NEW MINERALS, FOUGÈRITE, TRÉBEURDENITE AND MÖSSBAUERITE: FROM CORROSION TO MINERALOGY THROUGH WATER PURIFICATION

J.-M.R. Génin

Institut Jean Barriol FR2843 CNRS-Université de Lorraine, ESSTIN, 2 rue Jean Lamour, F-54500 Vandœuvre-Lès-Nancy, France

Fe^{II-III} hydroxysalts were originally studied in the eighties for understanding the corrosion of iron-based materials and steels since they are intermediate compounds between metallic iron and ferric oxyhydroxide end products; therefore, they are called commonly green rusts because of their color [1]. They belong to the double layered hydroxide family and own unchallenged redox properties since both divalent and trivalent cations come from the same iron element, where Mössbauer spectroscopy allows us to determine very easily the molar ferric ratio $x = \{[Fe^{III}]/ ([Fe^{II}] + [Fe^{III}])\}$. The discovery in 1996 of a green rust related mineral in the gleys of hydromorphic soils of aquifers opened a new field of potential applications since synthetic green rusts are able to reduce oxidized pollutants [2].

A detailed explanation of what actually occurs in the field was found recently by oxidizing carbonated green rust with H_2O_2 as demonstrated by Mössbauer spectroscopy [3]. The oxidation proceeded by *in situ* deprotonation of OH^- ions making think that a phase Fe^{II-III} oxyhydroxycarbonate with continuous formula $Fe^{II}_{6(1-x)}\,Fe^{III}_{6x}\,O_{12}\,H_{2(7-3x)}\,CO_3 \bullet 3H_2O$ does exist instead of dissolving in solution for precipitating a usual ferric oxyhydroxide FeOOH as it does with oxygen. However, long range ordering occurs among Fe cations giving well defined magnetic domains and three new minerals whose names have been accepted by the International Mineralogical Association (IMA) are considered: (i) fougèrite for Fe^{II-III} hydroxycarbonate green rust $Fe^{II}_4\,Fe^{III}_2\,(OH)_{12}CO_3 \bullet 3H_2O$, (ii) trébeurdenite for Fe^{II-III} oxyhydroxycarbonate $Fe^{II}_2\,Fe^{III}_4\,O_{12}\,H_{10}\,O_2\,CO_3 \bullet 3H_2O$ and (iii) mössbauerite for the ferric oxyhydroxycarbonate $Fe^{III}_6\,O_{12}\,H_8\,O_4\,CO_3 \bullet 3H_2O$, at definite x values of 0.33, 0.67 and 1, respectively. Any intermediate average value of x ratio comes from mixing domains that transform topotaxicaly during the redox reaction [4].

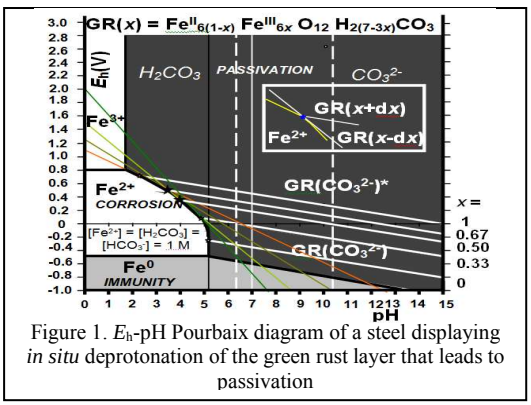

Figure 1. E_h-pH Pourbaix diagram of a steel displaying *in situ* deprotonation of the green rust layer that leads to passivation

A comparison of the E_h-pH Pourbaix diagrams between the dissolution-precipitation oxidation and the *in situ* deprotonation modes was made and this last mode can be used for several industrial applications (Fig. 1). Firstly, it explains the remarkable properties of weathering (CORTEN®) steels which were empirically discovered in the sixties; the protection of these steels comes from the *in situ* deprotonation of the green rust layer that forms at the steel surface giving the ferric green rust, homologous to mössbauerite. Other strategies than Cu addition for obtaining this protective layer can be envisioned.

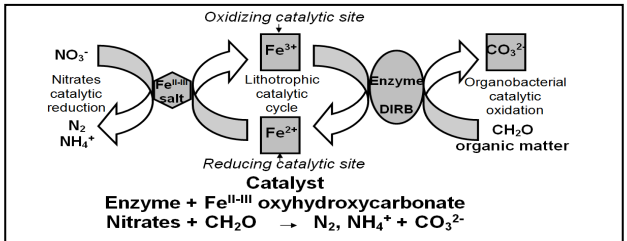

Figure 2.Principle of enzymatic reduction of Fe^{III} and oxidation of Fe^{II-III} oxyhydroxycarbonate by nitrates.

Another development is currently fully investigated; the minerals found in gleysols of characteristic bluish-green shade come from the bacterial reduction of natural ferric oxyhydroxides in anoxic conditions under the water table of aquifers. Moreover, since synthetic green rusts are able to reduce many oxidized pollutants, the idea arose to match the oxidation of green rust with its regeneration by bacterial activity (Fig. 2). In fact, denitrification actually occurs in aquifers by respiration of bacteria such as *Shewanella putrefaciens*; instead of breathing directly nitrates, they prefer to breathe Fe^{III} and by producing carbonates they form green rust related minerals that, at their turn, reduce nitrates into nitrogen gas. Results from the development of a tertiary treatment for waste water denitrification will be presented with continuous Mössbauer monitoring in reactors using a MIMOS spectrometer. Finally, the landscaping of "watered areas with reinforced iron purification" (WARIP) which is currently starting in Brittany for large scale treatment in the field will be discussed. This development is intended to solve in the long term the devastating proliferation of algae at the mouth of coastal rivers and beaches due to intense agricultural activity.

[1] J.-M.R. Génin et al., Hyperfine Interactions **29** (1986) 1355–1360.

[2] J.-M.R. Génin et al., Envir. Sci. Technol. **32** (1998) 1058–1068.

[3] J.-M.R. Génin et al., Solid State Science, **7** (2005) 545–572.

[4] J.-M.R. Génin et al., Hyper. Inter. (2012)DOI/10.1007/s10751-011-8

COEXISTENCE OF SUPERCONDUCTIVITY AND MAGNETISM IN THE Fe-As and Fe-Se NEW MAGNETO-SUPERCONDUCTORS

I. Felner and I. Nowik

"Racah" Institute of Physics, The Hebrew University, Jerusalem 91904, Israel

Since the discovery of Mössbauer spectroscopy (MS), superconductivity (SC) was one of the subjects the method was able to investigate. MS in conventional superconductors yield little information. However in the new magneto-superconducting systems where SC is confined to the Fe-As or Fe-Se layers, ^{57}Fe MS may contribute much, since the Fe ions are not probes, but rather part of the layers to which SC is confined.

MS and Magnetization studies of a large variety of AFe_2As_2 (A=Ba, Eu) and $B_xFe_2Se_2$ (B=K, Rb and Tl) single crystals, including substitutions (i) of Fe by Co or Ni or (ii) As by P in the AFe_2As_2 system have been performed. We shall summarize our present knowledge about the phenomena observed to date, including the results obtained in the $B_xFe_2Se_2$ systems, in which the high AFM state (T_N> 500 K) coexists with SC (below 30 K) within the **same** Fe layers. In some materials, the paramagnetic Meissner effect is observed. Of particular interest is the $EuFe_2(As_{1-x}P_x)_2$ system, for which two Mössbauer isotopes, ^{57}Fe and ^{151}Eu, enable to investigate simultaneously the mutual interactions between the magnetic Eu and the Fe layers. $EuFe_2(As_{1-x}P_x)_2$ is SC for $0.2<x<0.5$. For $x\leq0.2$ the Eu^{2+} ions are AFM ordered with the moments in the *ab* planes. Whereas for $x\geq0.2$ the Eu is FM ordered along the *c*-axis. In the FM region, the magnetic transition and the magnetic hyperfine fields (H_{eff}) of the Eu nuclei are higher than those in the AFM region. The ^{57}Fe Mössbauer studies show no magnetism in the iron site for x >0.2, yet exhibit at 5 K transferred magnetic hyperfine fields (~1 T) from the FM ordered Eu sub lattice, even in the SC region. The observation of superconductivity in the presence of ferromagnetism is rarely observed, transferred magnetic hyperfine fields in the superconducting state are observed here for the first time.

[1] I. Nowik, I Felner, Z Ren, G H Cao and Z A Xu, New J. Physics 13(2011) 023033

[2] I. Felner, S. Jin, S. Wang, K. Zhu, and T. Zhou, J. Supercon. Nov. Magn. 24(2011) 2033

Session 1(T15) I-3 In Memoriam Rudolf L. Mößbauer

DEFECT-FLUORITE OXIDES: Ln (Eu AND Gd)-MÖSSBAUER SPECTROSCOPIC STUDY COUPLED WITH NEW DEFECT-CRYSTAL-CHEMISTRY MODEL

A.Nakamura[1], N.Igawa[2], Y.Okamoto[2], J.Wang[3], Y.Hinatsu[4], M.Takahashi[5], M.Takeda[5]
[1]*Japan Atomic Energy Agency, Advanced Science Research Center, Tokai, Naka, Ibaraki 319-1195, Japan*
[2]*Japan Atomic Energy Agency, Ouantum Beam Science Directorate, Tokai, Naka, Ibaraki 319-1195, Japan*
[3]*Dalian Institute of Chemical Physics, Chinese Academy of Science, Dalien 116023, China*
[4]*Hokkaido University, Department of Chemistry, Sapporo 160-0810 Hokkaido, Japan*
[5]*Toho University, Department of Chemistry, Miyama, Funahashi, Chiba 274-8510, Japan*

Defect-fluorite (DF) oxides as a generic term of various grossly oxygen-deficit oxygen-vacancy (V_O) type $M_{1-y}Ln_yO_{2-y2}(V_{Oy/2})$ solid solutions (ss) formed between parent fluorite (F) MO_2 (M^{4+} = Zr, Hf, Ce, Th, U, Np and Pu *etc*) and its V_O-ordered superstructure, lanthanide (Ln) and light-Ln C-type $LnO_{1.5}$ (Ln^{3+} = La-Lu, Y, Sc, In *etc*), have been the object of enormous research efforts for over these several decades due to their technological importance in nuclear, ceramic and electrochemical *etc* areas. Yet, much has remained elusive till now as to their detailed defect (V_O)-related local structure and its correlations with many key defect properties such as oxygen conductivity (σ(ion)), radiation tolerance, catalytic ability and phase and structural stability *etc*. To serve this purpose in these years we have been engaged in their combined Ln (Eu and Gd)-Mössbauer and XRD lattice-parameter (a_0(ss)) studies [1-5], lately extending them to ^{170}Yb-Mössbauer, EXAFS and Y-MAS-NMR *etc* studies.

One basic controversy of such defect-structure study has been; albeit classified as the same DF oxides, whether those based on larger M^{4+}s (Ce, Th, U, Np, Pu and Am *etc*) which themselves adopt F structure and those based on smaller M^{4+}s (Zr and Hf) which are first stabilized into F structure by $LnO_{1.5}$→$Zr(Hf)O_2$ doping, the both have either mutually 'different or similar' local structure. Our ^{151}Eu-Mössbauer study of $M_{1-y}Ln_yO_{2-y2}$ (M^{4+} = Ce, Th, U, Zr and Hf) (Fig. 1 [1]) has given a clear answer to this controversy: Based on the well-known near inversely-proportional IS(Eu^{3+})-(Eu^{3+}-O) bond-length (BL) relationship, these data decisively reveal that:

(i)The parent F-based M^{4+}=Ce and Th have a naïve (but non-random) 'disordered DF-type' local structure in which both BL(Eu^{3+}-O)s decrease smoothly and similarly due to the steady oxygen coordination number (CN) decrease about Eu^{3+} from ~7.5 at y=0 to 6 at y=1.0.

(ii)The stabilized zirconia (SZ) and stabilized hafnia (SH) (M^{4+}=Zr and Hf) the both have a sharp BL(Eu^{3+}-O) maximum, that of the SH with the shorter a_0(ss) being even longer than that of the SZ with the longer a_0(ss). Such characteristic IS(Eu^{3+}) behavior of SZ and SH is entirely different from that of the above parent-F-based systems, and is almost a first direct experimental evidence that SZs and SHs have basically the same intermediate ordered pyrochlore (P $Zr(Hf)_2Eu_2O_7$ at y=0.50)-based strongly anisotropic local structure extending to either the y<0.50 or >0.50 region retaining its short-range (local) P-type ordering, and thus the both have the longest BL(Eu^{3+}-O) at y=0.50 at which the most highly-ordered and the most-dilated near-ideally P-type Eu-$8O^{2-}$ (CN=8) coordination structure is realized. Making these findings a major incentive, one of the authors (A.N) has recently proposed a new defect-crystal-chemistry (DCC) a_0(ss) model for parent-F-type M^{4+}=Ce and Th [2-4] which can provide not only a novel possibly unified picture of their non-Vegardianity and non-random defect structure as closely coupled two sides of 'distortion-dilation' phenomenon of C-type $LnO_{1.5}$ but also a new consistent description of their detailed mutually non-randomly coordinated cation-anion concentration variations and also of their intriguing σ(ion) maximum behavior in low y (<0.10-0.20) range.

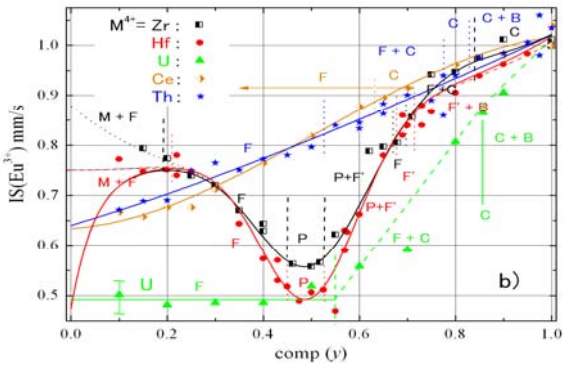

Figure 1. ^{151}Eu-Mössbauer Isomer-shift (IS) vs. composition (y) plot in the $M_{1-y}Ln_yO_{2-y2}(V_{Oy/2})$ (M^{4+}=Ce, Th, U, Zr and Hf)

We are now trying to extend this DCC a_0(ss) model to the more complex SZs and SHs involving the intermediate P (or δ)-type ordering and hence its-based extra distortion-dilation effect [5]. In the present talk, this ongoing efforts of our group, being in progress by piecing together their reported various a_0(ss), local-structure, σ(ion) and thermodynamic *etc* data with our own latest ^{155}Gd-Mössbauer, EXAFS and Y-MAS-NMR *etc* data obtained for several of them, will be described and discussed, in pursuit for the more global understanding of the whole DF oxides, either parent F- or stabilized P-type.

[1] A.Nakamura, N.Masaki, H.Otobe, Y.Hinatsu, J.Wang, M.Takeda, *Pure and Appl. Chem*. **2007**, *79*, 1691-1729.
[2] A.Nakamura, Solid State Ionics, **2010**, *181*, 1543-1564.
[3] A.Nakamura, Solid State Ionics, **2010**, *181*, 1631-1653.
[4] A.Nakamura et al, Hyperfine Interactions, **2012**, *207*, 67-71.
[5] A.Nakamura et al, Chap.5, in 'Mossbauer Spectroscopy: Applications in Chemistry, Biology, Nanotechnology, Industry, and Environment', V. K. Sharma, G. Klingelhoefer and T. Nishida eds, John-Wiley & Sons, in press, 2012.

^{151}Eu MÖSSBAUER STUDY OF LUMINESCENT Y_2O_3:Eu^{3+} CORE-SHELL NANOPARTICLES

E. Kuzmann[1], A. Vértes[1], G. Bohus[2], V. Hornok[3], A. Oszkó[1], I. Dékány[3,4]

[1]*Laboratory of Nuclear Chemistry, Institute of Chemistry, Eötvös University, Budapest Hungary*
[2] *Department of Physical Chemistry and Materials Science, University of Szeged, Szeged, Hungary*
[3] *Supramolecular and Nanostructured Materials Research Group of the Hungarian Academy of Sciences, University of Szeged, Szeged, Hungary*
[4] *Department of Medical Chemistry, University of Szeged, Szeged, Hungary*

More and more industrial interest was focused on semiconductor-based light-emitting diodes (LEDs). In their preparation the phosphors play a very important role. Among the phosphors Eu doped Y_2O_3 is one of the best luminophors regarding the emission efficiency of a red light. For the flat-panel display industry it became necessary to obtain nanoparticles with regular morphology and narrow size distribution.

In our study monosdisperse Y_2O_3:Eu^{3+} spherical nanoparticles and Y_2O_3@Eu^{3+} core-shell structured nanoparticles were synthetized by homogeneous precipitation method. TEM confirmed that spherical particles were obtained. Photoluminescence emission spectra of samples were observed in the range of 550-650 nm. ^{151}Eu Mössbauer parameters (Table I) undoubtfully proves that Eu atoms exist only in oxidation state Eu^{3+} in all spherical Y_2O_3:Eu^{3+} and Y_2O_3@Eu^{3+} core-shell nanoparticles. We have found small but significant differences between the ^{151}Eu Mössbauer spectra (Fig. 1 (a) and (b)) and the corresponding parameters (Table 1) of spherical Y_2O_3:Eu^{3+} and Y_2O_3@Eu^{3+} core-shell nanoparticles. Higher isomer shift and V_{zz} and smaller linewidth are characteristic of the spherical Y_2O_3:Eu^{3+} samples than those of belonging to the Y_2O_3@Eu^{3+} core-shell samples. This can be well understood in terms of the different structures of these nanoparticles. In the case of the spherical Y_2O_3:Eu^{3+} sample with 2.5% Eu^{3+} content the isomer shift is close to that reported for the Eu substitution in Y_2O_3 [1]. The relatively small linewidth also indicate that Eu occupy a well defined site in the lattice. The high Vzz in comparison to that of Eu in Eu_2O_3 can be originated from the change in the charge distribution probable due to lattice distorsion appearing at the incorporation of Eu into the Y site. All these parameters indicate that Eu occupies the Y site in Y_2O_3 in the spherical Y_2O_3:Eu^{3+} nanoparticles.

The observed isomer shift (Table 1) for all Y_2O_3@Eu^{3+} core-shell samples resonantly agrees with that found earlier for Eu_2O_3 [2]. This reflects that Eu locates in Eu_2O_3 in the core-shell samples (Fig. 2). The very high linewidth is associated with a highly defected Eu_2O_3 occurring in the shell of these nanoparticles.

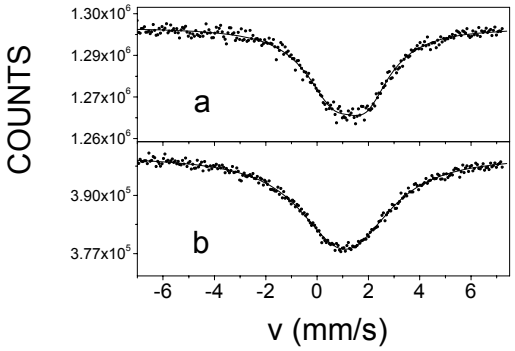

Figure 1. Typical room temperature ^{151}Eu Mössbauer spectra of Y_2O_3:Eu^{3+} and Y_2O_3@Eu^{3+} nanoparticles (a) Y_2O_3:Eu^{3+} containing 10% Eu^{3+} (b) Y_2O_3@Eu^{3+} with 75:25 of Y_2O_3:Eu_2O_3

Table I: ^{151}Eu Mössbauer parameters of Y_2O_3:Eu^{3+} and Y_2O_3@Eu^{3+} nanoparticles

	Y_2O_3:Eu^{3+} 2.5% Eu^{3+}	Y_2O_3:Eu^{3+} 10% Eu^{3+}	Y_2O_3@Eu^{3+} 75:25 Y_2O_3:Eu_2O_3	Y_2O_3@Eu^{3+} 10% Eu^{3+}
δ (mm/s)	1.28 (0.05)	1.19 (0.02)	1.03 (0.02)	1.02 (0.03)
V_{ZZ} (10^{21}V/m^2)	4.78 (0.52)	4.77 (0.16)	2.89 (0.81)	3.53 (0.95)
η	0.98 (0.21)	0.98 (0.07)	0.99 (0.38)	0.98 (0.34)
W(mm/s)	2.10 (0.22)	2.10 (0.08)	3.70 (0.27)	3.02 (0.40)

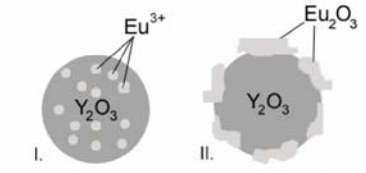

Figure 2. The schematic illustration of the nanoparticles

[1] H.T. Hintzen, H.M.van Noort, Phys. Chem. Sol. 49, (1988) 873-881
[2] E. Bauminger, G.M. Kalvius, I. Novik, In: Mössbauer Isomer Shifts (Eds. G. Shenoy, F. Wagner), North Holland, Amsterdam, New York, Oxford, 1978, pp.663-758.

Session 2(T14) I-5 In Memoriam Attila Vértes

NEW CONDUCTIVE VANADATE GLASS WITH HIGH CHEMICAL DURABILITY

T. Nishida*[1], I. Furumoto[1], H. Masuda[2] and S. Kubuki[2]

[1]*Kinki University, Kayanomori 11-6, Iizuka, Fukuoka 820-8555, JAPAN*

[2]*Tokyo Metropolitan University, Minami-osawa 1-1, Hachi-oji, Tokyo192-0397, JAPAN*

Electrical conductivity (σ) of semiconducting $20BaO \cdot 10Fe_2O_3 \cdot 70V_2O_5$ glass can be changed from the order of 10^{-7} to 10^{0} S cm^{-1} by changing temperature and duration of isothermal annealing [1-3]. Mössbauer atoms incorporated into glass matrix play a role of probe for the local structural study. Mössbauer spectrum of vanadate glass shows a marked decrease in quadrupole splitting (Δ) after isothermal annealing at temperatures higher than glass transition temperature (T_g) or crystallization temperature (T_c) [1-3]. Quadrupole splitting is expressed by:

$$\Delta = eq \cdot eQ/2 \times (1 + \eta^2/3)^{1/2}, \qquad (1)$$

in which eq and Q are electric field gradient and nuclear quadrupole moment. The former is composed of eq_{val}, caused by valence electrons, and eq_{lat} caused by steric configuration of neighboring atoms. In case of high-spin Fe^{III}, eq_{val} becomes zero, since five 3d-orbitals are equivalently occupied by five valence electrons. Since glass has isotropic structure, it is considered that asymmetry parameter (η) is zero.

Decrease of Δ is ascribed to a decreased distortion of $Fe^{III}O_4$ tetrahedra or *structural relaxation* of 3D-network, since eq is equal to eq_{lat} and hence Δ is directly proportional to eq_{lat}. *Structural relaxation* of distorted $Fe^{III}O_4$ tetrahedra detected by Mössbauer measurement is also the case for distorted $V^{IV}O_4$ or $V^{V}O_4$ tetrahedra, since they share corner oxygen atoms with $Fe^{III}O_4$ in the 3D-network.

In this study, local structure of new conductive vanadate glasses, $20BaO \cdot 10Fe_2O_3 \cdot xWO_3 \cdot (70\text{-}x)V_2O_5$, was investigated by means of Mössbauer spectroscopy. Mössbauer spectra of new vanadate glass with "x" of 20, annealed at 500 °C for 240 min, resulted in a marked decrease of Δ from 0.82 to 0.76 mm·s^{-1}. This reflects a decreased distortion of $Fe^{III}O_4$, $V^{IV}O_4$ and $V^{V}O_4$ tetrahedra, as observed in $20BaO \cdot 10Fe_2O_3 \cdot 70V_2O_5$ [1-3] and $20BaO \cdot 10Fe_2O_3 \cdot xMnO_2 \cdot (70\text{-}x)V_2O_5$ glasses [4]. In case of vanadate glass with "x" of 35, an identical Δ value of 0.80 mm·s^{-1} was observed in the Mössbauer spectra, irrespective of the isothermal annealing.

Isothermal annealing of vanadate glass with "x" of 20 at 500 °C for 240 min resulted in a marked increase of σ from 3.9×10^{-6} to 2.1×10^{-3} S·cm^{-1}, while comparable σ values of 0.88×10^{-5} and 1.6×10^{-5} S·cm^{-1} were obtained when "x" was 35. These results indicate that the marked increase of σ observed when "x" was 20 is due to a decreased distortion of the 3D-network.

Plot of T_g against the Δ of Fe^{III} gives a straight line, depending on the site occupation of Fe^{III} atoms; slope of the straight line becomes 680 K·(mm·s^{-1})$^{-1}$ when they occupy tetrahedral network forming (NWF) sites [5], while it becomes 260 in octahedral NWF sites [6]. This experimental rule, "T_g-Δ rule" [5], is valid for several inorganic glasses, and hence we can know "site occupation" of Fe^{III} in several glasses. In the present study, slope of 680 was obtained for glasses with "x" of 0-50, indicating that Fe^{III} evidently occupied substitutional sites of $V^{IV}O_4$ or $V^{V}O_4$ tetrahedra, not of $W^{VI}O_6$ octahedra.

Leaching test with boiling water for 120 min indicated that dissolution of vanadium ion was depressed from 30 to 11 and 10 mg·l^{-1} when "x" was changed from 0 to 20 and 35, respectively. These results evidently prove that introduction of $W^{VI}O_4$ and $W^{VI}O_6$ units into 3D-network of vanadate glass is effective for the improvement of water-resistivity. Leaching test with 20%HCl solution at 25 °C for 72 h showed higher chemical durability of vanadate glass when "x" was equal to or more than 20. Hence, it is concluded that introduction of 20 mol% WO_3 is effective for the preparation of chemical durable conductive vanadate glass.

References

[1] T. Nishida, *Japanese Patent No. 3854985* (2006).

[2] T. Nishida, *Japanese Patent, Tokugan 2006-99286* (2006) / *2008-508645* (2008).

[3] S. Kubuki, H. Sakka, K. Tsuge, Z. Homonnay, K. Sinkó, E. Kuzmann, H. Yasumitsu and T. Nishida, *J. Ceram. Soc. Jpn.*, **115** (2008) 776-779.

[4] S. Kubuki, H. Masuda, K. Akiyama, I. Furumoto and T. Nishida, *Hyperfine Interact*., DOI10.1007/ s10751-011-0433-2 (2011).

[5] T. Nishida, H. Ide and Y. Takashima, *Bull. Chem. Soc. Jpn.*, **63** (1990) 548-553.

[6] T. Nishida, M. Suzuki, S. Kubuki, M. Katada and Y. Maeda, *J. Non-Cryst. Solids*, **194** (1996) 23-33.

*nishida@fuk.kindai.ac.jp

Session 2(T13) I-6 In Memoriam Attila Vértes

CEMS STUDY OF TRANSPARENT SnO_2 FILMS DOPED WITH ^{57}Fe

Kiyoshi Nomura
[1]*Shool of Engineering, the University of Tokyo, Hongo7-3-1, Bunkyo-ku, Tokyo 113-8656*

The origin of magnetic interactions in diluted magnetic semiconductors (DMS) is an interesting issue as a basic problem in magnetism and its possible application in spintronics [1-2]. We have reported different types of magnetic source in case of Fe doped SnO_2 powders, prepared by sol-gel method and post annealing [3], and also the phonon density of states (DOS) of rutile type structures of SnO_2 and TiO_2 [4]. The dilution and clustering of doping Fe species can be estimated by Mössbauer spectra and phonon DOS. We have clarified that the diluted Fe species probe the phonon DOS in SnO_2 more faithfully than in TiO_2. When a large magnetization was obtained for diluted Fe doped SnO_2, a magnetic relaxation with broad lines was observed in room temperature Mössbauer spectra. However, when the small magnetization was observed, no magnetic component was found in Mossbauer spectrum. In the latter case, the magnetization disappeared by annealing for long time [3]. It is clear that defects in DMS can also contribute to enhance the saturation magnetization.

On the other hand, thin films of $Sn_{1-x}{}^{57}Fe_xO_{2-\delta}$ have been implanted at room temperature with $1x10^{17}$ Fe ions/cm^2 and at 300^{o}C with $5x10^{16}$ and $1x10^{17}$ Fe ions/cm^2, with an implantation energy of 100 keV in each case [5]. The as-implanted samples at room temperature and post-annealed samples did not show any Kerr effect, but the sample implanted with $1x10^{17}$ Fe ions/cm^2 at substrate temperature of 300^{o}C showed Kerr effect although magnetic sextets were not so clearly observed in the ^{57}Fe conversion electron Mössbauer (CEM) spectra. Kerr effect disappeared after annealing. This suggests that the number of magnetic defects decreases by absorption of oxygen due to annealing in air atmosphere [5]. We have also showed that the bulk magnetization is enhanced by introducing Sb^{5+} in the Fe doped SnO_2 powder [6]. We have tried to prepare ^{57}Fe implanted SnO_2 films at the substrate temperature of 500^{o}C, which showed Kerr effect [7]. The Kerr effect did not disappear after annealing. We have characterized tin oxide doped with ^{57}Fe and some transition metals.

SnO_2 (Sb) films with thickness of 200 nm were prepared on quartz glass by DC sputtering, and implanted with 5×10^{16} ^{57}Fe ions/cm^2 at the substrate temperature of 500 °C in vacuum, using an energy of 100 keV. From TRIM calculations of implantation conditions of 5×10^{16} Fe ions/cm^2, the iron profile peak is expected to be located at about 40 nm depth with a maximum Fe concentration of 5 at. %. Some samples were step by step post-annealed at 400 °C, 500 °C, 600 °C, 700 °C, and 800 °C. Polar Kerr effect of these samples was measured with magnetic circular dichroism (MCD) mode.

We have fabricated gas flow counter for CEMS and XMS, respectively, and further have also developed a dual counter to get both CEM and XM spectra simultaneously [7]. As another application, a He gas proportional counter can be applied to depth selective CEMS (DCEMS) by detecting the different energy electrons emitted from the surface. Three CEM spectra were simultaneously observed on each sample from different depths by discriminating the resonance electrons with three energy regions (2–6.5 keV, 6.5–11 keV, and 11–20 keV) using homemade Mössbauer system and He + 5% CH_4 gas flow counter [8,9] . This method provides the rough depth profile of layers, which is named as DCEMS. In contrast to DCEMS, a conventional CEMS, which detects all electrons, is called an integrated CEMS (ICEMS). Doppler velocity was calibrated with standard α-Fe foil at room temperature and a γ source of ^{57}Co/Cr matrix was used.

The Fe doped SnO_2 films annealed at various temperatures have been characterized by DCEMS using a back-scattered type of gas flow counter in order to study especially the effect of post annealing. The SnO_2 films implanted with ^{57}Fe at room temperature were measured at 15 K. The review on CEMS study of implanted samples and some additional results will be presented.

Acknowledgements
Author would like to express thanks to Dr. H. Reuther, Forschungszentrum Dresden-Rossendorf e.V., for implantation of samples and Dr. A. Nakanishi, Medical School, Shiga University, for measuring low temperature CEMS.

References

(1) J. M. D. Coey, M. Venkatesan, and C. B. Fitzgerald, Nat. Mater. 4, 173 (2005).
(2) A. Punnoose, J. Hays, A. Thurber, M. H. Engelhard, R.H. Kukkadapu, C. Wang, V. Shutthanandan, and S. Thevhuthasan S, Phys. Rev. B 72, 054402 (2005).
(3) K. Nomura, C. A. Barrero, J. Sakuma, and M. Takeda, Phys. Rev. B 75, 184411 (2007).
(4) A. I. Rykov, K. Nomura, J. Sakuma, C. Barrero, Y. Yoda, and T. Mitsui, Phys. Rev. B 77, 014302 (2008)
(5) K. Nomura and H. Reuther, Hyperfine Interact. 191, 159 (2009).
(6) K. Nomura, C. A. Barrero, K. Kuwano, Y. Yamada, T. Saito, and E. Kuzmann, Hyperfine Interact. 191, 25 (2009).
(7) K. Nomura, T. Okubo, and M. Nakazawa, Spectrochim. Acta B 59, 1259 (2004).
(8) K. Nomura, S. Iio, Y. Ujihira, and T. Terai, Industrial Applications of the Mössbauer Effect, Eds. M. Gracia, J. F. Marco, and F. Plazaola, AIP, CP 765, 108 (2005).
(9) K. Nomura, Z. Nemeth, and H. Reuther, ICAME09 proceeding, Journal of Physics: Conference Series (JPCS), 217(2010)012118.

APPLICATIONS OF MAGNETIC NANOSTRUCTURES AND RELEVANCE OF MÖSSBAUER SPECTROMETRY

J.M. Greneche

LUNAM Université du Maine, Institut des Molécules et Matériaux du Mans, UMR CNRS 6283, 72085 Le Mans Cedex, France

Nanotechnology which refers to the design of functional devices from manipulation and self-assembly of atoms, molecules or clusters, should be one of technologies most relevant and challenging in different industrial applications for the coming decades. Indeed, the use of nanomaterials does contribute to reduce ecological stress, energy consumption and natural resources. But the use of nanomaterials requires to evaluate carefully the risks to the workers during elaboration and manufacturing, to the environment and to the consumers for risks of exposure and toxicological aspects. Consequently, it is necessary to control the morphology and the chemical nature, the temperature and time stability and the physical properties of nanomaterials. Among the different techniques which can be used, ^{57}Fe Mössbauer spectrometry is relevant to probe surface and bulk structures, and to determine on the one hand the role of the surface or of the grain boundaries in the case of nanoparticles and nanostructured powders, respectively and on the other hand the hyperfine magnetic properties and their dynamics in correlation with superparamagnetic relaxation phenomena in the case of magnetic nanostructures.

The different types of nanostructures will be first established in conjunction with their potential applications allowing thus to discriminate the relevant parameters which influence the physical properties and their changes compared to bulk microstructures. We illustrate from selected examples how both the selectivity and the local probe character of ^{57}Fe Mössbauer spectrometry contributes to investigate *in situ* local atomic order and magnetic properties in different nanostructures, as nanocrystalline alloys, nanostructured powders, nanoparticles and assemblies of particles and functionalized nanostructures and mesoporous hybrides ((Metal Organic Frameworks, MOFs).

Session 3(T11) I-8 In Memoriam Igor Petrovich Suzdalev

MOSSBAUER SPECTROSCOPY OF ZIRCONIUM ALLOYS

V.P. Filippov, A.B. Bateev, Yu.A. Lauer, N.I.Kargin,
Russia, Moscow, National Research Nuclear University "MEPhI"

Zirconium is used in nuclear reactors as a construction material. In Russia, the most widely used alloys are such as E110, E125, E635 having the approximate compositions of Zr-1% Nb, Zr-2.5% Nb, Zr-1% Nb +0.35% Fe-1, 2% Sn, respectively. Abroad such alloys as Zircaloy-2 (Zr-1.2-1. 7% Sn-0.07-0.2% Fe-0.05-0.15% Cr), Zircaloy-4, M4, M5 and NSF are used. Thus, in order to improve mechanical and corrosion properties of zirconium alloys they are modified with alloying elements as iron, tin, niobium, nickel, chromium, copper in varying amounts to 1.5 mas.% depending on country of manufacture and conditions of using. Iron and tin have the Mossbauer isotopes and therefore it is possible to carry out a study of their state and their influence on the properties of zirconium alloys by Mossbauer spectroscopy. One can study the state of the atoms in solid solutions and formed intermetallic compounds. The solubility of the iron atoms in the α-Zr is determined. It is 0.015 mas.% at 600 °C. The parameters of the Mossbauer spectra of the solid solution of iron atoms α-Zr at room temperature are δ =-0.10 ± 0.02 mm/s (isomer shift), ΔE=0.32 ± 0.02 mm/s (quadrupole splitting) [1]. Studying of penetration of oxygen in solid solution of iron atoms in the α-Zr showed that the iron atoms leave the solid solution and form intermetallic compounds. This indicates that the iron atoms in the α-Zr are in a state solid solution, since the oxygen atoms form a solid solution taking places of the iron atoms.

With the help of Mössbauer spectroscopy it was experimentally demonstrated the formation of intermetallic compounds Zr_2Fe in the Zr-Fe alloys [2] (δ = - 0.32±0.02 mm/s, η = 0, ΔE = (0.60 ÷ 0.72) mm/s). Aubertin [3] carried out measurements in magnetic fields and stated that in binary Zr-Fe alloys in addition to Zr_2Fe the stable compound Zr_3Fe is formed, whose parameters of Mossbauer spectra differ only by the value of the quadrupole splitting and sign of the electric field gradient (δ = -0.32 ± 0.02 mm / s, η = 0.6, ΔE = -(0.75÷0.90) mm/s). Adding other elements (W, Ni, Cu) [4] leads to changing in the values of the quadrupole splitting, or in the case of Cr, Nb - both the values of the quadrupole splitting and isomer shift [5-12]. Reducing the electric field gradient at the ^{57}Fe nuclei indicates the formation of a mixed phase composition on the basis of ZrV_2 $ZrCr_2$ and with the substitution of atoms of vanadium and chromium atoms with iron atoms [7-9]. As to the alloys with niobium, there may be formation of intermetallic compounds of two types - $(Zr_{1-x}\ Nb_x)_2Fe$, with the spectra parameters (ΔE= 0.5 ÷ 0.75 mm/s, δ= - (0.28÷0.34 mm/s) and $(Zr_{1-x}\ Nb_x)Fe_2$ with a smaller quadrupole splitting (ΔE= (0.20 ÷ 0.51) mm&s, = - (0.16÷0.28) mm/s). During heat treatment the iron atoms in alloys tend to move to the surface and enrich the surface layer of the intermetallic particles. In thin layers (0.1 mm) this enrichment can reach 5 mas.%, with the initial concentration 0.35mas.% Fe in alloy. Effect of laser irradiation on the enrichment of the surface layers manifests itself differently for the annealed and deformed samples. The reason for this behavior of the iron atoms can be explained both the fast diffusion of iron atoms and the presence of defects in deformed samples of the alloys. In alloys containing iron, tin, and chromium atoms it is found the conversion of one type of intermetallic particles to another type in the surface layers even at room temperature [10]. Irradiation of the surface of zirconium alloys by argon ions leads to the changing of ratio of intermetallic compounds concentrations in near surface layers [12]. The changes were detected for all investigated samples of E635, NSF and Zyrcaloy-2 alloys. In particular for cold deformed NSF alloy relative increase of compound $(Zr_{1-x}\ Nb_x)Fe_2$ is noticed. Relative changes of concentration Zr_3Fe in near surface layers aren't observed. For specimens of Zyrcaloy-2 alloy after the ionic irradiation the substantial growth of concentration of compound with nickel near surfaces of the sample is revealed, i.e. the concentration of $Zr_2(Fe,Ni)$ compound increases and the concentration of $Zr(Fe,Cr)_2$ (C14) decreases.

With regard to the state of tin, which concentration in alloys is 0.5-1.3 mas.%, most researchers find it in the form of a solid solution of Sn atoms in α-Zr and with parameters of Mössbauer spectra δ=1.72±0.04 mm/s, ΔE=0.32±0.02 mm/s (relative to $BaSnO_3$). In the ternary alloys with Fe and Nb after quenching the lines of β–Sn and compounds Nb_3Sn are visible. Formation of β–Sn is explained due to the occurrence of oxide films on the surface of the quenched samples. In oxide films the particles of metallic tin are formed, which go into α-Zr solid solution in the process of thermal treatment once again.

[1] M.M. Stupel, M. Bamberger and B.Z. Weiss., Scripta metallurgica 19 (1985) 739-740.
[2] Yu.Ph. Babikova, V.P. Filippov, I.I. Shtan. Atomnaya energia (rus), 32, 6(1972)484-487.
[3] F. Aubertin, et all. Z. Metallkde, Bd. 76, H4(1985)237-244.
[4] Yu.Ph. Babikova, et all. J. Ph. Met.i metalloved., 48, 5(1979)916-920.
[5] D. Pecheur, V.P. Filippov, F.B. Bateev, Yu. Yu. Ivanov. Zirconium in the Nuclear industry. 13 international symposium ASTM STR 1423, Cherry D Moan, Eds. ASTM International, PA (2002) 135-153.
[6] J.A. Sawiski. JNM, 228(1996)238-247.
[7] V.G. Kirichenko, A.I. Kirdin. Vestnik Khar'kovskogo Universiteta: physica, 823(2008)25-45.
[8] V.V. Igrushin et.al. FMM (rus), 55, 6(1983)1143-1149.
[9] M. Tanaka. J. Phys. Soc. Japan, 25, 6(1968)1541-1543.
[10] V.P. Filippov, Yu.A. Shikanova. FHOM(rus), 1(2004)90-91.
[111] .V.P. Filippov, V.I. Petrov, Yu.A. Shikanova. Izvestia RAN:physics. 69, 10(2005)1488-1491.
[12] V.P. Filippov et.al. Izvestia Ran :physics. 74, 3(2010)405-409..

Session 4(T5) I-9

Role of iron in neurodegenerations

J.Galazka-Friedman[1], and A. Friedman[2]
[1] *Faculty of Physics, Warsaw University of Technology, Poland,* [2]*Department of Neurology, Medical University of Warsaw, Poland*

Progressive atrophy of brain structure is referred to as neurodegeneration. The mechanisms of this process, leading to several neurological diseases of older age, are not well known. Among several causes the oxidative stress injury is taken into account. It is known that the oxidative stress may be triggered by an excess of divalent iron, which can initiate Fenton reaction:

$$Fe^{2+} + H_2O_2 \rightarrow Fe^{3+} + OH^{\bullet} + OH^{-}$$

The possible role of iron in neurodegeneration was studied by various techniques: Mössbauer spectroscopy (MS), electron microscopy, enzyme-linked immuno-sorbent assay (ELISA), atomic absorption, ultrasonography and magnetic resonance imaging (MRI). The measurements were made on human tissues extracted from liver and from brain structures involved in diseases of the human brain: substantia nigra (Parkinson disease, PD), hippocampal cortex (Alzheimer disease, AD) and globus pallidus (progressive supranuclear palsy, PSP). Mössbauer spectroscopy of all these structures has shown that most of iron is ferritin-like iron [1]. Ferritin is the main iron-storage compound in human body [2]. Ferritin is composed of the protein shell and inner cavity filled with iron. The protein shell is build of 24 ferritin H and L chains. H and L ferritins play various roles: H ferritin is mostly related to an absorption of iron into the protein shell of ferritin, while L ferritin is involved in the safe storage of iron within the protein shell. The sizes of the iron cores of ferritin assessed with the use of electron microscopy were found to be smaller in brain than in liver – 3.5 nm vs. 6.5 nm [3]. These values correlate well with the blocking temperatures determined by Mössbauer spectroscopy [4]. Brain ferritin has a higher proportion of H to L chains compared to liver (H/L in hippocampus – 14, in globus pallidus – 5, in substantia nigra – 4, in liver – 0.4) [5]. With the use of ELISA a significant decrease of the concentration of L chains in PD compared to control was found – 98 ng/mg wet tissue vs. 52 ng/mg wet tissue [6].

No increase in the concentration of iron in PD vs. control was detected, however there was an increase of labile iron, which constitutes only 2‰ of brain iron [7]. In AD an increase in the concentration of ferritin was noticed, without a significant increase in iron concentration [8]. In PSP an increase of total iron was observed [9].

Although the post mortem studies add a lot to the understanding of the mechanisms of neurodegeneration, the possibility to assess iron in vivo in patients with neurodegenerative diseases would be of ultimate importance. The discovery of hyperechogenicity of parkinsonian SN by TCS was originally interpreted as the result of a higher concentration of iron in the tissues [10]. It was shown however, that insertion of iron-loaded ferritin to the animal brain does not produce hyperechogenicity. On the other hand, insertion of glial tissue to the same animal brain, gives a hyperechogenic signal similar to the one found in PD. One may suspect therefore that the hyperechogenicity is not the result of higher iron concentrations in the tissues, but of higher proportions of glial cells, which replace dying nervous cells [11].

MRI was also used in studies of the possible role of iron in the pathogenesis of PD. The published studies gave, however, controversial results. As in some studies the change of the T2 MRI signal in PD patients was attributed to an increase of the concentration of iron in parkinsonian SN [12] and our MS studies did not confirm such an increase, we tried to assess, how much iron loaded ferritin and/or non-ferritin iron is needed to cause the change of the MRI signal. In this study, phantoms containing a one liter water solution of five metabolites present in the human brain grey matter tissue were used [13]. This experiment showed that the change of the T2 signal appears only when the ratio of ferrous/ferritin iron is bigger than one. As such high concentration of ferrous, non-ferritin bound iron was excluded by our MS studies there must be another cause for the change observed by MRI.

Our findings suggest that the mechanisms leading to nervous cells death in these three, investigated by us, diseases may be different, although all may be related to iron mediated oxidative stress.

[1] Galazka-Friedman J, Hyperfine Interactions, 182, (2008), 31-44
[2] Harrison PM, Arosio P, Biochim Biophys Acta 1275 (1996), 161-203
[3] Galazka-Friedman J, Bauminger ER, Tymosz T, Friedman A. Hyperfine Interactions (C), 3, (1998), 49-52
[4] Galazka-Friedman J, Bauminger ER, Friedman A, Koziorowski D, Szlachta K, Hyperfine Interactions 165, (2005), 285-288
[5] Galazka-Friedman J, Bauminger ER, Koziorowski D, Friedman A. Biochim. Biophys. Acta 1688, (2004), 130-136
[6] Koziorowski D, Friedman A, Arosio P, Santambrogio P, Dziewulska D. Park Rel Disord 13, (2007), 214-218
[7] Wypijewska A, Galazka-Friedman J, Bauminger ER, Wszolek ZK, Schweitzer KJ, Dickson DW, Jaklewicz A, Elbaum D, Friedman A. Park Rel Disord 16, (2010), 329-333
[8]Gałązka-Friedman J, Bauminger ER, Szlachta K, Koziorowski D, Tomasiuk R, Jaklewicz A, Wszolek ZK, Dickson D, Kaplinska K, Friedman A. Acta Phys Pol 119, (2011), 81-83
[9] Galazka-Friedman J, Bauminger ER, Szlachta K, Schweitzer K, Wszolek Z, Dickson D, Friedman A. Acta Phys Pol 115, (2009), 431-433
[10] Berg D, Roggendorf W, Schröder U, Klein R, Tatschner T, Benz P et al. Arch Neurol 59, (2002), 999-1005
[11] Sadowski K, Szlachta K, Serafin-Król M, Galazka-Friedman J, Friedman A. J Neural Trasm, (2011) doi.org/10.1007/s00702-011-0707-5
[12] Antonini A, Leenders KL, Meier D, Oertel WH, Boesiger P, Anliker M. Neurology 43, (1993), 697-700
[13] Szlachta K, Sadowski K, Kuliński R, Galazka-Friedman J, Friedman A. Acta Phys Pol (in press)

MÖSSBAUER SPECTROSCOPY IN CATALYSIS

K.Lázár[1]
[1]Centre for Energy Research, Institute of Isotopes, Budapest , P.O.B. 49, H-1525, Hungary

Among other fields, Mössbauer spectroscopy is an efficient tool to study various catalysts. The method is linked inherently to gamma rays which may penetrate through low mass number media, thereby providing a mean for in situ studies on supported catalysts.

The utilisation of the method in this direction commenced in the 1970's. Studies have been focussed on various fieds of catalysis since then [1].

An overview is given on various topics in which the method provided principal contributions to the analysis of catalysts and to reveal their state during catalytic processes. Certain selected examples are presented to illustrate various facets of the potentials of the method.

Among others

- initial stages of the formation of carbide phases in supported Fischer-Tropsh catalysts,

- early stages of formation and stabilisation of bimetallic Pd_xFe (x = 1,3) phases on SiO_2 and NaX zeolite cages and correlation with catalytic performance in CH_3OH formation, [2]

- variation of composition of $PtSn_x$ (x = 1-4) and correlated Sn(IV) $\leftrightarrow$ Sn(0) reversible processen on supported SiO_2 catalysts during hydrodechlorination, [3]

- framework-extraframework dinuclear iron centres in zeolites, [5]

- early stages of formation of carbide phases in $Cu_{1-x}Co_xFe_2O_4$ ferrospinels, and its correlation with the catalytic performance in alkylation, [4]

- comparison of redox changes of iron in ferrisilicates and in FeAlPO-s , [6]

- performance of composite Fe_2O_3/SBA-15 mesoporous catalysts in total oxidation of phenol, [7]

are demonstrated and interpreted in relation with the catalytic performance. [8]

Future perspective directions are also mentioned briefly [9].

References
[1] J.-M.M. Millet, Advances in Catalysis, 51 (2007) 309
[2] B.M. Choudary et al., J. Chem. Soc., Faraday Trans., 86 (1990) 419
[3] W.D. Rhodes, et al., Journal of Catalysis, 230 (2005) 86
[4] K. Lázár et al., Phys. Chem. Chem. Phys., 4 (2002) 3530
[5] K. Lázár et al., Catalysis Today, 110 (2005) 239
[6] K. Lázár et al., Stud. Surf. Sci. Catal., 135 (2001) 14-P-22
[7] K. Lázár et al., Stud. Surf, Sci. Catal., 154 (2004) 805
[8] K. Lázár, Hyperfine Interactions, 206 (2012) 51
[9] T. Belgya, K. Lázár, Hyperfine Interactions, 167 (2006) 87

Session 5(T1) Oral-1

IDENTIFICATION AND QUANTIFICATION OF Sn-BASED SPECIES IN TRIMETALLIC Pt-Sn-In/Al_2O_3-Cl NAPHTHA-REFORMING CATALYSTS

J.-C. Jumas[1], M.T. Sougrati[1], J. Olivier-Fourcade[1], A. Jahel[2], P. Avenier[2] and S. Lacombe[2]

[1] *Institut Charles Gerhardt (UMR 5253), Université Montpellier 2, Place E. Bataillon, CC1502 34095 Montpellier Cedex 5 (France)*
[2] *IFP Energies nouvelles, BP 3, 69360 Solaize (France)*

Catalytic naphtha reforming is a major petroleum refining process for the production of hydrogen and high-octane gasoline and one of the largest users of catalysts in the chemical industry. If Pt/Al_2O_3 was the first naphtha-reforming catalyst, great progress has been achieved with the introduction of supported bimetallic-reforming catalysts in which Pt is promoted by another metal (Re, Sn, Ge, Ir). Among these the Pt-Sn based catalysts are particularly selective at low pressure and highly resistant to Pt sintering. More recently the addition of a second promoter as In [1] leading to a significant selectivity improvement has been evidenced. ^{119}Sn Mössbauer Spectroscopy (MS) is powerful tool to identify the different Sn-based species using diagrams previously established from model compounds and reference catalysts (Figure 1) [2]. MS has been used to elaborate a clear insight on the distribution diagram regarding Sn-species formed in these catalysts in different activation forms.[3-6].

The quantification of these Sn-species can be estimated from the contribution of their sub-spectra provided that their ***f*** Lamb Mössbauer factors are known. The objective of this communication will be to determine these ***f*** factors.

From the temperature dependence of Mössbauer spectra of a reference catalyst $Pt/Al_2O_3SnIn_{0.59}$ under different forms (oxidized, reduced and re-oxidized) the ***f*** factors of the main Sn-based species (pure oxides, interfacial oxides, pure alloys, oxometallics) have been determined (Table I). The results were thoroughly used in the quantification of Sn-based species observed for $Pt/Al_2O_3SnIn_x$-Cl catalysts with different amounts of $In_{x\ =\ wt.\%}$ (x = 0.06, 0.21, 0.39, 0.59) in activated form (reduced). Discussion will be provided in view of catalytic performances.

Acknowledgements

The Mössbauer platform has been implemented at the University of Montpellier 2 with supports from the EC (NoE ALISTORE SES6-CT-2003-503532), Région Languedoc Roussillon (Contracts n° 2006-Q086 and 2008-094192). The authors are grateful to these institutions and to IFP Energies nouvelles, CNRS and University of Montpellier 2 (contract n° 31229) for financial supports.

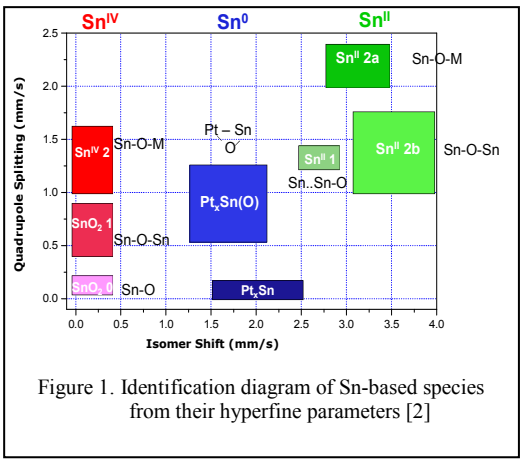

Figure 1. Identification diagram of Sn-based species from their hyperfine parameters [2]

Table I: *f* factors of the different Sn-based species (according labels from Figure 1)

Catalyst	Sn-based species	*f* factors at 300K
$Pt/Al_2O_3SnIn_{0.59}$-Cl oxidized	SnO_2 1, Sn^{IV} 2	0.53 (1)
$Pt/Al_2O_3SnIn_{0.59}$-Cl reduced	SnO_2 1, Sn^{IV} 2	0.72 (9)
	Pt_xSn	0.27 (4)
	Sn^{II} 2a	0.35 (5)
	Sn^{II} 2b	0.31 (7)
$Pt/Al_2O_3SnIn_{0.59}$-Cl re-oxidized	SnO_2 1, Sn^{IV} 2	0.62 (1)
	$Pt_xSn(O)$	0.34 (1)
	Sn^{II} 2b	0.23 (1)

[1] P.Y Le Goff et al., French Patent 2 910 347 (2008)
[2] J. Olivier-Fourcade et al., ChemPhysChem 5 (2004) 1734.
[3] A. Jahel et al., J. Phys. :Conf. Ser. ,217 (2010) 012045.
[4] A. Jahel et al., J. Catal., 272 (2010) 275.
[5] A. Jahel et al., Hyperfine Interactions (2012, in press)
[6] A. N. Jahel et al., J. Phys. Chem. (2012, in press)

MÖSSBAUER STUDY ON Fe-SUBSTITUTED SPINEL OXIDES: SYNERGY OF Fe^{2+} AND Fe^{3+} FOR ETHYLBENZENE DEHYDROGENATION WITH CO_2

Min Ji[1, *], Xiaoyan Zhang[1], Junhu Wang[2], Huihong Yin[1]

[1] *School of Chemisty, Dalian University of Technology, Dalian 116023, PR China, jimin@dlut.edu.cn*

[2] *Mössbauer Effect Data Center, Dalian Institute of Chemical Physics, Chinese Academy of Sciences, Dalian 116023, PR China*

Styrene is one of the most important basic chemicals as a monomer of polymers and one way to synthesize it is dehydrogenation of ethylbenzene in the presence of CO_2, which is widely investigated due to its environmental and economical benefits. Spinel oxides that contain iron ions as catalysts for ethylbenzene dehydrogenation have been screened extensively [1, 2]. However, there are still some disputes about the roles of Fe^{2+} and Fe^{3+} in the reaction so far. In this study, ternary-composite oxides of iron-incorporated catalysts were prepared and reduced in the atmosphere of H_2 at different temperatures. Their catalytic performance was evaluated and the coordination environment and valence state of iron species was investigated with ^{57}Fe Mössbauer spectroscopy.

Three catalysts of Fe_2O_3–MgO/γ-Al_2O_3, Fe_2O_3/$MgAl_2O_4$ and $MgFe_{0.1}Al_{1.9}O_4$ with the same molar ratio of Mg/Fe/Al were prepared by impregnation and sol–gel methods. The properties of the solids were characterized by X-ray diffraction (XRD), H_2-temperature programmed reduction (H_2-TPR) and Mössbauer spectroscopy (MS). XRD revealed the spinel structure of the catalysts. For all three catalysts, there are no diffraction peaks of α-Fe_2O_3, but diffraction peaks of MgO in Fe_2O_3–MgO/γ-Al_2O_3, which indicated that Fe has incorporated into spinel lattice or highly decentralized in the catalyst. H_2-TPR showed different reduction behaviours of the catalysts and gave information about the nature of the iron species present in the catalysts. It could be seen from MS that there was α-Fe_2O_3 dispersed in Fe_2O_3–MgO/γ-Al_2O_3 and Fe_2O_3/$MgAl_2O_4$, but α-Fe_2O_3 was hardly found in $MgFe_{0.1}Al_{1.9}O_4$.

The preparation method has great influence on the catalytic performance of iron oxide-based catalysts. $MgFe_{0.1}Al_{1.9}O_4$ prepared by sol–gel methods showed high catalytic activity and stability. The catalysts were reduced by hydrogen at 450 °C and 650 °C on the basis of the results of H_2-TPR, and investigated by Mössbauer spectroscopy. After the catalysts were reduced, ethylbenzene conversion was increased (Fig.1) and the styrene selectivity kept more than 90%. MS showed that the content of Fe^{2+} in the tetrahedral site of spinel were increased after being reduced and there was a new doublet with isomer shift of 0.60 mm/s that assigned to Fe^{2+} in $FeAl_2O_4$ after being reduced at 650 °C. It suggests that Fe^{2+} also contribute to ethylbenzene dehydrogenation to styrene in the atmosphere of CO_2 as well as Fe^{3+}, in other words, there is a synergetic function between the Fe^{2+} and Fe^{3+} species existing in the spinel skeleton during ethylbenzene dehydrogenation.

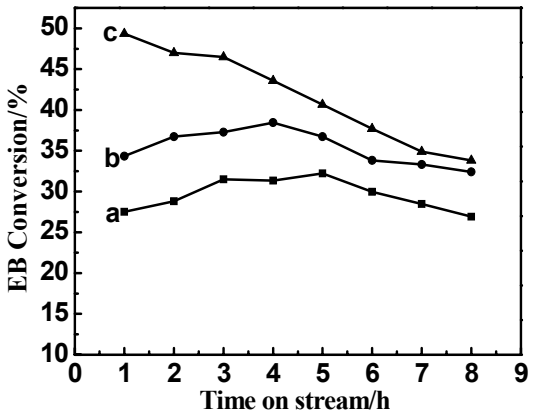

Fig.1 EB conversion as a function of time on stream over catalysts: (a) fresh $MgFe_{0.1}Al_{1.9}O_4$ (b) $MgFe_{0.1}Al_{1.9}O_4$ reduced at 450 °C (c) $MgFe_{0.1}Al_{1.9}O_4$ reduced at 650 °C

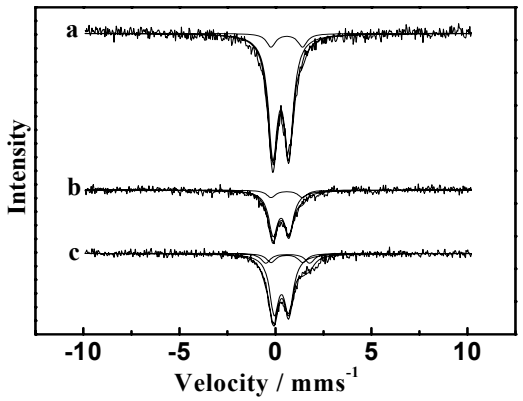

Fig.2 ^{57}Fe Mössbauer spectra of catalysts: (a) fresh $MgFe_{0.1}Al_{1.9}O_4$ (b) $MgFe_{0.1}Al_{1.9}O_4$ reduced at 450 °C (c) $MgFe_{0.1}Al_{1.9}O_4$ reduced at 650 °C

Sample	IS (mm/s)	QS (mm/s)	Area (%)	Remarks
Fresh	0.28	0.82	89.6	Fe^{3+} in Oh
	0.59	1.64	10.4	Fe^{2+} in Td
Reduced at 450 °C	0.29	0.82	85.2	Fe^{3+} in Oh
	0.59	1.64	14.8	Fe^{2+} in Td
Reduced at 650 °C	0.64	2.29	13.0	Fe^{2+}
	0.32	0.76	75.0	Fe^{3+} in Oh
	0.60	1.65	12.0	Fe^{2+} in Td

[1] Min Ji, Guili Chen, Junhu Wang, Xinkui Wang, Tao Zhang. Catalysis Today 158 (2010) 464.

[2] Xingnan Ye, Ning Ma, Weiming Hua, Yinghong Yue, Changxi Miao, Zaiku Xie, Zi Gao. Journal of Molecular Catalysis A: Chemical 217 (2004) 103.

Session 5(T1) I-11

MECHANISTIC STUDIES ON PREFERENTIAL OXIDATION OF CO IN H_2-RICH ATMOSPHERE OVER IRFE CATALYSTS

Kuo Liu, Junhu Wang and Tao Zhang
Mössbauer Effect Data Center, Dalian Institute of Chemical Physics, Chinese Academy of Sciences

Preferential oxidation of CO in H_2-rich stream (PROX) is becoming attractive with the fast development of the proton exchange membrane fuel cells. Among the PROX catalysts, bimetallic catalyst is one of the most effective candidates, such as PtFe[1-3] and IrFe[4-8] catalysts. In the present text, IrFe catalyst was chosen as a model catalyst for studying the mechanism of the PROX reaction on bimetallic catalysts.

IrFe bimetallic catalysts supported on SiO_2 was prepared by co-impregnation method.[6] It has been found that the presence of H_2, even in a slight excess (such as 2 %), could led to a large increase in the CO oxidation rate on IrFe/SiO_2.[7] In order to reveal the promotional role of Fe related with the presence of H_2, quasi in situ Mössbauer spectroscopy, in combination with microcalorimetry and in situ DRIFTS, was employed. The results showed that Fe^{3+} in the IrFe catalyst could be easily reduced to Fe^{n+} ($2 < n < 3$), Fe^{2+}, FeIr alloy and Fe^0 with the aid of Ir, and the low valence Fe species could also be easily oxidized when exposed to O_2. The relative amount of Fe^{2+} increased when increasing the H_2 concentration in the gas mixture, as shown in Figure 1, which was well consistent with the trend of the CO oxidation rate. In addition, Fe^0 remained intact in the oxidation atmosphere, probably because it was encapsulated by ferric oxide. The results above strongly suggested that Fe^{2+} was the active site for oxygen activation. During the PROX reaction, FeIr alloy disappeared due to oxidation, forming intimately contacted Fe^{2+} species and Ir particles. H_2 promoted CO oxidation by stabilizing Fe^{2+} in IrFe/SiO_2.

Based on the results of characterization and the steady state kinetic data in a microreactor, the microkinetic model which could predict the experimental results well was proposed.[8] The elementary steps (1) - (7) were involved in the PROX reaction, while the steps (1) - (3) were involved in CO oxidation:

$CO + Ir \leftrightarrows Ir\text{-}CO$ (1)
$O_2 + 2* \rightarrow 2O*$ (2)
$Ir\text{-}CO + O* \rightarrow CO_2 + Ir + *$ (3)
$H_2 + 2Ir \leftrightarrows 2H\text{-}Ir$ (4)
$H\text{-}Ir + O* \leftrightarrows OH\text{-}* + Ir$ (5)
$OH\text{-}* + H\text{-}Ir \rightarrow H_2O + * + Ir$ (6)
$OH\text{-}* + Ir\text{-}CO \rightarrow CO_2 + H\text{-}Ir + *$ (7)

Where * denotes Fe^{2+} species. The model suggested that for CO oxidation, no competitive adsorption between CO and O_2 was observed on IrFe catalyst. For CO oxidation, the surface reaction between adsorbed CO and O was rate limiting. For PROX, the reaction between adsorbed H and O for OH formation was rate determining, and the rate constant of step 7 was faster than step 3 (Table I), suggesting that the oxidation of adsorbed CO by surface OH was the dominant pathway for CO_2 formation. According to the model, the increasing trend of OH coverage coincides with the increase of the CO oxidation rate, as shown in Figure 2. Thus, it can be concluded that the presence of H_2 increased the surface concentration of OH and hence lowered the activation energy and increased the reaction rate of PROX.

Therefore, H_2 not only stabilized Fe^{2+} species, but also increased OH groups on the surface, both of which could promote CO oxidation.

Table I: Rate constants for elementary steps for PROX.

T (K)	333	353	373	393
k_1/k_{-1}	1.33×10^8	1.14×10^7	1.27×10^6	1.78×10^5
k_2	2000	2000	2000	2000
k_3	0.009	0.026	0.07	0.16
k_4/k_{-4}	1.08×10^4	3.88×10^3	1.56×10^3	6.85×10^2
k_5/k_{-5}	0.12	0.19	0.27	0.37
k_6	0.11	0.24	0.50	0.97
k_7	0.43	0.96	2.00	3.86

k: rate constant

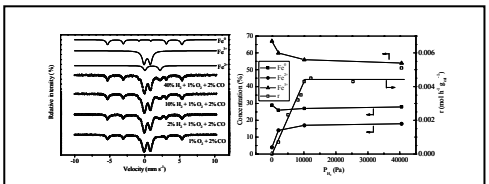

Figure 1. The relationship between Fe^{2+} and the CO oxidation rate (r).

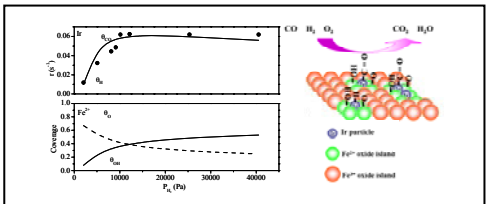

Figure 2. The relationship between OH and the CO oxidation rate (r).

[1] BT.Qiao et al., Nature Chem 3 (2011) 634-641
[2] Q.Fu et al., Science 328 (2010) 1141-1144
[3] J.Yin et al., Catal Lett 125 (2008) 76-82
[4] WS.Zhang et al., Catal Lett 121 (2008) 319-323
[5] WS.Zhang et al., Catal Today 131 (2008) 457-463
[6] WS.Zhang et al., Int J Hydrogen Energy 35 (2010) 3065-3071
[7] K.Liu et al., J Phys Chem C 114 (2010) 8533-8541
[8] K.Liu et al., Ind Eng Chem Res 50 (2011) 758-766

ROOM-TEMPERATURE FERROMAGNETISM IN TRANSITION-METAL CO-DOPED SnO_2

Jun Okabayashi[1], Kiyoshi Nomura[2], Shin Kono[3], and Yasuhiro Yamada[3]
[1]*Research Center for Spectrochemistry, The University of Tokyo, 113-0033, Japan*
[2]*Department of Applied Chemistry, The University of Tokyo, 113-8656, Japan*
[3]*Department of Chemistry, Tokyo University of Science, 162-8601, Japan*

Transition-metal (TM) doped TiO_2, ZnO, and SnO_2 have attracted a great deal of attention because of their potential use as functionalities in optical and carrier controlling [1]. SnO_2, in particular, is widely utilized as a gas sensor, because of its chemical sensitivity and structural stability. The main challenge is to fabricate a diluted magnetic semiconductors (DMS) with a high Curie temperature (T_C) and to control its magnetic properties. Although Fe-doped SnO_2 and Ni-doped SnO_2 have been fabricated [2-4], magnetic properties are not controlled in single-ion-doping cases. We focus on the co-doping of Fe and Ni into SnO_2 for the development of new kinds of DMS controlling the magnetic properties at room temperature.

In this paper, we report upon the TM concentration dependence of the magnetic properties of Fe and Ni co-doped SnO_2. We also systematically discuss its magnetic and electronic properties in TM co-doped SnO_2.

Fe and Ni co-doped SnO_2 samples were synthesized using sol-gel method. $SnCl_2 \cdot H_2O$, metallic Fe and Ni solutions were mixed and then condensed at 80 ℃ and calcinated at 250 ℃ for 2 h, finally annealed 550 ℃ in air for 4 h. The obtained nanoparticles became a white-brown color with increasing TM concentration.

For the Fe or Ni single-ion doped SnO_2, no clear hysteresis loop was observed by vibrating sample magnetometer (VSM) at room temperature. On the other hand, for the Fe and Ni co-doped SnO_2, hysteresis with 500 Oe of coercive filed H_c was observed. With increasing Fe concentration, the M_s was enhanced.

Mössbauer spectra for the Fe and Ni co-doped SnO_2 are shown in Fig. 1. The spectra consist of two kinds of doublets (D1, D2), the sextets (S1, S2), and a broad magnetic relaxation component (R1). The values of the isomer shift (IS) in all components were almost 0.3 mm/s, which suggests Fe^{3+} states. D1 originates from the substitution of Fe in the Sn site. D2 is assigned as the presence of oxygen vacancies around the Fe ions, which is brought about by the large QS and small IS. Sextet peaks are derived from the magnetic ordering. With increasing Fe concentrations, the peak intensity of S1 increases. An internal field of about 50 T is estimated, which is almost consistent with the results obtained for Fe-doped SnO_2 [4]. S1 origineted from the magnetization for the substitution of Fe ion. On the other hand, a S2 component with a hyperfine field of 51 T and QS of -0.2 mm/s appears over 3% Fe doping. The Mössbauer parameters of the S2 component are quite similar to those of hematite, suggesting that antiferromagnetic α-Fe_2O_3 or ferromagnetic γ- Fe_2O_3 segregations occur. However in the case of 5% Fe doping, the intensity of S2 component decreases. The broad R1 components represent the spin relaxation within the detection time of 10^{-7} sec in Mössbauer spectrometry. For less than 5% of Fe doping, the R1 component is needed for the fitting. The presence of R1 is related to the polarons induced by spin interaction between magnetic defects and Fe^{3+} ions. With an increase in the Fe concentration, S1 is enhanced, which is related to the enhancement of M_s in VSM.

In the presentation, we will discuss the magnetic and electronic properties depending on the Fe and TM concentrations using Mössbauer spectrometry and X-ray absorption spectroscopy [5,6].

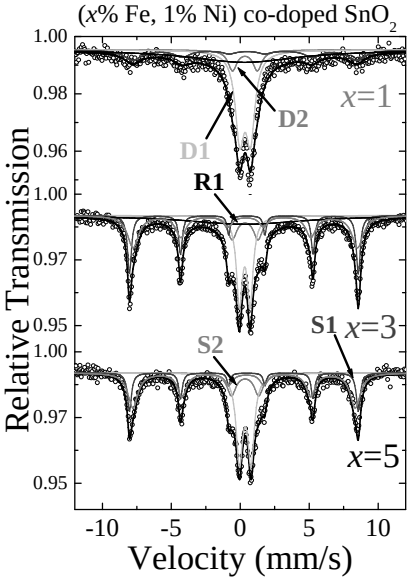

Fig. 1 : Mössbauer spectra of *x*% Fe and 1% Ni co-doped SnO_2.

References

1. J. M. D. Coey, M. Venkatesan, and C. B. Fitzgerald, Nature Mat. **4**, 173 (2005).
2. A. Punnoose, J. Hays, A. Thurber, M. H. Engelhard, P. K. Kukkadapu, C. Wnag, V. Shutthanandan, and S. Thevuthasan, Phys. Rev. B **72**, 054402 (2005).
3. P. I. Archer, P. V. Radovanovic, S. M. Heald, and D. R. Gamelin, J. Am. Chem. Soc. **127**, 14479 (2005).
4. K. Nomura, C. A. Barrero, J. Sakuma, and M. Takeda, Phys. Rev. B **75**, 184411 (2007).
5. K. Nomura, J. Okabayashi, K. Okamura, and Y. Yamada, J. Appl. Phys. **110**, 083901 (2011).
6. J. Okabayashi, S. Kono, Y. Yamada, and K. Nomura, Jpn. J. Appl. Phys. **51**, 023003 (2012).

Session 6(T10) Oral-3

EMISSION MÖSSBAUER SPECTROSCOPY OF GRAIN BOUNDARIES

V.V. Popov[1]
[1] *Institute of Metal Physics, Ural Branch of RAS, S. Kovalevskaya str., 18, Ekaterinburg, Russia*

This study analyzes capabilities of application of emission nuclear gamma-resonance (NGR) spectroscopy for investigation of grain boundaries (GB) and its advantages compared to absorption NGR technique.

The main drawback of the absorption NGR spectroscopy is its relatively low sensibility, which makes it practically impossible to use this method for GB studies in coarse-grained materials where the volume fraction of GBs is very small. A method of GB studies in polycrystals based on combination of the phenomenon of accelerated diffusion along GB with the emission Mössbauer spectroscopy was suggested in [1]. In this case a radionuclide is deposited on a polycrystalline specimen surface. Then the specimen is annealed at temperatures when the volume diffusion is frozen ($\sim 0.2T_m$), and at such annealing the Mössbauer atoms are localized in GBs. After the first annealing a Mössbauer spectrum is taken, and then the specimen is annealed at higher temperatures, and after every annealing the spectrum is taken again. GBs in a number of transition and precious metals were studied by this method, and it was found that at all the annealing temperatures there were two components in the Mossbauer spectra (Fig. 1).

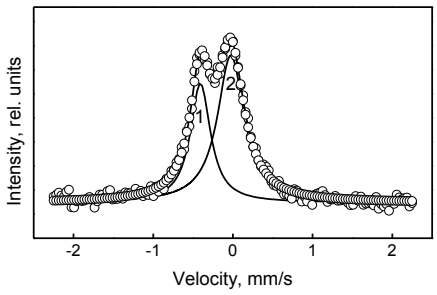

Figure 1. Emission Mössbauer spectrum of $^{57}Co(^{57}Fe)$ in polycrystalline Cu annealed at 373 K

It was difficult to explain this phenomenon based on the available models of grain-boundary diffusion. Recently a specified model of grain-boundary diffusion was suggested [2], according to which component 1 is formed by atoms localized in GBs and component 2 by atoms in monatomic near-boundary layers. In the treatment of NGR spectroscopy data based on this model one can determine the grain-boundary diffusion mechanism, segregation factor, local Debye temperatures, effective diffusion coefficient in near-boundary areas, segregation of impurity atoms, etc.

In case of nanocrystalline materials, in which the GB fraction is high, it is possible to apply the absorption NGR spectroscopy, and in most of the available publications on such materials this method was applied. However, in this case certain difficulties in distinguishing of GB components emerge as well, and they are analyzed in detail in [3]. In particular, for the absorption Mössbauer experiments to be performed, the iron content has to be rather high, resulting in solute - solute interactions and magnetic ordering phenomena. Hence, the results of absorption NGR studies of grain boundaries are often debatable.

Application of the emission Mössbauer spectroscopy for nanocrystalline materials also involves difficulties since heat treatments are required to transfer the Mossbauer atoms to GBs, but at annealing GBs may migrate and their structure may change because of low thermal stability of such materials. Nevertheless, we demonstrated considerable potentials of the emission NGR spectroscopy for the studies of GBs in nanocrystalline materials [4]. For instance, three components were found in the spectra taken from nanocrystalline Au obtained by gas condensation (Fig 2), two of which (components 1 and 3) are formed by atoms located at internal interfaces and another one (component 2) by atoms localized in near-boundary areas. As demonstrated by the analysis of this spectrum, component 1 is formed by atoms located at boundaries of nanocrystallites and component 2 by those at boundaries of agglomerates formed of nanoparticles.

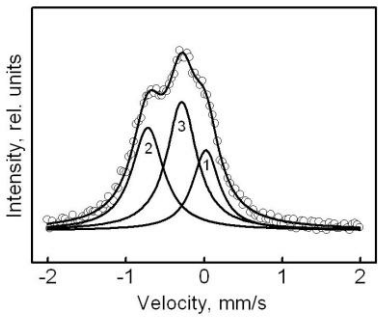

Figure 2. Emission Mössbauer spectrum of $^{57}Co(^{57}Fe)$ in nanocrystalline Au annealed at 423 K

Investigation of non-equilibrium grain boundaries in metals obtained by severe plastic deformation (SPD) reveals distinctions in hyperfine parameters of GB spectra of such materials from those in coarse-grained materials with equilibrium boundaries. It is demonstrated that these studies enable to judge on the degree of non-equilibrium state of GBs in such materials and on changes of their physical properties at heating before the GB migration starts.

The work has been done with partial support of RFBR (project No. 10-03-00530)

[1] V.N. Kaigorodov and S.M. Klotsman, Pisma v JETF. **28** (1978) 386.
[2] V.V. Popov, Solid State Phenomena. **138** (2008) 133.
[3] G. Rixecker, Solid State Comm. **122** (2002) 299.
[4] V.V. Popov. Structure and properties of grain boundaries / Chapter 3 in Current Trends in Chemical Engineering. Editor: J.M.P.Q. Delgado. Studium Press LLC. 2010.

ROOM TEMPERATURE FEROMAGNETISM OF $CoFe_{2-x}Cu_xO_4$ NANOPARTICLES

Khalid Mujasam batoo.
King Abdullah Institute for Nanotechnology, King Saud University, P.O. Box 2460, Riyadh,

11451-Saudi Arabia

Abstract

Ferrimagnetic oxides may contain single or multi domain particles and they convert into superparamagnetic state near a critical size. To explore the existence of these particles CoFe2-xCuxO4 mixed ferrite nanoparticles of different sizes were prepared through citrate-gel method. The structural aspects of the samples were explored by a wide variety of experimental techniques namely, X-ray diffraction, field emission transmission electron microscopy, vibrational sample magnetometery and Mössbauer spectroscopy. The magnetic and Mössbauer properties were strongly dependent on size. The saturation magnetization (Ms) increased with the growth of the grain size while the coercitivity decreased. The saturation magnetization (Ms) was found quite high between 35.606 emu/g to 64.35 emu/g. Magnetization data reveal the presence of room temperature ferromagnetism (RTFM).

[1]. T.Dietl, H. ohno, F. Matsukura, J. Cibert, D. Ferrand, Science 287 (2000) 1019.
[2]. K. Sato, H. Katayama-Yoshida, Jpn. J. Appl. Phys. Part 2 39 (2000) L555.
[3]. M. Venkateshan, C.B. Fitzgerald, J.G. Lunney, J.M. D. Coey, Phys. Rev. Lett. 93 (2004) 177206.
[4]. S. Yin, M. X. Xu, L. Yang, J.F. Liu, H. Rosner, H. Hahn, H. Gleiter, D. Shild, S. Doyle, T. Liu, T.D. Hu, E. Takayama-Muromachi, J.Z. Jing, Phys. Rev. B 73 (2006) 224408.

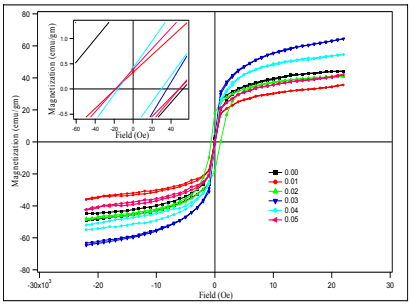

Figure 1. Hysterisses curve at RT.

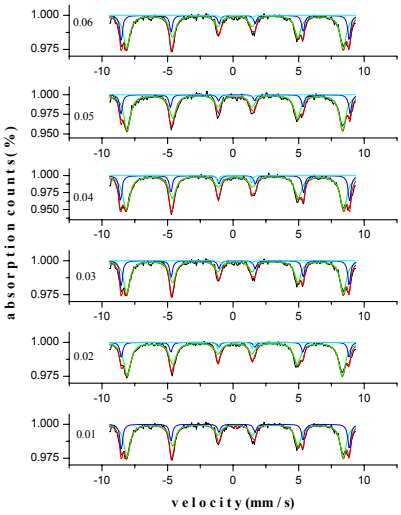

Figure 2. RT Mossbauer spectra

Session 6(T10) I-13

POLYMORPHOUS TRANSITIONS OF NANOMETRIC Fe_2O_3 BY VIEW OF MÖSSBAUER SPECTROSCOPY

L. Machala[1], J. Tuček[1], and R. Zboril[1]

[1] *Regional Centre of Advanced Technologies and Materials, Palacký University in Olomouc, Šlechtitelů 11, 78 371 Olomouc, Czech Republic*

Each of the four different known crystalline Fe_2O_3 polymorphs (alpha, beta, gamma, and epsilon-Fe_2O_3) has unique biochemical, magnetic, catalytic, and other properties that make it suitable for specific industrial applications. High temperature treatment is a key step in most syntheses of iron(III) oxides, but often induces polymorphous transformations that result in the formation of undesired mixtures of Fe_2O_3 polymorphs. On the other hand controlled polymorphous transformation can be use as a method to get given polymorph. It is therefore important to control the parameters that induce polymorphous transformations when finding routes to prepare given Fe_2O_3 polymorph as a single phase. The dependence of the mechanism and kinetics of the polymorphous transformations of Fe_2O_3 on the intrinsic properties of the material and external parameters of synthetic and/or natural conditions such as temperature, atmosphere, and pressure are discussed. In addition, the question of whether different Fe_2O_3 polymorphs are formed sequentially or simultaneously during thermal processes is discussed. ^{57}Fe Mössbauer spectroscopy presents a powerful experimental tool for unambiguous identification of each ferric oxide polymorph irrespective of particle size and crystallinity. In this context, Mössbauer spectra and their typical hyperfine parameters at various temperatures are introduced for individual Fe_2O_3 polymorphs. Finally, particular solid-state syntheses of ferric oxide based nanomaterials, they characterization and industrial applications are presented.

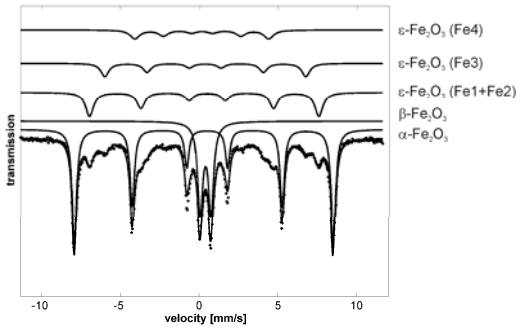

Figure 1. Mössbauer spectrum of sample, which contains α-Fe_2O_3, β-Fe_2O_3 and ε-Fe_2O_3

[1] L. Machala, J. Tuček, R. Zboril, Chem. Mater. 23(14) (2011) 3255-3272.
[2] L. Machala, R. Zboril, A. Gedanken, J. Phys. Chem. B (2007) 4003-4018.

NEW SENSORS BASED ON THERMO AND PHOTOSWITCHABLE IRON(II) SPIN CROSSOVER MATERIALS

Y. Garcia[1]

[1]*Université Catholique de Louvain, Institute of Condensed Matter and Nanosciences, MOST – Inorganic Chemistry, Place L. Pasteur 1, 1348 Louvain-la-Neuve, Belgium. Email: yann.garcia@uclouvain.be*

Iron(II) spin crossover (SCO) materials belong to an attractive class of switchable functional solids with spin state that can be reversibly triggered by temperature, pressure or electromagnetic radiation,[1] and that can be tracked by numerous physical techniques including ^{57}Fe Mössbauer spectroscopy [2] and muon spin relaxation [3]. Although the origin of the SCO phenomenon is molecular, its cooperative manifestation depends on an efficient coupling between active magnetic species in the crystal lattice through covalent and supramolecular interactions [4].

In this context, iron(II) 1,2,4-triazole 1D coordination polymers have attracted great interest as their abrupt spin transition (ST) is generally associated to both hysteretic and spectacular thermochromic effects, thus providing a basis for their potential use in thermal display, memory devices and sensors [5]. Various applications were proposed ranging from smart bank cards and temperature overheating alert systems [6], cold channel tracking sensors [7] and more recently functional paints. The nature of intrachain interactions can be mediated by the triple ligand bridge between iron centres and intramolecular H-bonding in some cases. Interchain interactions are also to be considered in these materials [8], but the role of the anionic sublattice dynamics on the ST mechanism of these compounds, which was probed by ^{119}Sn Mössbauer spectroscopy, is not to be neglected too [7] to tune their magnetic properties. Gas sensing associated to a colour and spin state change is also another appealing facet of these functional materials [6].

Size reduction as well as an effective deposition on suitable surfaces is desirable for implementation of SCO materials into devices. In a unique approach under green technology, we recently introduced an inner epidermis of onion bulb (*Allium cepa*) [9] as a novel support to grow single crystals of desired size and for thin film processing of SCO materials. This radical approach differs from the classical one using conventional supports like glass, quartz, Si-wafer and so on. As a proof of concept, we selected an illustrious thermochromic iron(II) complex, $[Fe(1\text{-propyl-tetrazole})_6](BF_4)_2$ (**1**), whose thermally and light-induced spin transition has been very well documented [e.g. 1]. Non-conventional method of 'seeding' and capillary deposition as well as dip coating were employed for crystal growth and thin film processing of **1**, which was probed by AFM on both abaxial and adaxial sides of the membrane [10]. The nature of the deposition was explained thanks to a detailed ^{57}Fe Mössbauer investigation [11].

Unprecedented photomagnetic properties at room temperature were recorded for the photochromic coordination complex $[Fe(BM\text{-}4TP)_2(NCS)_2\cdot 2MeOH$ including a diarylethene ligand, whose origin were explained thanks to ^{57}Fe Mössbauer spectroscopy at variable temperature [12]. More recently, we have revisited the optical-structural properties relationship for *N*-salicylidene N-heterocycles derivatives affording a new range of solid state thermochromic and photochromic switches operating at room temperature [13]. These molecules were included in mononuclear coordination complexes as a proof of concept [14] as well as in oligomeric SCO complexes [15,16]. For the dinuclear iron(II) complex, $[Fe_2(Hsaltrz)_5(NCS)_4]\cdot 4MeOH$, with Hsaltrz = *N*-salicylidene-4-amino-1,2,4-triazole [16], the abrupt ST phenomenon occurring at ~ 150 K could be tracked by temperature dependence fluorescence spectroscopy for the first time in the crystalline state, thus opening new sensing perspectives, e.g. in thermometry.

We acknowledge financial support from FRFC-FNRS.

[1] P. Gütlich, Y. Garcia, H. Spiering, Magnetism: From Molecules to Materials IV, Wiley-VCH 8 (2003) 271.
[2] (a) P. Gütlich, Y. Garcia, J. Phys. Conf. Ser., 217 (2010) 012001. (b) P. Gütlich, Y. Garcia, Eds. Y. Yoshida, G. Langouche, Springer (2012, in press).
[3] Y. Garcia, S. J. Campbell, J. S. Lord, P. Gütlich, Inorg. Chim. Acta 361 (2008) 3577.
[4] Y. Garcia, V. Niel, M. C. Muñoz, J. A. Real, Top. Curr. Chem. 233 (2004) 229.
[5] Y. Garcia, V. Ksenofontov, P. Gütlich, Hyperfine Interact. 139/140 (2002) 543
[6] Y. Garcia, P. J. van Koningsbruggen, E. Codjovi, R. Lapouyade, O. Kahn, L. Rabardel, J. Mater. Chem. 7 (1997) 857.
[7] Y. Garcia, V. Ksenofontov, S. Mentior, M. M. Dîrtu, C. Gieck, A. Bhatthacharjee, P. Gütlich, Chem. Eur. J. 14 (2008) 3745.
[8] M. M. Dîrtu, C. Neuhausen, A. D. Naik, A. Rotaru, L. Spinu, Y. Garcia, Inorg. Chem. 49 (2010) 5723.
[9] J. Schönherr, J. Expt. Botany 57 (2006) 1.
[10] A. D. Naik, L. Stappers, J. Snauwaert, J. Fransaer, Y. Garcia, Small 6 (2010) 2842.
[11] A. D. Naik, Y. Garcia, Hyperfine Interact. (2012, in press).
[12] Y. Garcia, V. Ksenofontov, R. Lapouyade, A. D. Naik, F. Robert, P. Gütlich, Opt. Mater. 33 (2011) 942.
[13] (a) F. Robert, A. D. Naik, B. Tinant, R. Robiette, Y. Garcia, Chem. Eur. J. 15 (2009) 4327. (b) F. Robert, A. D. Naik, F. Hidara, B. Tinant, R. Robiette, J. Wouters, Y. Garcia, Eur. J. Org. Chem. (2010) 621.
[14] F. Robert, A. D. Naik, B. Tinant, Y. Garcia, Inorg. Chim. Acta 380 (2012) 104.
[15] (a) F. Robert, A. D. Naik, Y. Garcia, J. Phys. Conf. Ser. 217 (2010) 012031. (b) F. Robert, A. D. Naik, Y. Garcia, Möss. Eff. Data Ref. J. 34 (2011) 200.
[16] Y. Garcia, F. Robert, A. D. Naik, G. Zhou, B. Tinant, K. Robeyns, S. Michotte, L. Piraux, J. Am. Chem. Soc. 133 (2011) 15850.

Session 8(T13) I-15

SURFACE STUDIES IN ULTRATHIN BINARY IRON OXIDE FILMS: ANCIENT MATERIALS, NEW OPPORTUNITIES

M. Monti[1], J. de la Figuera[1], and J.F. Marco[1]
[1]*Instituto de Química Física "Rocasolano", CSIC. Serrano 119, 28006 Madrid. Spain.*

Binary iron oxides (FeO, Fe_3O_4, γ-Fe_2O_3, α-Fe_2O_3) are well-known compounds. From the Mössbauer spectroscopic point of view they have been extensively studied and an overwhelming amount of information is available in the literature both for the bulk materials as for other forms of these materials (for example, nanoparticles). The properties of these oxides in ultrathin films (a few atomic layers thick), however, have not been studied at too much extent. This is mainly due to the difficulties of (i) handling ultra high conditions to avoid sample contamination and/or deterioration and (ii) dealing with a small number of atoms where sample enrichment in ^{57}Fe is compulsory. The recent communication of the interesting catalytic activity of FeO for CO oxidation [1], as well as the potential application of Fe_3O_4 and γ-Fe_2O_3 in spintronic devices, have boosted the interest in studying these oxides in ultrathin film form [2]. The use of Mössbauer spectroscopy in this type of studies has been, nevertheless, limited.

Relevant aspects in the investigation of these type of systems as, for example, the influence of the fabrication parameters on the structural, chemical and magnetic properties of these compounds, the conditions under which these oxides can be oxidized or reduced to obtain a different phase or the influence of thickness on their magnetic properties (e.g. spin re-orientation transitions), need to be studied in order to obtain the knowledge required for these materials to be used in the above-mentioned applications.

In this talk we will review some of the recent studies on the applications of Conversion Electron Mössbauer Spectroscopy to this kind of systems and will show how the use of complementary surface imaging and spectroscopic techniques can help to understand the growth of the various oxides on Ru (0001) as well as to follow the transformations occurring among them when the thin layers deposited are exposed to NO_2-controlled atmospheres. We will also discuss briefly on our recent activity in building an Integral Low Energy Electron Spectrometer (ILEEMS) and its ability to study thin layers of iron-containing materials.

[1] B. Quiao, A. Wang, X. Yang, L.F. Allard, Z. Jiang, Y. Cui, J. Liu, J. Li and T. Zhang, Nature Chemistry **3**, 634-641 (2011).
[2] M. Bibes, J.E. Villegas and A. Barthélémy, *Advances in Physics* **60**, 5-84 (2011).

APPLICATION OF MÖSSBAUER SPECTROSCOPY ON CORROSION PRODUCTS OF NNP

J.Dekan[1], J.Lipka[1] and V.Slugeň[1]
[1]*Institute of Nuclear and Physical Engineering, Faculty of Electrical Engineering and Information Technology, Slovak University of Technology, Bratislava, Slovakia*

Steam generator (SG) is generally one of the most important components at all nuclear power plants (NPP) with close impact to safe and long-term operation. Material degradation and corrosion/erosion processes are serious risks for long-term reliable operation. Steam generators of four VVER-440 units at nuclear power plants V-1 and V-2 in Jaslovske Bohunice (Slovakia) were gradually changed by new original "Bohunice" design in period 1994-1998, in order to improve corrosion resistance of SGs.

Corrosion processes before and after these design and material changes in Bohunice secondary circuit were studied using Mössbauer spectroscopy during last 25 years. Innovations in the feed water pipeline design as well as material composition improvements were evaluated positively. Mössbauer spectroscopy studies of phase composition of corrosion products were performed on real specimens scrapped from water pipelines or in form of filters deposits. Newest results in our long-term corrosion study confirm good operational experiences and suitable chemical regimes (reduction environment) which results mostly in creation of magnetite (on the level 70% or higher) and small portions of hematite, goethite or hydrooxides.

Regular observation of corrosion/erosion processes is essential for keeping NPP operation on high safety level. The output from performed material analyses influences the optimisation of operating chemical regimes and it can be used in optimisation of regimes at decontamination and passivation of pipelines or secondary circuit components. It can be concluded that a longer passivation time leads more to magnetite fraction in the corrosion products composition.

Session 8(T13) Oral-6

MOSSBAUER SPECTROSCOPY OF FROZEN SOLUTIONS FOR STEPWISE CONTROL IN PREPARATION OF BIOCOMPATIBLE HUMIC-STABILIZED FEROXYHYTE NANOPARTICLES

A.Polyakov[1], T.Sorkina[2], A.Goldt[1], D.Pankratov[2], I.Perminova[2] and E.Goodilin[1, 2]
[1]*Faculty of Material Science, Lomonosov Moscow State University, Moscow, Russia*
[2]*Faculty of Chemistry, Lomonosov Moscow State University, Moscow, Russia*

Iron oxide and oxyhydroxide magnetic nanoparticles have widespread biomedical application because of their usefulness as contrast agents for magnetic resonance imaging, colloidal mediators for magnetic hyperthermia, cell separation, drug delivery, etc. [1]. Aggregation is a serious problem in the preparation and storage of such magnetic nanoparticles limiting considerably their practical application. This problem is usually solved by a surface modification of nanoparticles with organic macromolecules [2]. A whole number of commercial and experimental biocompatible preparations based on magnetic nanoparticles are prepared by one-pot techniques directly into solution of stabilizers, which serve to limit the magnetic core growth and to stabilize via steric and electrostatic repulsions the nanoparticles dispersion in aqueous medium [3]. However, it's very complicated to control the formation of required magnetic phase during such one-pot preparation especially in the case of iron oxides which are inclined to numerous interphase transformations.

Mossbauer spectroscopy has been extensively used for the investigation of frozen aqueous solutions (FAS) [4]. This technique is highly effective for studying of intermediates in synthesis of iron compounds.

In the present work Mossbauer spectroscopy of FAS was suggested for the stepwise control in synthesis of magnetic feroxyhyte (δ′-FeOOH) nanoparticles stabilized *in situ* by humic substances (HS). HS (natural polyelectrolytes) are usually used as stabilizers to prevent nanoparticle agglomeration and precipitation. For example, HS have been applied as an effective stabilizing agent for iron oxide nanoparticles [5].

One-pot synthesis of feroxyhyte nanoparticles involved rapid oxidation of $FeCl_2$ solution at pH 8 by 30% H_2O_2 in presence of potassium humate. A set of aliquots was taken from reaction mixture at different stages of synthesis, rapidly frozen by immersion into liquid nitrogen and studied by transmission Mossbauer spectroscopy for identification of intermediates formed. Final feroxyhyte nanoparticles were also characterized by XRD, TEM, magnetic measurements and cytotoxicity test.

According to spectra obtained, ultradispersed $Fe(OH)_2$ was formed from $FeCl_2$ solution in alkali medium before oxidation and stabilized by humic macromolecules, whereas no complex formation between ferrous ions and HS was registered. Rapid oxidation of $Fe(OH)_2$ with 30% H_2O_2 plays significant role in the synthesis and leads to direct formation of feroxyhyte (δ′-FeOOH), while slower oxidation results in a number of impurities (e.g. γ-FeOOH, β-FeOOH). TEM images show that the feroxyhyte nanoparticles obtained represent nanoflakes with the size along the largest axis about 20 nm and thickness 2-3 nm (Fig. 1). According to Mossbauer spectra registered at different temperatures (Fig. 2), humic-stabilized δ′-FeOOH nanoparticles are found to be superparamagnetic at room temperature. Hyperfine parameters of the nanoparticles at 5K are given in Table I; two sub-spectra identified for this sample were ascribed to surface and bulk iron atoms. The MTT-tests on fibroblasts show that the nanoparticles are not cytotoxic. The results obtained show evident efficiency of Mossbauer spectroscopy of FAS for controlled one-pot preparation of biocompatible magnetic nanoparticles.

Table I: A hyperfine parameters of the humic-stabilized feroxyhyte nanoparticles at 5K.

Sample	δ	Δ mm/s	Γ_{exp}	H_{in}, kOe	S, ±0.05 %
δ′-FeOOH-	0.50	-0.08	0.73	507.1	60
HS	0.48	-0.08	0.91	463.3	40

[1]*δ - isomer shift relative to α-Fe, Δ - quadruple splitting, H_{in}- internal magnetic field (Oe)*

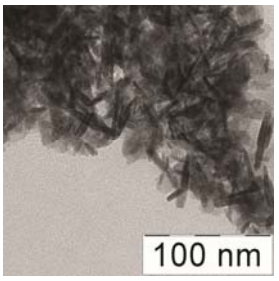

Figure 1. TEM image of humic-stabilized feroxyhyte nanoparticles.

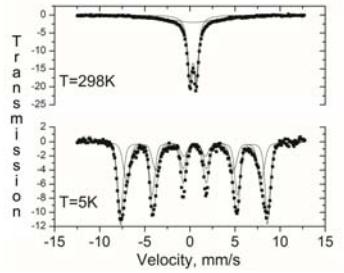

Figure 2. Mossbauer spectra of humic-stabilized feroxyhyte nanoparticles registered at room and liquid-helium temperatures.

[1] A.Figuerola, et al., Pharm. Res. 62 (2010) 126–143
[2] S.Mornet, et al., J. Mater. Chem. 14 (2004) 2161–2175
[3] J.Park, et al., J. Mater. Chem. 19 (2009) 6412–6417
[4] S.Morup, et al., J. Chem. Phys. 65 (1976) 536-543
[5] A.E.Chekanova, T.A.Sorkina et al., Mendeleev Commun. 19 (2009) 72-74

MÖSSBAUER SPECTROSCOPY STUDY OF THE IRON ACTIVE SITES IN ZEOLITES FOR N_2O DECOMPOSITION

E. Tabor*, Z. Sobalík

J. Heyrovský Institute of Physical Chemistry, Academy of Sciences of the Czech Republic
Dolejškova 2155/3 182-23 Prague 8, Czech Republic
**Corresponding author: edyta.tabor@jh-inst.cas.cz*
Phone number: +420 266 053 535; FAX: +420+ 420 286 582 307

Iron ferrierites (Fe-FER) are known as catalysts for decomposition of nitrous oxide. It is assumed that Fe-FER ─ N_2O system could provide the solution for the environmentally relevant problem of eliminating of harmful nitrous oxide that strongly contributes to the greenhouse effect [1-3]. Despite the apparent simplicity of the reaction that takes place during N_2O decomposition over various iron zeolites, mechanistic details of this process have not been completely characterised. It is suggested that the main role in this process play the Fe ions in cationic positions [1,4]. Therefore, this contribution is focused on the identification of Mössbauer parameters of Fe sited in cationic positions, which can be further, apply for determination of the reactivity of Fe species in N_2O decomposition.

A series of Fe-FER with Fe/Al < 0.1 were prepared by impregnation of NH_4-FER by actetylacetone solution of $^{57}FeCl_3$ [1]. This method makes possible introduction the Fe ions into cationic positions. FTIR and UV-Vis spectroscopy were used to check the location of Fe ions in Fe-FER. Catalytic activity of Fe-FER in N_2O decomposition was carried out in batch reactor. Both the Mössbauer and *in-situ* FTIR spectroscopies were used as main methods for monitoring the nature of Fe species as well as their behavior under oxidized conditions. Mössbauer spectra were acquired under vacuum at RT after: (a) evacuation at 450 °C for 3 h, (b) evacuation at 450 °C for 3 h, followed by O_2 at 450 °C adsorption (c) evacuation at 450 °C for 3 h, followed by adsorption of N_2O at 280 °C. FTIR measurements were performed during the interaction of the evacuated sample (450 ˚C for 3 h) with N_2O at 280 ˚C for various interaction times.

Catalytic results have shown that in spite of low Fe loading in FER all samples exhibited high N_2O conversion. UV-Vis and FTIR measurements of evacuated samples confirmed absence of Fe oxide species and location of Fe ions in cationic positions.

By Mössbauer spectroscopy of Fe-FER with low content of iron and well-defined composition the Mössbauer parameters of Fe ions in α and β cationic sites. Moreover, thanks to high sensitivity of the Mössbauer spectroscopy, the two types of β sites (β_1 and β_2) were distinguished. In Fe-FER with Fe/Al lower than 0.036 iron was exclusively present as Fe(II) and located in α and β cationic positions. In the samples with Fe/Al 0.018 and 0.036 the population of β sites was 83 % and 75 %, respectively. At higher iron content (Fe/Al 0.072), Fe(III) was present as well (27 %); Fe(II) ions were equally distributed between α and β sites.

The reactivity of Fe species in Fe-FER was checked by interaction with O_2 or N_2O. Mössbauer spectra of all investigated samples treated by O_2 led to the oxidation of about the same proportion of the Fe cations, i.e. presenting about 20% of the Fe(II) present in the samples. These results clearly suggest that only part of the iron located in cationic positions could be transformed into oxidized form by molecular oxygen. It further confirmed higher resistance of β sites to O_2 oxidation. On the other hand, nearly total transformation of Fe(II) to Fe(III) was observed after oxidation by N_2O at 280 ºC. On the Mössbauer spectrum of Fe-FER after N_2O interaction the relaxation component was appeared, which characterized the paramagnetic hyperfine interaction and indicates a change in the microenvironment of Fe species after N_2O treatment. The presence of this component can be assigned to formation of Fe-NO_x species.

Analysis of FTIR spectra after N_2O adsorption at 280 ºC showed that after short interaction time Fe-O species are formed. But, with an increasing of interaction time of N_2O with Fe-FER, the amount of Fe(III)-NO_x species increases with simultaneous decreasing of the amount of Fe(III)-O, in agreement with the sequence: Fe(II) → Fe(III)-O → Fe(III)-NO_x.

The studied Fe-FER samples with Fe/Al < 0.1 provide a standard for reliable establishing of Mössbauer parameters of iron cations in α and β cationic positions. Moreover, Mössbauer spectroscopy brings the first experimental support for the presence of two types of β sites in Fe-FER. Recently, based on experimental results (FTIR, UV-VIS, MBS) supported by DFT calculation was shown that iron cations in Fe-FER are preferably located in β cationic positions [1, 5]. It is suggested that part of Fe(II) in β sites is located in adjacent positions across the FER channel. Because the majority of Fe(II) is located in β positions, as evidenced by Mössbauer spectroscopy, it is possible that the observed nitrates are primarily bridged between two Fe(II) ions located in adjacent β positions. Once formed Fe-NO_x species were stable during the subsequent N_2O decomposition and enhanced the reaction rate.

References

[1] K. Jisa, J. Novakova, M. Schwarze, A. Vondrova, S. Sklenak, Z. Sobalik, J. Catal. 262 (2009) 27-34.
[2] K.A. Dubkov, N.S. Ovanesyan, A.A. Shteinman, E.V. Starokon,G.I. Panov, J. Catal. 207 (2002) 341-352.
[3] G.D. Pirngruber,P.K. Roy, Catal.Today 110 (2005) 199-210.
[4] E. Tabor, K. Zaveta, N.K. Sathu, A. Vondrova, P. Sazama, Z. Sobalik, Catal.Today 175 (2011) 238-244.
[5] E. Tabor, K. Zaveta, N.K. Sathu, Z. Tvaruzkova,Z. Sobalik, Catal.Today 169 (2011) 16-23.

Session 9(T1) I-17

ACCURATE PREDICTION OF ^{57}FE MöSSBAUER PARAMETERS VIA DENSITY FUNCTIONAL THEORY: PREDICTION OF REACTION INTERMEDIATES AND CATALYTIC CYCLES OF IRON ENZYMES

Jorge H. Rodriguez[1]

[1]*Theoretical and Computational Biomolecular Physics Group, Department of Physics, Purdue University, West Lafayette IN 47907, USA*

Computational methods of electronic structure can predict the electron density, $\rho(\mathbf{r})$, at the site of ^{57}Fe nuclei ($\mathbf{r} = 0$) and, therefore, Mössbauer isomer shifts (δ_{Fe}). In addition, one can predict electric field gradient tensors and quadrupole splittings (Δ_{EQ}). We report the implementation of a computational methodology for the accurate prediction of Mössbauer spectral parameters via spin density functional theory (SDFT). Given the crystallographic structure, the method can be applied to any molecular or biomolecular system and, in addition to predicting spectral parameters, allows the microscopic interpretation of experimental spectra. Herein, we use SDFT to predict and elucidate complex spectra (Figure 1) of antiferromagnetic binuclear iron proteins (Figure 2). We also describe the phenomenological simulation of spectra of antiferromagnetic diiron centers based on the use of spin Hamiltonians with a leading Heisenberg term, $J\mathbf{S}_1 \bullet \mathbf{S}_2$, where $\mathbf{S}_1$ and $\mathbf{S}_2$ are the intrinsic spin operators of each iron site.[1-3]

M□ssbauer spectra of spin-coupled diiron proteins, recorded as a function of applied magnetic field (Figure 1) and temperature, are highly informative but difficult to interpret. We have combined the use of phenomenological spin Hamiltonians and spin density functional theory [2] to predict and interpret spectroscopic parameters of several antiferromagnetic binuclear iron proteins. In particular, we have predicted Mössbauer parameters of methane monooxygenase hydroxilase (MMOH), an enzyme that catalyzes the conversion of methane to methanol.[4] In addition, by incorporating the effects of spin-orbit coupling (SOC) via perturbation theory (PT) on top of conventional SDFT calculations, we predict with a high degree of accuracy the zero-field splittings (ZFS) of the iron centers. This

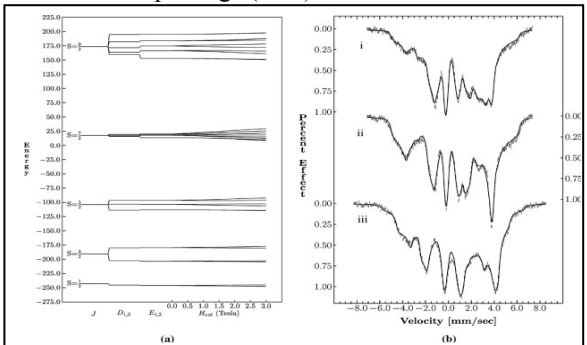

Figure 1. (a) Energy levels of the antiferromagnetic diiron protein uteroferrin (Ufr) obtained from diagonalization of a spin Hamiltonian. [1] The ground doublet (S = 1/2) and higher spin multiplets are shown as the Heisenberg exchange, zero field splitting (ZFS), and Zeeman interactions are turned on. (b) Spectra recorded at 4.2K under variable external fileds.[1]

SDFT-PT methodology allows us to establish a direct relationship between electronic structure, geometric structure, and ZFS parameters. Finally, we describe the prediction of geometric structures of reaction intermediates in catalytic cycles of iron enzymes using Mössbauer parameters as a reference.[4]

Supported, in part, by National Science Foundation (NSF) award CHE-0349189 (J.H.R.)

[1] J.H. Rodriguez in *Quantum Biochemistry*, Ed. by C.F. Matta, Wiley-VCH Verlag GmbH & Co. KGaA, Weinheim, Germany (2010) 537.
[2] J.H. Rodriguez et al., J.Am.Chem.Soc. 121 (1999) 7846.
[3] J.H. Rodriguez *et al*., J. Phys. Chem. **100** (1996) 6849.
[4] T. Chachiyo and J.H. Rodriguez, Dalton Trans. **41**, (2012) 995.

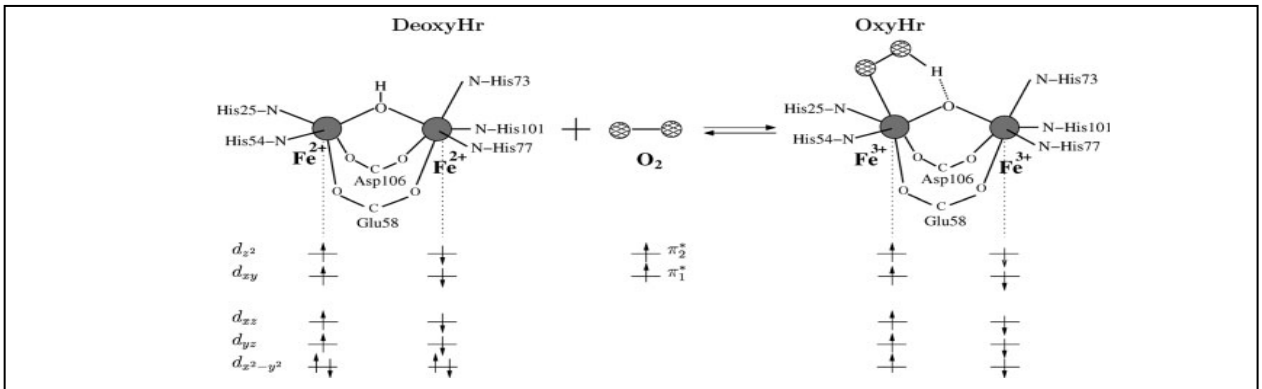

Figure 2. DeoxyHr, an oxygen transporting protein, has an antiferromagnetic binuclear where the unpaired electrons of one ferrous ion are antiparallel to those of the other. This gives rise to an open-shell singlet ground state. Upon binding to the triplet ground state of O_2 the protein cycles to the oxidized state (OxyHr), where the unpaired electrons of one ferric ion are antiparallel to those of the other, also giving rise to an open-shell singlet.[1] The antiferromagnetic interaction between the irons is described by the Heisenberg operator $J\mathbf{S}_1 \bullet \mathbf{S}_2$.[1,2,3]

MÖSSBAUER STUDIES OF MATERIALS USED TO IMMOBILISE INDUSTRIAL WASTE

S.D.Forder[1], P.A.Bingham[1], R. J. Hand[2], M. C. Stennett[2] and N. C. Hyatt[2]
[1] *Materials and Engineering Research Institute, Sheffield Hallam University, Howard Street, Sheffield, S1 1WB, UK*
[2] *Immobilisation Science Laboratory, Department of Material Science and Engineering, University of Sheffield, Mappin Street, Sheffield, S1 3JD, UK*

Today's society produces toxic wastes ranging from nuclear wastes, with various levels of activity, to incinerator ashes such as sewage sludge ash which contains harmful heavy metals. The harmful nature of some components of these wastes means that safe immobilisation can be necessary. Methods have been, and are being, developed to immobilise these wastes. Vitrification is used in the UK to immobilise high level liquid waste (HLLW) from nuclear fuel reprocessing. The study and development of suitable methods and materials to immobilise waste is the focus of the work reported in this paper. ^{57}Fe Mössbauer spectroscopy has been used during these studies to identify the valence state and coordination of iron in glasses and ceramics.

A material designed to immobilise waste requires structural stability, compositional flexibility, thermal stability and chemical durability. Optimum properties are obtained by modifying the composition and production parameters of glasses and ceramics.

UK high level waste (HLW) borosilicate glasses have been studied to determine the effects of Fe_2O_3 addition on glass chemical durability, thermal properties, density and redox [1]. Results indicated that 5–10 wt% Fe_2O_3 addition provides optimum improvement in chemical durability. ^{57}Fe Mössbauer spectroscopy revealed Fe is in these glasses as Fe^{3+} ions in tetrahedral coordination, strengthening the glass network through increased network polymerisation.

Also ^{57}Fe Mössbauer spectroscopy has been widely used to study iron-containing phosphate glasses to investigate the redox and structure [2]. The particular attraction of these glasses is their combination of low melting temperatures and high chemical durability. Extensive studies have been performed [3] on the doping of iron-phosphate glasses to improve the properties that make them suitable for waste immobilisation. We have shown that modification of these glasses by a number of components substantially improves physical properties. However, interestingly, ^{57}Fe Mössbauer spectroscopy has shown that such modifications produce only small changes in Fe coordination and in Fe^{2+}/Fe^{3+} redox ratio. Therefore the iron in these glasses is relatively immune to compositionally-induced changes in these glasses [4].

Vitrification is being considered as a possible technology for safe disposal of toxic waste streams such as sewage sludge combustion ashes (SSA), since vitrification of such waste is becoming more economically viable due to higher landfill costs and stricter legislation. ^{57}Fe Mössbauer spectroscopy has been used [5] to determine the coordination of the Fe in the glass. The glass composition has been modified to improve the glass forming properties of the waste and the potential of the glass to be used in another application.

Alternative energy efficient methods of vitrifying waste such as dielectric heating have also been investigated. The effect of internal heating, choice of precursor, local atmosphere, and melt time on the iron redox in iron phosphate glasses has been investigated by ^{57}Fe Mössbauer spectroscopy. Short melt times coupled with reducing local sample environments have enabled homogeneous glasses to be formed with significantly higher Fe^{2+}/Fe^{3+} redox ratio than the corresponding conventionally melted glasses.

Ceramics are an alternative option to vitrification for the immobilisation of actinide rich waste streams where iron (and other transition metals) may be present either as a component of waste stream or added for the purpose of charge compensation. Iron valence, coordination and site partitioning in a number of proposed and novel ceramic systems have been investigated by ^{57}Fe Mössbauer spectroscopy.

Vitrification is also being considered for immobilising some "legacy wastes" that are by-products of the UK's early nuclear power programmes. These wastes are often present in relatively small volumes and may be chemically diverse and poorly characterised. They include several wastes that are rich in the problematic actinide plutonium.

[1] N.J.Cassingham et.al., Glass Technol.: Eur. J. Glass Sci. Technol. A **49** (1) (2008) 21–26
[2] T. Nishida et al., Journal of Non-Crystalline Solids **43** (1981) 115
[3] Yu, X.et al., Journal of. Non-Crystalline Solids **215** (1997) 21
[4] P.A. Bingham et. al., Journal of Non-Crystalline Solids 355 (2009) 1526–1538
[5] O.M. Hannant et.al., Glass Technol.: Eur. J. Glass Sci. Technol. A **49** (1) (2008) 27–32

Session 10(T3) Oral-7

MÖSSBAUER ANALYSIS OF BIOX TREATMENT OF ORES AT WILUNA GOLD MINE, WESTERN AUSTRALIA

F.M.Gagliardi[1*] and J.D.Cashion[1]
[1]*School of Physics, Building 27, Monash University, Melbourne, Victoria 3800, Australia*

The treatment of refractory gold ores has long been a problem for the gold mining industry. The gold in these sulphide ores is incorporated in the structure and is not accessible for leaching by cyanide or other leachants. The traditional treatments have been by roasting, pressure oxidation or nitric acid leaching.

A more recent technique, originally developed by Gencor Process Research in Johannesburg under the name BIOX®, and now owned by Biomin Technologies SA, a subsidiary of Gold Fields Ltd, uses three natural strains of bacteria to oxidize the sulphidic ores. The sulphur and iron-loving bacteria break down the ore matrix in a series of stirred reactors. Maintenance of the optimum conditions requires control of the temperature and pH, the input of air to aid the oxidation, and carbon dioxide, nitrogen, phosphorus and potassium to assist bacteria growth. The residence time is typically 4 – 6 days. The optimum conditions must be determined for each ore body and the large number of variables makes this difficult. We have used Mössbauer spectroscopy to analyse the types and concentrations of the iron-containing compounds under operating conditions at nine points in the BIOX® plant at the Wiluna Mine in central Western Australia.

The BIOX® plant takes a continuous feed of a flotation concentrate slurry which initially goes to three stirred, primary reactors in parallel, followed by another three reactors in series. The output of the final reactor goes through a wash and thickening process from which it is separated into the leach feed for cyanidation and the tails. Our analysis is of samples taken from each of these parts. Spectra were taken at room temperature, 78 K and 5 K, with some spectra also taken in applied magnetic fields in order to identify poorly crystalline species.

The spectrum of the input feed is dominated by the doublets of pyrite, FeS_2, and arsenopyrite, FeAsS, with a smaller contribution from szomolnokite, $FeSO_4.H_2O$. The fraction of arsenopyrite approximately halved after the primary reactors, in agreement with the known fact that the bacteria attack arsenopyrite preferentially. An apparent increase in the spectral area of arsenopyrite, accompanied by a small change in parameters, was attributed to the development of a jarosite.

The proportion of szomolnokite increased fairly steadily through the series due to oxidation of the sulphides. A small amount of the higher hydrated ferrous sulphates rozenite, $FeSO_4.4H_2O$, and melanterite, $FeSO_4 7H_2O$, appeared during the processing but essentially disappeared again by the final products. The liberated arsenic was similarly incorporated as scorodite, $FeAsO_4.2H_2O$, which is a reasonably stable entity.

A doublet with a non-specific quadrupole splitting also appeared during the processing. Suspicion that this was a poorly crystalline ferric oxyhydroxide required spectra at 5 K with a magnetic field to confirm that this was due to goethite, although it is possible that ferrihydrite is also present in the earlier samples.

Comparison with a similar investigation of processing at the Fairview mine [1] showed that while the majority of our iron phases were ferrous, theirs were ferric, with magnetically ordered oxyhydroxides and jarosite appearing early in the processing.

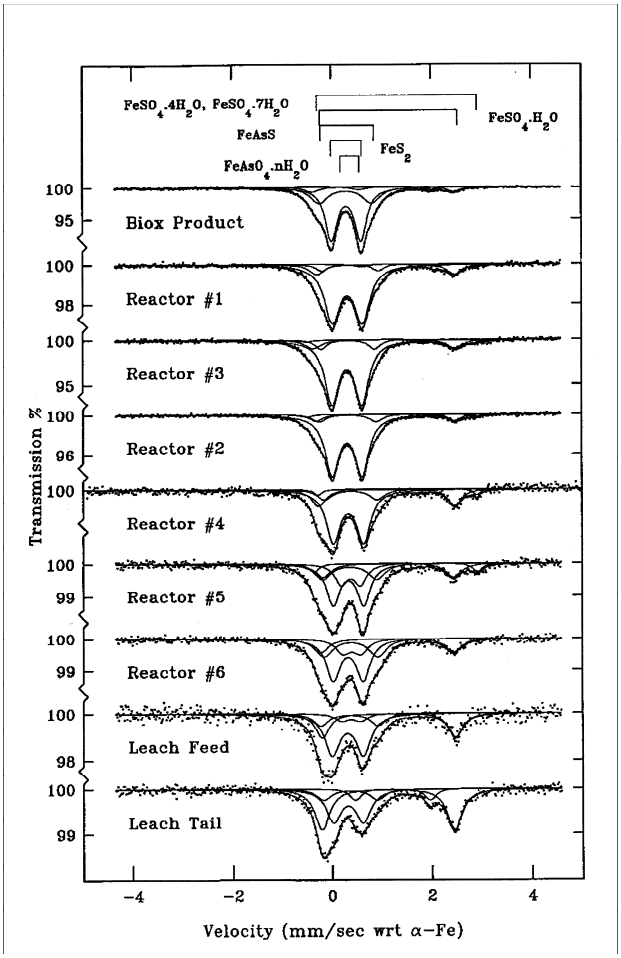

Fig. 1. Room temperature Mössbauer spectra of the Wiluna gold ore at different stages of the BIOX® treatment.

*Present address: William Buckland Radiotherapy Centre, The Alfred, Melbourne, Victoria 3004, Australia.

[1] J. Friedl et al., XV[th] CMMI Congress, Johannesburg, SAIMM, 2 (1994) 403.

MÖSSBAUER SPECTROSCOPY AND QUALITY CONTROL IN FERRATE TECHNOLOGY

S.K.Dedushenko, Yu.D.Perfiliev and L.A.Kulikov
FacultyF of Chemistry, Moscow Lomonosov State University

The usage of the tetraoxoferrate (VI) anion (*ferrate(VI)-ion, FeO_4^{2-}*) for oxidation of the undesired substances and/or their removal from water is now seriously considered as a prospective branch of future water treatment technology. Several FeO_4^{2-}-containing reactants as well as devices for their production can be easily found by the internet search. Production of the reactants and their application for water cleaning is now conventionally called "ferrate technology".

FeO_4^{2-}-ions are used for water treatment in dissolved form, its common target concentrations being less than 10^{-3} M. Thus, the water solutions are not good objects for routine Mössbauer analysis. But Mössbauer spectroscopy is the most important technique for quality control of solid reactants used to prepare the solutions.

FeO_4^{2-} solutions can be prepared by the following ways:

1. dissolution of soluble ferrates (VI) in water;
2. interaction of ferrates (IV,V) with water;
3. exchange reaction with insoluble ferrates (VI);
4. electrochemical oxidation of metallic iron or iron compounds in alkaline solutions;
5. chemical oxidation of iron (II,III) in alkaline solutions;
6. dissolution of Fe(VI)-containing alkali melts in water.

The huge disadvantage of the last three approaches is high alkalinity of the target solutions. The first three methods use solid substances which can be synthesized in almost pure form. Thus, final level of alkalinity is determined only by OH^--ions evaluated during reduction of FeO_4^{n-}-ions.

Among known soluble ferrates (VI) only K_2FeO_4 and $K_3Na(FeO_4)_2$ can be used for water treatment. The other ferrates are insoluble, contain toxic cations or are complicated for synthesis in industrial quantities. These two salts are synthesized by precipitation from alkaline solutions followed by washing and drying. The salts are stable for a very long time. Nevertheless the salts are quite sensitive for storage conditions and can decompose by different mechanisms. Mössbauer parameters of the salts [1] allow one to easily evaluate the relative content of each ferrate in their mixture as well as the content of the impurity of trivalent iron.

Electrochemical generation of FeO_4^{2-} in alkaline mother liquor with continuous crystallization of the salts is, in our opinion, the best way to obtain ferrates (VI) in large quantities. But large-scale production by this way needs very high electric currents. Therefore the electrochemical technology needs solid capital investments.

The alternative way is the solid-state synthesis of ferrates (VI,V,IV). This way is fast and flexible. Changing the synthesis conditions, initial reactants and their ratio we can obtain pure ferrates or the mixtures. And consequently this allows us to reach the necessary concentration of FeO_4^{2-}-ion and, at the same time, to get the desired quantity of colloidal iron hydroxide and to adjust Na-K ration in the final solution. Solid-state approach is a simple way to produce large quantities of the reactant using relatively inexpensive equipment and small space. The main disadvantage of the solid-state approach is higher alkalinity of the final solutions. The price of the row substances also seems to be higher.

Solid-state synthesis of ferrates is a sophisticated multi-step process. It is very sensitive to many conditions and can lead to different products; some of them could be unknown [2,3]. Moreover, the ferrates obtained can undergo structural changes by different mechanisms. Mössbauer spectroscopy allows one to see all iron derivatives and to compare their relative contents. It makes it also possible to identify them determining iron oxidation state and coordination polyhedron as well as magnetic properties for each iron compound. Thus, it is considered to be an essential technique for quality control in solid-state ferrate production.

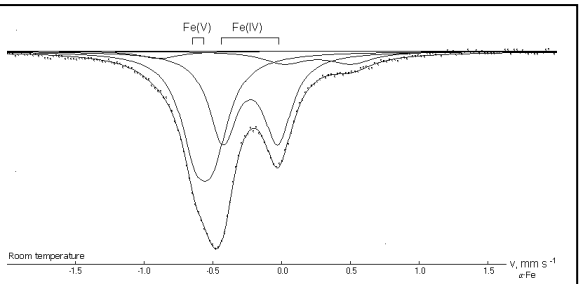

Figure 1. Mössbauer spectrum of reactant, Fe(V):Fe(IV) ≈ 1:1. Impurities of Fe(VI) and Fe(III) are present.

To obtain FeO_4^{2-}-solution with different counter cations, the exchange reaction between $BaFeO_4$ and the respective carbonate can be used:

$$BaFeO_4\downarrow + CO_3^{2-} \rightarrow BaCO_3\downarrow + FeO_4^{2-}.$$

Very low solubility of barium ferrate (VI) and barium carbonate makes this reaction applicable for water treatment. This reaction can be also used for ferrate recycling. Barium ferrate (VI) can be synthesized in a pure form. It is stable and easy to handle. The content of ferrate (VI) in the reactant as well as its purity can be quantitatively controlled by Mössbauer technique.

[1] S.K.Dedushenko et al., Hyp.Int. 136/137 (2001) 373
[2] S.K.Dedushenko et al., J.Alloys Compd. 262-263 (1997) 78
[3] S.K.Dedushenko et al., Hyp.Int. 185 (2008) 197

Session 10(T3) Oral-9

DECOMPOSITION MECHANISM OF METHYLENE BLUE CAUSED BY METALLIC IRON-MAGHEMITE MIXTURE

S.Kubuki[1], K.Shibano[1], K.Akiyama[1], Z.Homonnay[2], E.Kuzmann[2], M.Ristić[3], and T.Nishida[4]
[1]*Tokyo Metropolitan University, Minami-Osawa 1-1, Hachi-Oji, Tokyo 192-0397, JAPAN*
[2] *Eötvös Loránd University, Pázmany P. s., 1/A, Budapest 1117, HUNGARY*
[3]*Ruđer Bošković Institute, P.O.Box 180, Zagreb 10008, CROATIA*
[4]*Kinki University, Kayanomori 11-6, Iizuka, Fukuoka 820-8555, JAPAN*

1. Introduction

Chlorinated volatile organic compounds(CVOC), such as trichloroethylene(TCE) were widely used as solvent and degreaser in cleaning facilities and semi-conductors industry until the 1980s. The use of TCE is now prohibited because it may cause cancer. Several TCE detoxification methods applying metallic alloy catalyst [1] or activated charcoal filter have been developed, but the TCE decomposition rate is known to be slow. Kubuki *et al.* have recently reported that a mixture of industrial by-product of metallic iron(Fe^0) and iron oxide rapidly decreased the TCE concentration from 10 to 0.5 ppm after 7 days [2]. In the present study, methylene blue(MB) was used as a simulating material of TCE, and a relationship between the decomposing process and the structural change of Fe^0-γFe_2O_3 mixture was investigated by means of ^{57}Fe-Mössbaur spectroscopy, X-ray diffractometry, electrospray ionization mass spectroscopy(ESI-MS) and UV-VIS spectroscopy.

2. Experimental

Fe^0-γFe_2O_3 mixture was prepared from reagent grade chemicals. 500 milligrams of Fe^0-γFe_2O_3 mixture with the mass ratio of 1:9, 3:7, 5:5, 7:3, and 9:1 was soaked in 20 mL aqueous solution of methylene blue (MB) with the concentration of 10^{-2} mM. The leaching test was conducted at the temperature of 30 °C for 10 days. Mass of products originating from MB was measured by an electron spray ionization mass spectroscopy (ESI-MS) within m/z of 50 and 350. For the structural characterization of the metallic iron-maghemite mixture, Mössbauer spectra were measured at room temperature in a conventional constant acceleration mode using a 925 MBq ^{57}Co(Rh) source. The velocity scale and Mössbauer parameters refer to metallic α-Fe. The Mössbauer spectra obtained were analyzed by Mosswinn 3.0i XP assuming Lorentzian curves. XRD pattern was recorded from 2Θ = 10 to 90° at 0.02° intervals at a scanning rate of 5° min^{-1}, using Cu-K_α X-rays (λ = 0.1541 nm) generated by setting the tube voltage and the current to 50 kV and 300 mA.

3. Results and Discussion

ESI-MS profiles of 10^{-2} mM MB before and after leaching with the Fe^0-γFe_2O_3 mixture ratio of 3:7 are shown in Fig. 1. A peak intensity ratio of Azure B (m/z = 270) / MB(m/z = 284) increased from 5.1 to 52.6 % after the leaching. This result suggests that the MB was oxidatively decomposed by substituting –H at the terminal position of MB for –CH_3. Mössbauer spectra of

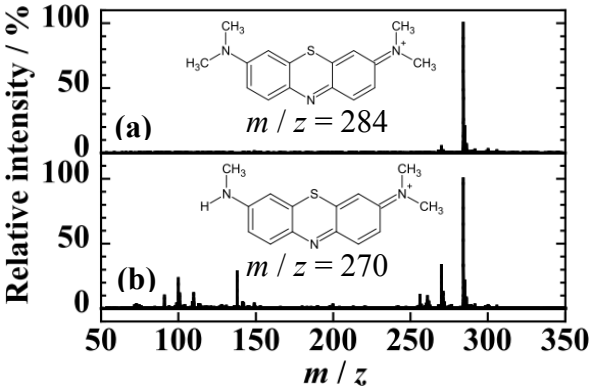

Figure 1. ESI-MS profiles of 10^{-2} mM MB (a) before and (b) after 10-day leaching with Fe^0-γFe_2O_3mixture(3:7).

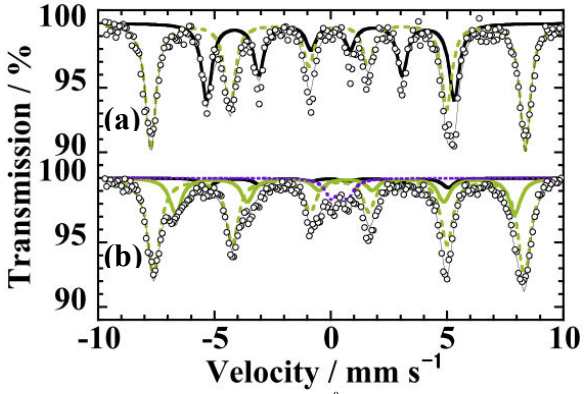

Figure 2. Mössbauer spectra of Fe^0-γFe_2O_3mixture (3:7) (a) before and (b) after 10 day leaching with 10^{-2} mM MB.

the Fe^0-γFe_2O_3 mixture (3:7) before leaching (Figure 2(a)) consisted of two hyperfine sextets due to α-Fe with the isomer shift(δ) and internal magnetic field(H) of 0.00 mm s^{-1} and 33.0 T, and to γFe_2O_3 with δ and Δ of 0.32 mm s^{-1} and 49.5 T, respectively. While a paramagnetic doublet due to tetrahedral Fe^{3+}(δ: 0.38 mm s^{-1}, quadrupole splitting (Δ): 0.79 mm s^{-1}) and another sextet due to octahedral Fe^{3+}(δ: 0.63 mm s^{-1}, H: 45.3 T) were newly observed for the mixture of post leaching (Figure 2(b)). These results indicate that lepidocrocite(γ-FeOOH) and magnetite (Fe_3O_4) precipitated when Fe^0-γFe_2O_3 mixture reacted with MB. It can be concluded that the decomposition of MB proceeds under the oxidation of metallic iron from Fe^0 to Fe^{3+} and that Fe^0-γFe_2O_3 mixture is effective for decomposing CVOCs.

Reference

[1] C. Liu, D. Tseng, C. Wang, J. Hazardous Materials, **B136** (2006) 706-713.
[2] S. Kubuki, H. Matsutomi, Z. Homonnay, E Kuzmann, and T. Nishida, 239th American Chemical Society National Meeting, San Fracisco, 21-25 Mar.(2010).

"SOLUBLE" IRON HEXACYANOCOBALTATE PRUSSIAN BLUE ANALOGUE

A.I. Rykov[1], J. Wang[1], T. Zhang[1] and K.Nomura[2]

[1]*Mössbauer Effect Data Center, Dalian Institute of Chemical Physics, Chinese Academy of Sciences, 457 Zhongshan Road, Dalian 116023, China*

[2]*Graduate School of Engineering, The University of Tokyo, Hongo 7-3-1, Bunkyo-ku, Tokyo 113-8656, Japan*

So-called "soluble" and "insoluble" Prussian Blues (PB) are two cubic modifications of hexacyanometallate frameworks, described by structure models of Keggin[1] and Ludi[2], respectively, when the interstitials of these frameworks are either filled with ions of alkali metals, or empty. In spite of their obsolete naming, compounds of both these families are insoluble, and differ rather by their peptisation property than by solubility. When the "filled" and "empty" structures are built of metal M(II) ion and ferricyanide complex $Fe(III)(CN)_6$, the formulas of the "soluble" and "insoluble" ferricyanides are implied to be KM[Fe(CN)] and $M_3[Fe(CN)_6]_2$, respectively. In hexacyanocobaltate (III) family, the "insoluble" PB analogues $Fe_3[Co(CN)_6]_2$ are indeed well documented [3,4]. However, no ferrous hexacyanocobaltates(III), enclosing alkaline ions, were characterized so far. We report the synthesis and Mössbauer spectra in the "soluble" PB analogues, containing K, Rb and Cs ions. These compounds are interesting as sorbents of radiocesium. While our sorption experiments showed that insoluble hexacyanocobaltates are rather poor sorbents, the soluble PB analogue could have much larger sorption capacity accessible via ionic exchange mechanism.

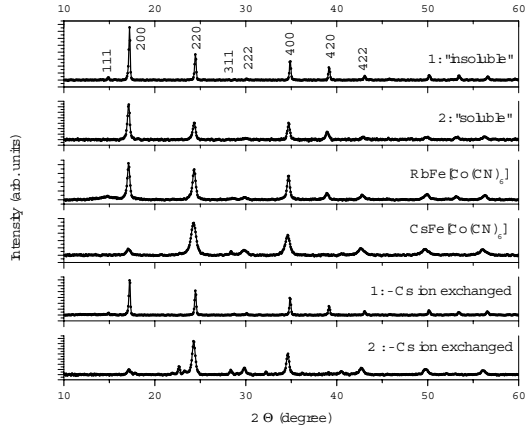

Figure 1. Cu Kα X-ray diffraction patterns of the as prepared and ion-exchanged ferrous hexacyancobaltates (III).

The "soluble" hexacyanocobaltates were prepared from the solutions of ferrous chloride tetrahydrate and $K_3[Co(CN)_6]$ in excess of the latter. Oppositely, when the excess of $FeCl_2$ was allowed the precipitation of the potassium-free "insoluble" phase was observed.

In the x-ray diffraction patterns (Fig.1) the intensity ratio of the reflections 200 and 220 changes when K, Rb or Cs ions enter into the structure. For Cs ion this ratio changes more than 10 times.

Table I: Parameters of Mössbauer spectra in the hexacyanocobaltates

Compound	δ(mm/s)	Δ(mm/s)	Γ(mm/s)	%
"insoluble" **(1)** $Fe[Co(CN)6]_{0.67}$	1.114(2)	1.65(1)	0.45(1)	64
	1.104(2)	0.86(1)	0.38(1)	31
	0.33(1)	0.23(2)	0.26(3)	5
"soluble" **(2)** $KFe[Co(CN)_6]$	1.144(3)	1.77(1)	0.44(2)	32
	1.104(2)	1.03(1)	0.52(2)	64
	0.39(1)	0.66(2)	0.23(3)	4
Precipitated **(3)** $RbFe[Co(CN)_6]$	1.091(5)	0.992(8)	0.60(1)	100
Precipitated **(4)** $CsFe[Co(CN)_6]$	1.116(3)	1.077(4)	0.71(1)	100
Ion-exchanged **(1)** $Fe[Co(CN)_6]_{0.7}$	1.113(4)	1.62(2)	0.65(2)	70
	1.106(7)	0.88(3)	0.46(3)	24
	0.35(6)	0.36(6)	0.5(2)	6
Ion-exchanged **(2)** $CsFe[Co(CN)_6]$	1.111(5)	1.80(3)	0.69(4)	64
	1.084(9)	0.94(3)	0.45(4)	23
	1.123(8)	2.98(2)	0.33(4)	13

The x-ray patterns showed no significant changes for the "insoluble" phase stirred in 0.1 M solution of CsCl for 24 hours. In contrast, in the "soluble" phase, the K^+ ions were replaced with Cs^+.

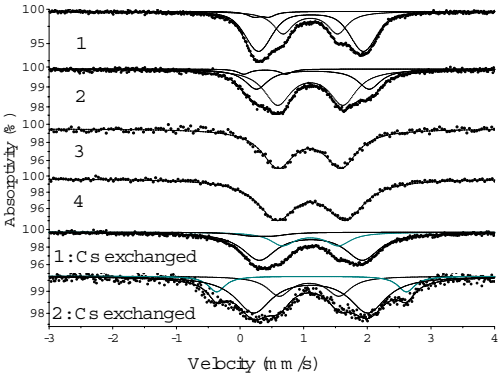

Figure 2. Mössbauer spectra of the ferrous hexacyanocobaltates (from top to bottom according to Fig.1 and Table I)

Mössbauer spectra confirmed the first result, showing a little change for the "insoluble" phase after the ion exchange. However, the Mössbauer spectrum of the ion-exchanged "soluble" phase (Fig. 2) showed the unusual guadrupole states of the high-spin Fe^{2+} ions, dissimilar to Fe^{2+} in small crystals of precipitated $CsFe[Co(CN)_6]$. This result may suggest that the larger ion-exchanged crystals are in a strained metastable state.

[1] J. F. Keggin, and F.D. Miles, *Nature (London)* **1936**, *137*, 577-578.
[2] A. Ludi, H.U. Güdel, *Struct. Bonding* **1973**, *14*, 1-21.
[3] P.G. Rasmussen and E.A. Meyers, *Polyhedron.* **1984**, *3*, 183-190.
[4] E. Reguera, H. Yee-Madeira, S. Demeshko, G. Eckold, and J. Jimenez-Gallegos, *Z. Phys. Chem.* **2009**, 223, 701-711.

THE PRESSURE INDUCED UNUSUAL MAGNETIC PHASE TRANSITION IN IRON PNICTIDE SUPERCONDUCTORS

Chang Qing Jin[1], Jungjie Wu[1,2], Jung Fu Lin[2]
[1] *Institute of Physics, Chinese Academy of Sciences, Beijing, China*
[2]*Department of Geological Sciences, The University of Texas at Austin, TX 78712, USA*

The discovery of iron pnictide superconductors opens a new era for condensed matter physics [1~8]. The parent compounds of iron superconductors form a spin density wave state that can proceed to superconductor upon chemical doping or applied pressure, therefore one of key points of the iron based superconductors is to understand the high pressure behaviors. Here we report the systematic studies of how pressure affects the magnetic ordering of iron pnictitides using synchrotron Mössbauer spectroscopy combined with X-ray diffraction at high pressure low tempearture, indicating unusual phase evolution sequence between magnetic order versus crystal structure symmetry change.

Acknoledgements :

The works are supported by NFS and MOST of China through research projects. The experiments are performed at HPCAT (sector 16), Advanced Photon Source (APS), Argonne National Laboratory. HPCAT is supported by CIW, CDAC, UNLV and LLNL through funding from DOE-NNSA, DOE-BES and NFS. APS is supported by DOE-BES, under Contract No. DE-AC02-06CH11357. Work at UT Austin is supported by Energy Frontier Research in Extreme Environments (EFree) and the Carnegie/DOE Alliance Center (CDAC).

References :

[1] Y. Kamihara, T. Watanabe, M. Hirano, and H. Hosono, J. Am. Chem. Soc. 130 (2008)32902

[2] M. Rotter, M. Tegel, and D. Johrendt, Phys. Rev. Lett. 101(2008) 107006

[3] X. C. Wang, Q. Q. Liu, Y. X. Lv, W. B. Gao, L. X. Yang, R. C. Yu, F. Y. Li, and C. Q. Jin, Solid State Commun. 148 (2008)538.

[4] F.-C. Hsu, J.-Y. Luo, K.-W. Yeh, T.-K. Chen, T.-W. Huang, P. M.Wu, Y.-C. Lee, Y.-L. Huang, Y.-Y. Chu, D.-C. Yan, and M-K Wu, Proc. Natl. Acad. Sci. USA 105 (2008)14262.

[5] C. de la Cruz, Q. Huang, J. W. Lynn, J. Y. Li, W. Ratcliff II, J. L. Zarestky, H. A. Mook, G. F. Chen, J. L. Luo, N. L. Wang, and P. C. Dai, Nature (London) 453 (2008)899

[6] Y. Qiu, W. Bao, Q. Huang, T. Yildirim, J. M. Simmons, M. A. Green, J. W. Lynn, Y. C. Gasparovic, J. Li, T. Wu, G. Wu, and X. H. Chen, Phys. Rev. Lett. 101(2008)257002

[7] Q. Huang, Y. Qiu, W. Bao, M. A. Green, J. W. Lynn, Y. C. Gasparovic, T. Wu, G. Wu, and C. H. Chen, Phys. Rev. Lett. 101(2008)257003

[8] K. Ishida, Y. Nakai, and H. Hosono, J. Phys. Soc. Jpn. 78(2010)62001.

THE RELEVANCY OF MöSSBAUER SPECTROSCOPY AND OTHER ANALYTICAL TECHNIQUES IN COAL RESEARCH

F.B.Waanders

School of Chemical and Minerals Engineering, North-West University, Potchefstroom, 2531, South Africa

Coal consists mainly of hydrocarbons with inorganic constituents mainly being minerals occurring in various amounts from just a few percent to as much as 40% in some South African coal sources [1]. Mössbauer spectroscopy can be, amongst others, a useful tool to characterise these minerals and also monitor the changes that occur with heating of the coal during combustion or gasification. Even weathering (or oxidation) and corrosion effects can be studied by means of Mössbauer spectroscopy that can in turn assist environmentalist in predicting pollution occurrence and the control thereof.

Various other techniques, such as XRD, SEM, Microwave and optical investigations, are described in this paper to augment the Mössbauer findings.

The composition of the coal samples 1-7 (Table 1) differ and represent different South African coal fields. A characterisation of the coal fields is thus possible by means of Mössbauer spectroscopy. Weathered samples 1 and 2 (Table 1) exposed to air and water during different conditions indicate that the pyrite present changed to a ferrous sulphate in less than a week with a drop in pH of the water from pH = 7 to less than pH = 5. The amount of ferrous sulphate increased from 0% to more than 60% with a resultant decrease in the pyrite content.

During coal combustion, in a typical power plant, mineral changes occur and the resultant ash or fly ash contains hematite and an iron rich glassy component. A comparison with laboratory prepared ash yielded similar results as was found for the power plant coal. The relevant Mössbauer parameters are shown in Table 1.

In South Africa a large quantity of coal is used to produce syngas via a gasification plant for the production of synthetic fuels. The change of mineral matter during gasification was studied and the changes occurring during the gasification process could be followed [2]. The solid ash fusion temperature (AFT) is determined by; amongst others the presence of iron and the effect of the amount of iron to the AFT was also studied. Literature [3] suggests the formation of pyrrhotite in the reduction zone and magnetite in the final combustion zone but due to process conditions and subsequent oxidation only hematite and an iron rich glass phase was observed with a typical spectrum shown in Figure 1.

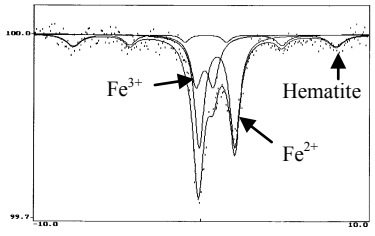

Figure 1. Mössbauer spectrum of gasifier ash

Table 1: Room temperature Mössbauer parameters of samples studied[1]

Sample	Mineral	δ (mm.s^{-1}) ±0.01	Δ (mm.s^{-1}) ±0.01	H (T)	Rel area (%)
Coal 1	Pyrite	0.33	0.58	-	58
	Ankerite	1.17	1.59	-	42
Coal 2	Pyrite	0.30	0.62	-	75
	Illite	1.04	2.52	-	25
Coal 3	Pyrite	0.30	0.61	-	77
	Illite	1.02	2.40	-	23
Coal 4	Pyrite	0.30	0.59	-	76
	$FeSO_4$	1.61	2.87	-	24
Coal 5	Pyrite	0.32	0.63	-	90
	Jarosite	0.20	0.96	-	10
Coal 6	Pyrite	0.31	0.62	-	78
	Illite	0.82	2.40	-	22
Coal 7	Pyrite	0.32	0.59	-	100
Weathered sample 1	Pyrite	0.31	0.59	-	100
Weathered sample 2	Pyrite	0.31	0.60	-	
	$FeSO_4$	1.63	2.88	-	x[2]
Fly ash (power plant)	Fe^{2+}	0.93	2.11	-	27
	Fe^{3+}	0.38	1.01	-	38
	Fe_2O_3	0.34	-0.08	49.3	35
Fly ash (lab. product)	Fe^{2+}	0.89	2.12	-	39
	Fe^{3+}	0.41	1.02	-	38
	Fe_2O_3	0.35	-0.07	49.5	23
AFT	Pyrite	0.28	0.63	-	80
	Fe	-0.02	0.00	32.8	20
	Fe_2O_3(1)	0.37	-0.20	51.5	100
	Fe^{2+}	0.85	1.88	-	20
	Fe^{3+}	0.32	0.57	-	8
	Fe_2O_3(2)	0.36	-0.16	51.5	72
Gasifier top	Pyrite	0.23	0.58		100
1/3 down	Pyrite	0.23	0.59		52
	Fe^{2+}	1.05	2.39		48
2/3 down	Pyrite	0.23	0.58		37
	Fe^{2+}	1.07	2.29		52
	Fe^{3+}	0.70	1.10		11
Bottom of gasifier	Fe^{2+}	1.06	2.22		56
	Fe^{3+}	0.68	1.10		26
	Fe_2O_3	0.33	-0.08	49.7	18

[1] *δ = Isomer shift relative to α-iron, Δ = Quadrupole splitting and H = magnetic hyperfine field*

[2] *Weathering measurements taken at various intervals*

[1] Pinheiro, H.J., (ed). Bulletin 113, A techno-economic and historical review of the South African coal industry in the 19th and 20th centuries and analyses of coal product samples of South African collieries, 1998-1999, Department of Minerals and Energy and the SABS Coal and Minerals Services, (1999), 97p.

[2] Waanders, F.B., and Bunt, J.R. Transformation of the Fe-mineral associations in coal during gasification, Hyperfine Interactions (2006) 171: 287-292.

[3] Bandyopadhyay, D., Study of kinetics of iron minerals in coal by ^{57}Fe Mössbauer and FT-IR spectroscopy during natural burning. Hyperfine Interactions (2005), 163 nr 1-4, 167-176.

Session 11(T6) Oral-12

THE METAMICT STATE CHARACTERIZED WITH MÖSSBAUER SPECTROSCOPY. IMPLICATIONS FOR STABILIZATION OF HIGH-LEVEL NUCLEAR WASTE

Dariusz Malczewski
Faculty of Earth Sciences, University of Silesia; Bedzińska 60, 41-200 Sosnowiec, Poland.
e-mail: dariusz.malczewski@us.edu.pl

Stabilization and immobilization of nuclear high-level waste (HLW) in a solid form is an important problem in the nuclear industry. In most cases, HLW will be immobilized by homogeneously distributing them inside glass waste forms. In potentially crystalline nuclear waste forms, such as oxides, silicates, and phosphates structures, radionuclides may occupy specific atomic positions within these periodic structures as dilute solid solutions. Some of the coordination polyhedra in each phase exhibit specific size, charge, and bonding characteristics, making it possible to incorporate the radionuclides into the structures. Since the required storage times are long (10^4 - 10^6 years), an understanding of the long-term cumulative effects of radiation damage on both of these waste forms is essential. Metamict minerals, a class of natural amorphous minerals which were initially crystalline, contain radioactive elements such as uranium and thorium that degrade the crystal structure mainly by α-decay events. Progressive overlap recoil nuclei collision cascades from ^{235}U, ^{238}U, ^{232}Th, and their daughter products are critical to this process.

The extent of the structural damage is radiation dose-dependent and is also controlled by the competition between the rate of damage production and the rates of various recovery processes. Hence, metamict minerals are found with a wide range of damage states, ranging from highly crystalline to fully metamict (amorphous). Because of the natural occurrence of uranium and thorium in metamict minerals, they serve as natural analogues for radiation effects in high level nuclear waste over extremely long time periods (10^8 – 10^9 years).

This presentation summarizes recent research findings of representative metamict minerals using ^{57}Fe Mössbauer spectroscopy. In this case, ^{57}Fe Mössbauer spectroscopy is a probe for the local structure around the Fe^{2+} and Fe^{3+} positions, and indirectly provides information on the ordering of adjacent polyhedra occupied by large cations such as U, Th, and rare earth elements. Application of the Mössbauer effect holds great potential for the future of this field.

IRON AND SULFUR SPECIATION OF SLIDING MUD FROM THE XIELIUPO LANDSLIDE IN ZHOUQU COUNTY, NW CHINA

G. D. Zheng[1], S. Y Liang[1,2], N. Zhang[2] and X. Li[2]

[1] *Key Laboratory of Petroleum Resources Research, Institute of Geology and Geophysics, Chinese Academy of Sciences, Lanzhou 730000, China*

[2] *Key Laboratory of Mechanics on Disaster and Environment in Western China (Lanzhou University), Ministry of Education, Lanzhou 730000, China*

Gray and/or black mud materials are often observed within slipping zones of many landslides, especially the landslides in large scale and long history of action. Such mud materials are always called as sliding mud and considered as key factors corresponding to landslide development and evolution even the slipping actions. Thus the sliding mud along with the slip zones is attractive to many researchers and engineers working on landslide protection. However, there is still large space to understand the formation mechanism and accumulation process of sliding mud (Zheng et al., 2002a; 2002b). In this study, a profile crossing a slip zone of the giant Xieliupo Landslide is selected for the sliding mud formation conditions based on iron and sulfur speciation.

The Xieliupo Landslide, located along the Bailongjiang River in Longnan District, Gansu province, NW China, is famous in very large size, continuous and frequently actions (Chen et al., 2006), which induced huge damages to local society. There are many sliding surfaces occurred in the debris layer, some of them have been cut by water and displayed as outcrops in the streams. One vertical profile crossing a sliding surface in a stream on the western part of the Xieliupo Landslide was selected for this study, and 13 samples were collected from this profile during a fieldwork and analyzed for their mineral and chemical compositions as well as chemical species of iron and sulfur using XRD, XRF, and Mössbauer spectroscopy and K-edge XANES, respectively. The sliding surface displays a very clear plane with a sharp deformation within a special layer or zone of rocks in deep gray color. This zone contains much more clays than the rocks above and beneath the zone. The mineral and chemical compositions of the samples in gray color are almost the same as other debris samples collected from the upward debris rock above the zone and the bedrocks underneath the zone. However, the Mössbauer spectroscopy revealed a clear variation of iron species between the samples in gray from the zone and other debris and bed rocks. The samples in deep gray contain much more ferrous iron than other debris rocks and the bedrocks, indicating a relatively stronger reducing condition within the slip zone. K-edge XANES also revealed the vertical variation of sulfur species that was similar to iron speciation, the samples in gray collected from the slip zone were enriched with reduced sulfur species whereas other debris and bed rocks contain relatively much more oxidative sulfur species. Iron and sulfur speciation indicate redox change on the vertical profile studied. The relatively reducing conditions may be important factors controlling the variation of the materials in deep gray color and fine particles within the slip zone, and furthermore inducing the weakness of the sliding zone along with the process of landslide development.

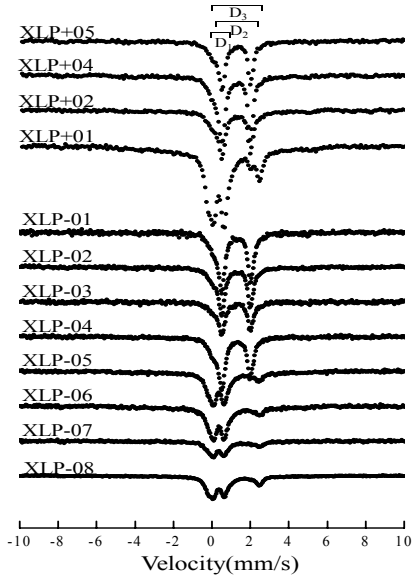

Figure 1. Mössbauer spectra of rock samples from the Xieliupo Landslide. The samples XLP+01 through XLP+05 were collected from the up section above the sliding surface, and XLP-01 though XLP-08 from the lower section under the sliding surface

Reference

[1] B-P. Wen et al., Environmental Geology 47(2003)140
[2] B.P. Wen and H.Y. Chen, Earth Science Frontiers 14(2007) 98
[3] G.D. Zheng et al., Journal of Asian Earth Sciences 20(2002a) 955
[4] G.D. Zheng et al., Chinese Science Bulletin 47(2002b) 2018
[5] G.D. Zheng et al., Environmental Geology 51(2007) 1455
[6] G.D. Zheng et al., Journal of Earth Science 21(2010) 954
[7] W.W. Chen et al., Study on Engineering Geological Problems along the Gansnu Part of the Lanzhou-Haikou Highway (2006) Laznhou University Press, pp240

Session 11(T6) I-20

ROLE OF Fe-MINERALS ON RADIONUCLIDE MOBILITY IN SUBSURFACE

R.K.Kukkadapu[1], T.S.Peretyazhko[1], J.M.Zachara[1], Y.Bi[2], and K.F.Hayes[2]
[1]*Pacific Northwest National Laboratory, Richland, WA 99352, USA*
[2]*University of Michigan, Ann Arbor, Michigan, MI,48103, USA*

The U.S. Department of Energy faces the challenge of cleaning up groundwater plumes contaminated by radioactive metals, e.g., uranium and technetium. The mobility of these metals in contaminated aquifers is governed by a complex assortment of site-specific biogeochemical and hydrological properties, sediment Fe-mineralogy, and redox status. Among other effects, there is a particular interest in understanding the role of Fe(III)-(oxyhydr)oxides and Fe-containing clay minerals, ubiquitous in soils and sediments, on metal attenuation. Secondary Fe(II)-minerals, such as Fe-sulfides and Fe-carbonates generated under reducing conditions by (bio)transformation of the Fe(III)-(oxyhydr)oxides convert oxidized soluble contaminates to sparingly soluble phases, e.g., $Tc(VII)_{aq}$ to Tc(IV)-oxide. Reduced clays also are reactive toward soluble contaminates. However, upon the return of oxic conditions, these Fe minerals are vulnerable to oxidative mineral transformation. Thus, the temporal fate of the contaminants in the subsurface is, in part, a function of the Fe-redox state.

Two case studies regarding the role of Fe-minerals on radionuclide mobility under different scenarios are presented here. In the first example, sediments obtained at different depths from the Columbia River corridor (WA State, USA) were reacted with soluble Tc(VII) to gain insights into the nature of reactive Fe(II). Detailed Mössbauer spectroscopy measurements, coupled with Tc-extended X-ray absorption fine structure (EXAFS), microscopic observations, and selective chemical extraction studies, have shown the Fe-mineralogy of the transect varied with the depth, and Tc reactivity of the sediment is dependent on the Fe(II)-mineral suite of the sample. Sediments containing siderite, $FeCO_3$, exhibited the highest reactivity toward Tc. Figure 1 shows Mössbauer spectra of a siderite-rich sample before and after Tc reaction.

Biogenic Fe-sulfide minerals have been reported to slow down the oxidation of $U(IV)O_2$ precipitate to soluble U(VI). However, the delaying effect of Fe-sulfides on UO_2 oxidative dissolution and its implication for long-term U immobilization is not well understood. To understand the mechanistic details of the role of Fe-sulfide on UO_2 dissolution, products of laboratory-synthesized mackinawite ($Fe(II)S_{0.9}$) and UO_2 mixture reacted with dissolved oxygen (DO) were studied. Mössbauer spectroscopy, X-ray diffraction (XRD), and solution analysis indicated: a) $Fe(II)S_{0.9}$ effectively scavenges DO and inhibits UO_2 oxidation until $Fe(II)S_{0.9}$ is completely depleted, and b) $Fe(II)S_{0.9}$ is converted to nanogoethite and lepidocrocite via an Fe(II)/Fe(III) intermediate product state that was not readily discernible from XRD (Figure 2).

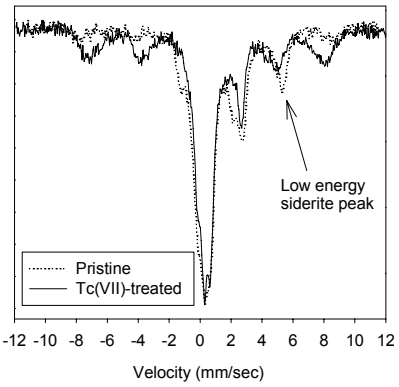

Figure 1. 12 K spectra of pristine and Tc(VII)-treated sediments showing siderite oxidation by Tc(VII) to a new Fe(III)-phase.

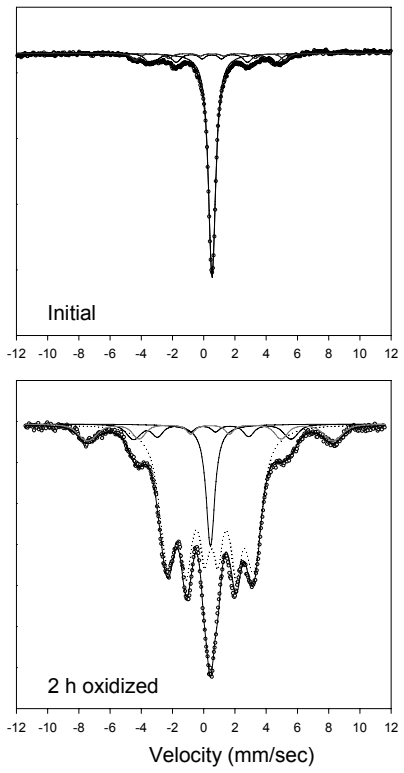

Figure 2. 4.5 K Mössbauer spectra of initial and 2-h oxidized $FeS_{0.9}$ samples. The singlet in the initial sample is due to low-spin Fe(II) in a tetrahedral environment in mackinawite. Bulk transformation of the singlet occurred within 2 hours. The inner sextets are due to Fe(II) and Fe(III) in modified mackinawite structure. The outer sextet is due to ferrihydrite

INFLUENCE OF INTERFACES ON MAGNETIC HYPERFINE FIELD

M. Ghafari[1] , D. Sopu[2], H. Hahn[1], H. Gleiter[1], R. Brand[1], K. Albe[2], S. Kamali[3],

[1]Institute for Nanotechnology, Karlsruhe Institute of Technology, Karlsruhe, Germany.
[2]Institut für Materialwissenschaft, TU Darmstadt, Petersenstr. 23, D-64287 Darmstadt, Germany
[3]University of California Davis, Department of Applied Science, Davis, California, USA

Compacting nanoparticles leads to the formation of a bulk material with a significant fraction of interface. The atomistic short-range order of interfaces is very different from the well known amorphous and crystalline materials. Transmission electron microscopy (TEM), X-ray diffraction studies as well as Mössbauer spectroscopy have been applied to elucidate physical and magnetic properties. The iron-partial phonon density of states (PDOS) was measured showing dramatic differences between the bulk and Materials with significant fraction of interfaces. Molecular dynamics (MD) simulations of the atomic structure of nanomaterials were made and reproduce well the experimental results. The magnetic properties of these materials have been investigated in details. The results show that transition temperature and magnetic moment are different from the well-known materials.

Session 12(T4) Oral-14

Magnetic and microstructural properties of (Nd,Pr)-(Tb,Dy,Gd)-(Fe,Co,Al,Cu)-B type magnets

O.A.Arinicheva[1], A.S.Lileev[1], M.Reissner[2], A.A.Lukin[3] and A.S.Starikova[3]
[1]*National University of Science and Technology "MISIS", 119991 Moscow, Russia*
[2]*Vienna University of Technology, 1040 Wien, Austria*
[3]*Ltd. Research and production Complex "Magnets and magnetic systems", 127238 Moscow, Russia*

Magnets based on NdFeB are together with SmCo high energy magnets. They have very high energy product at room temperature, which have made them indispensable for many applications where small magnets with high fields are necessary, which range from automotive sensors to consumer electronics like handys and PCs, but also are in use in factory automation and medical applications [1]. The market is around several billion dollars a year. NdFeB magnets are cheaper than SmCo ones, but suffer from less good temperature stability, which restricts the use of standard NdFeB magnets to temperatures below 100°C, which is a problem for applications in motors, with temperatures of at least 180°C. Alloying with Dy and Tb has been shown to increase the temperature stability. Further NdFeB magnets are very sensitive to corrosion. Therefore they have to be covered by protective sheaths, like Ni, Zn or epoxy. Addition of Co decreases the corrosivity of the material.

Beside the intrinsic properties, the microstructure plays an important role. Large crystals are very unstable against demagnetization. Therefore small well separated grains are important. Special sinter procedures allow production of fine-grain samples where the rare earth elements are enriched at the grain boundaries, which helps to separate the magnetic particles [2]. Alloying with other rare earth elements like Dy and Tb does not only help in that way but also increase anisotropy field and in consequence also the coercive field. But these elements are expensive and lower the remanence field. Therefore cheaper alternatives are under investigation.

In this work we present results of an investigation of magnets of the type (Nd,Pr)-(Tb,Dy,Gd)-(Fe,Co,Al,Cu)B. Samples were prepared by standard sinter method: melting of constituent elements in water cooled Cu-boat under pure Ar atmosphere, milling in isopropylalcohol to particles of 3 to 4 µm, pressing with 500 kg/cm^2 in cross field of 10 kOe, followed by sintering at 1100°C for 2 hours. Afterwards samples were thermally annealed under different conditions. Sample A was annealed for 2 hours at 900°C followed by quenching in Ar atmosphere to room temperature. Sample B was annealed for 2 hours at 900°C followed by cooling to 400°C with 1°C/min, hold at 400°C for 3 hours, heated up to 500°C, hold there for 1 hour, and finally quenched in Ar atmosphere to room temperature. The composition was checked by EDX. Microstructure was investigated by SEM. Magnetic properties were determined by QD-PPMS-9T with VSM option. Mössbauer transmission spectroscopy was performed on powdered samples in constant acceleration mode.

Obtained grain sizes are between 10 and 20 µm. Grains of sample B are more "clean" (Figure 1). Several phases could be identified. Whereas the structure sensitive magnetic properties like coercive and demagnetizing field are different for both samples, remanent field and energy product are the same.

O.A. wants to thank ERASUMS-MUNDUS Action 2 MULTIC 10-1483 for a five month scholarship at Vienna University of Technology.

[1] D.Brown, B.-M.Ma, Z.Chen, J.Magn.Magn.Mat. 248 (2002) 432
[2] I.Betancourt, H.A.Davies, Mat.Sci.Technol. 26 (2010) 5

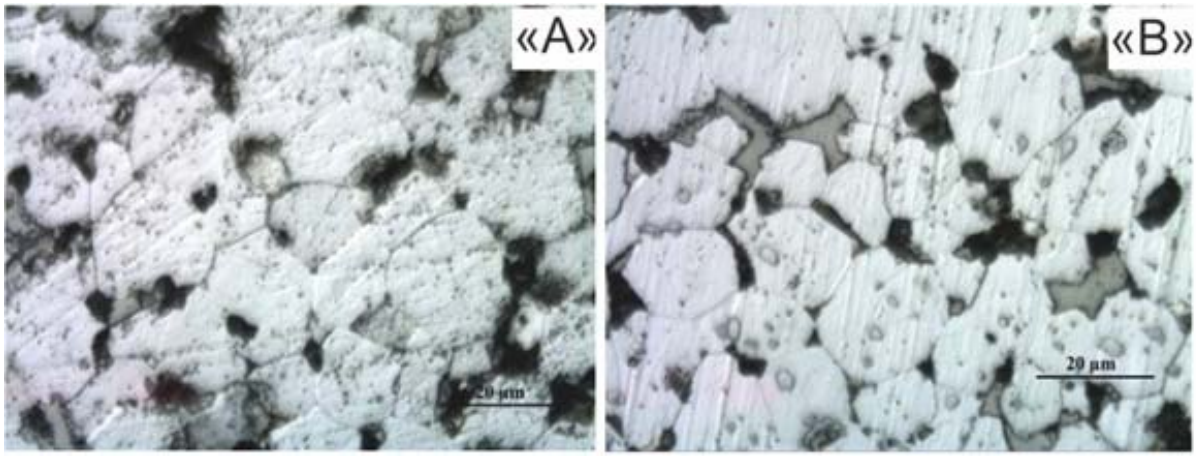

Figure 1. Microstructure of samples A and B

MAGNETISM INFLUENCED BY STRUCTURAL DISORDER IN MELT-SPUN $DyMn_{6-x}Ge_{6-x}Fe_xAl_x$ (x=2.5, 3) ALLOYS

B. Idzikowski[1], Z. Śniadecki[1], J.-M. Greneche[2]
[1]*Institute of Molecular Physics, PAS, M. Smoluchowskiego 17, PL-60-179 Poznań, Poland*
[2]*LUNAM Université du Maine IMMM UMR CNRS 6283, F-72085 Le Mans, France*

The intermetallic compounds $DyMn_{6-x}Ge_{6-x}Al_xFe_x$ with limiting compositions x=0 ($DyMn_6Ge_6$) and x=6 ($DyFe_6Al_6$) crystallize in hexagonal and tetragonal structures, respectively. Metastable crystalline as well as amorphous states appear as a consequence of phase competition during the rapid quenching process [1].

Different chemical and/or geometrical order was found in x=2.5 and 3 melt-spun samples, which possess mixed (crystalline and amorphous) and amorphous structure, respectively. Thermal variations of magnetization from liquid helium up to room temperature for both samples are similar. Magnetization value reaches about 0.1 μ_B per formula unit at 2 K and then increases. In-between two maxima are visible, first at 50 K (sharp effect) and second very broad ranged from 150 to 200 K with the transition to the paramagnetic state above 400 K. 300 K ^{57}Fe Mössbauer spectrum illustrated in Figure 1 reveals a remaining magnetic component in addition to a prevailing quadrupolar feature. This statement is also confirmed by the macroscopic magnetization measurements.

The Mössbauer spectrometry investigations on the $DyMn_3Ge_3Fe_3Al_3$ alloy suggest the existence of magnetic fluctuations. Application of weak external magnetic field causes the increase of mean hyperfine magnetic field B_{hyp} and the volume fraction of magnetic component. The Mössbauer spectra for $DyMn_{3.5}Ge_{3.5}Fe_{2.5}Al_{2.5}$ are similar with strong indication of Zeeman splitting. For $DyMn_3Ge_3Fe_3Al_3$ alloy at 77 K, the content of the magnetic fraction increased from 36% without field to 45% in $\mu_0 H$=0.04 T. For x=3 ac-susceptibility measurements confirm the presence of spin dynamics. One can observe also a cusp in the temperature dependence of the real part of magnetic susceptibility. There is a significant shift in freezing temperature T_f measured at different frequencies.

The Vogel-Fulcher law $\tau = \tau_0 \exp [E_a k_B^{-1} (T_f - T_0)]^{-1}$ and critical slowing-down power law $\tau = \tau_0 (T_f T_g^{-1} - 1)^{-z\nu}$ were helpful in characterization of observed spin dynamics. Both approximations (Vogel-Fulcher and power laws) give comparable values for the spin flipping time necessary to obtained equilibrium state $\tau_0 = 8 \times 10^{-7}$ and 1×10^{-9}s, respectively. Additionally the product of the dynamic critical exponent yielded $z\nu \approx 3.5$ values characteristic for cluster spin glass systems (for ordinary spin glasses $z\nu \approx 8$).

All results confirm the occurrence of mictomagnetic ordering in the alloy investigated. With decreasing Fe content (x=2.5) an increase in the hyperfine field strength B_{hyp} as well as in the volume of the magnetic fraction in the alloy is observed.

It can be stated to summarize that on the basis of the ^{57}Fe Mössbauer spectrometry, magnetic measurements

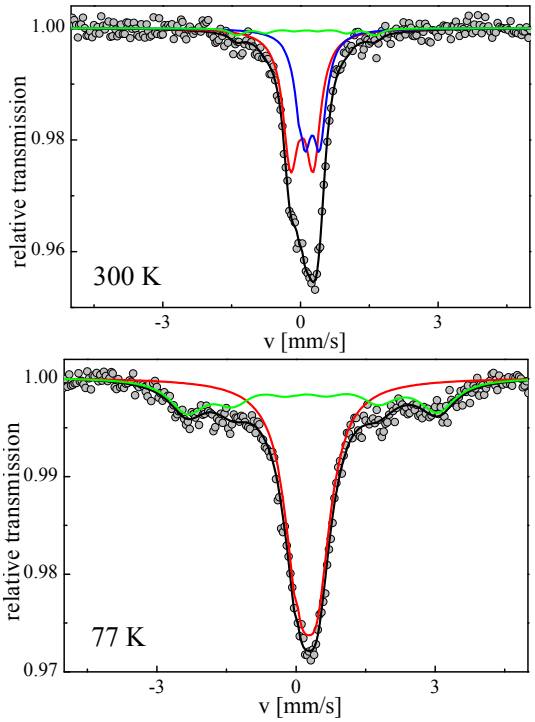

Figure 1. ^{57}Fe transmission Mössbauer spectra of $DyMn_3Ge_3Fe_3Al_3$ sample measured at 300 and 77 K.

M(T), *M(H)* and ac-susceptibility, short-range ordered crystallographic zones were characterized in melt-spun $DyMn_{6-x}Ge_{6-x}Al_xFe_x$ (x=2.5, 3) alloys. A related magnetic ordering exists, called mictomagnetism or cluster spin glass, with frozen entities representing small magnetic clusters rather than elementary magnetic moments, as in the spin glass.

The presence of clusters with frustrated magnetic interactions was also investigated by us in structurally disordered metastable cobalt [2], iron [3] or yttrium containing systems, *e.g.*, in polycrystalline structures with Y and Co.

[1] Z. Śniadecki, B. Idzikowski, J.-M. Greneche, P. Kerschl, U.K. Rößler, L. Schultz, „Independence of magnetic behavior for different structural states in melt-spun $DyMn_{6-x}Ge_{6-x}Al_xFe_x$ ($0 \le x \le 6$)", J. Phys.: Condens. Matter **20** (2008) 425212
[2] U.K. Rößler, B. Idzikowski, D. Eckert, K. Nenkov, K.-H. Müller, M. Kopcewicz, A. Grabias, „Structural, magnetic and magneto-transport properties of melt-spun $Fe_{10}Cu_{90}$", IEEE Trans. Magn. **35** (1999) 2841
[3] B. Idzikowski, U.K. Rössler, D. Eckert, K. Nenkov, K.-H. Müller, „Spin-glass-like ordering in giant magnetoresistive CuCo", Europhys. Lett. **45** (1999) 714

Acknowledgments
This work was supported by the PHC Polonium program (project No. 8405/2011) and the funds of the National Science Center as a research project No. N N202 381740.

Session 12(T4) Oral-16

STUDY OF $NiFe_2O_4$ NANOPARTICLES USING MAGNETIC MEASUREMENTS AND MÖSSBAUER SPECTROSCOPY WITH A HIGH VELOCITY RESOLUTION

M.I. Oshtrakh[1,2], M.V. Ushakov[1,2], B. Senthilkumar[3], R. Kalai Selvan[3], C. Sanjeeviraja[4], I. Felner[5], V.A. Semionkin[1,2]

[1]Department of Physical Techniques and Devices for Quality Control and [2]Department of Experimental Physics, Ural Federal University, Ekaterinburg, 620002, Russian Federation;
[3]Solid state Ionics and Energy Devices Laboratory, Department of Physics, Bharathiar University, Coimbatore – 641 046, India;
[4]School of Physics, Alagappa University, Karaikudi – 630 006, Tamil Nadu, India;
[5]The Racah Institute of Physics, The Hebrew University of Jerusalem, 91904 Jerusalem, Israel

Among the spinel ferrites, $NiFe_2O_4$ nanoparticles applied in information storage, microwave devices, spintronics and magnetic resonance imaging and, recently, have been identified as the suitable electrodes for Li-ion batteries and supercapacitors. $NiFe_2O_4$ has inverse spinel structure in which Ni^{2+} cation occupies octahedral B sites and Fe^{3+} cation occupies both octahedral B and tetrahedral A sites. It is well-known that cation distribution affects the physical, chemical and electrochemical properties of this material. Moreover, it is interesting to analyse Fe^{3+} local environment in both A and B sites. For this reason we studied two samples of $NiFe_2O_4$ nanoparticles with different preparation using magnetic measurements and Mössbauer spectroscopy with a high velocity resolution.

The nanocrystalline $NiFe_2O_4$ particles have been prepared by solution combustion synthesis technique using different fuels such as ethylene-diamine-tetra-acetic acid (NA sample) and urea (NB sample). These samples were characterized using XRD, TEM and SEM with chemical microanalysis with EDS techniques. Magnetic measurements were carried out using SQUID technique. These measurements demonstrated some differences in magnetic features for NA and NB sample (see Fig.1).

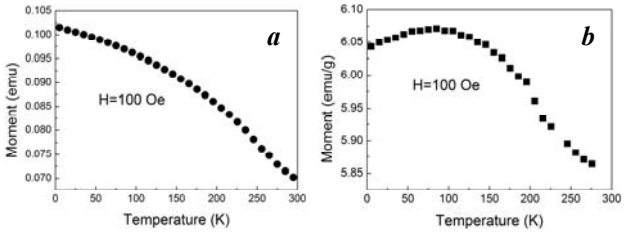

Figure 1. Temperature dependence of magnetic moments for the NA (***a***) and NB (***b***) samples.

Then Mössbauer spectra of the NA and NB samples were measured using automated precision Mössbauer spectrometric system with a high velocity resolution at room temperature with spectra registration in 4096 channels. These spectra look like other Mössbauer spectra of $NiFe_2O_4$ (Fig. 2). However, these spectra were not fitted well using widely used model of two sextets related to the ^{57}Fe in the A and B sites. Therefore, the probabilities of various numbers of Ni atoms in local environment of the A and B sites were calculated. Basing on these results Mössbauer spectra of the NA and NB samples were fitted using 10 magnetic sextets (5 sextets with larger values of H_{eff} were related to the ^{57}Fe in the A sites while 5 sextets with lower values of H_{eff} were related to the ^{57}Fe in the B sites).

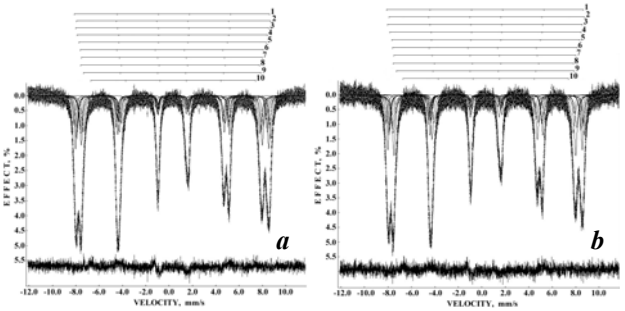

Figure 2. Mössbauer spectra of NA (***a***) and NB (***b***) samples measured in 4096 channels. T=295 K.

These fits may be considered as controversial taken into account usually used model. However, for instance, calculated probabilities of various numbers of Ni atoms in local environment of the B sites within the sphere of 3.45 Å (of about 10 % and more) may be compared with relative areas of 5 magnetic sextets related to the ^{57}Fe in the B sites obtained for the NA sample (Fig. 3). It was also shown that the total relative areas of sextets related to the ^{57}Fe in both A and B sites of NA and NB samples were about 50 % that corresponded to the equal ^{57}Fe content in the A and B sites of studied $NiFe_2O_4$ nanoparticles.

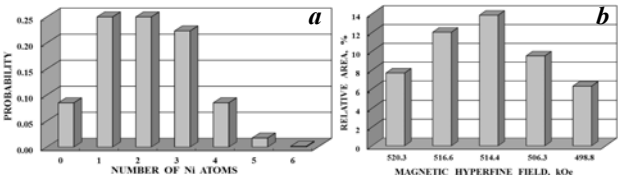

Figure 3. Probabilities of the numbers of Ni atoms in local environment of the B sites within the sphere of 3.45 Å in the NA sample (***a***) and relative areas of 5 magnetic sextets related to the ^{57}Fe in the B sites obtained from Mössbauer spectrum of the NA sample (***b***).

Comparison of Mössbauer parameters obtained from the spectra of the NA and NB samples using the same fitting model demonstrated some differences. This result correlates with some differences in magnetic data for two samples. Thus, the results obtained show the effect of fuel used for nanoparticles preparation.

CATIONIC DISTRIBUTION OF OXIDES IN THE MN_3O_4-FE_2O_3 SYSTEM SYNTHESIZED AT 1200°C

R. Wang[2], C. X. Yang[1], Y. G. Shi[3], Y. Z. Sun[1], G. B. Li[1], T. N. Jin[2], G. W. Qin[3], F. H. Liao[1], J. H. Lin[1]

[1]*Beijing National Laboratory for Molecular Sciences, State Key Laboratory of Rare Earth Materials Chemistry and Applications, College of Chemistry and Molecular Engineering, Peking University, Beijing 100871, P. R. China*
[2]*College of Material Science and Engineering, Beijing University of Technology, Beijing 100022, P. R. China*
[3]*Key Laboratory for Anisotropy and Texture of Materials (Ministry of Education), Northeastern University, Shenyang 110819 , P. R. China*

Manganese iron oxides have been extensively studied due to their applications to many electronic devices.[1] A lot of studies have been performed on the phase relationships, magnetic and electronic properties of the FeO_x-MnO_y system.[2] Several phases, such as hausmannite, spinel, hematite, and bixbyite, have been found in this system. It is interesting that there are several different points of view presented in the literature on how the cations (Fe^{2+}, Fe^{3+}, Mn^{2+}, Mn^{3+}) distribute between the tetrahedral (A) and octahedral (B) sites for $Mn_{3-x}Fe_xO_4$ (both hausmannite and spinel phases) because both Fe^{3+} and Mn^{2+} intend to occupy the tetrahedral A sites.[3-6] In order to present a clear picture for this question, X-ray diffraction, ^{57}Fe Mössbauer spectra, and X-ray photoelectron spectroscopy (XPS) have been performed on the samples in the system Fe-Mn-O synthesized at 1200 °C and quenched to room temperature.

Three solid solutions, $Mn_{3-3x}Fe_{3x}O_4$ ($0.00 \le x \le 0.278$), $Mn_{3-x}Fe_{3x}O_4$ ($0.291 \le x \le 0.667$), and $Mn_{2-2x}Fe_{2x}O_3$ ($0.89 \le x \le 1.00$), have been found by powder X-ray diffraction as shown in Figure 1. Rietveld refinement of the powder X-ray data of these samples show that they belong to hausmannite phase with the space group *I4$_1$/amd*, spinel phase with the space group *Fd3m*, and hematite phase with the space group *R-3c,* respectively. Between them are two-phase regions.

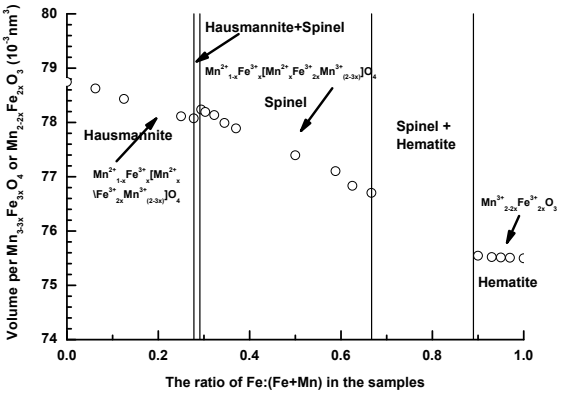

Figure 1. Phase relationship for the system Fe-Mn-O synthesized at 1200 °C and quenched to room temperature.

^{57}Fe Mössbauer spectra indicate that the valence state of Fe in these three solid solutions is +3, in addition there are two crystallographically independent Fe^{3+} ions in the unit cells of hausmannite or spinel phase, one Fe^{3+} in hematite phase, the corresponding data are shown in Figure 2. After considering ^{57}Fe Mössbauer spectra and XPS for the studied sample, it is found that a formula of $Mn^{2+}_{1-x}Fe^{3+}_x[Mn^{2+}_xFe^{3+}_{2x}Mn^{3+}_{2-3x}]O_4$ can be used to describe the cations distribution of both the hausmannite and spinel phases, and that for hematite phase is $Mn^{3+}_{2-2x}Fe^{3+}_{2x}O_3$.

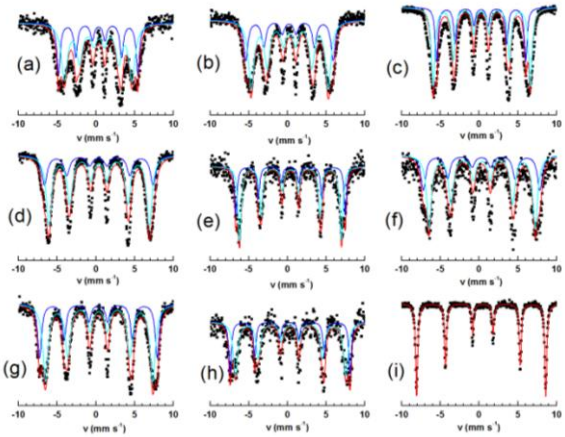

Figure 2. ^{57}Fe Mössbauer spectra of the samples $Mn_{3-3x}Fe_{3x}O_4$ (a, x=0.278 ; b, x=0.303; c, x=0.400; d, x=0.500; e, x=0.556; f, x=0.588; g, x=0.625; h, x=0.667) and $Mn_{2-2x}Fe_{2x}O_3$ (i,x=0.96). The solid black squares are measured data, the blue line is the simulated data for the site A, the green line for site B, and the red line is the total simulated data.

[1] K.Y. Kim, W. S. Kim, S. Y. Hong, *IEEE Trans. Magn.* 29(1993)2134.
[2] J. Blasco, J. Garcia, G. Subias, *Phys. Rev. B* 83(2011) 104105.
[3] A.H. Eschenfelder, *J. Appl. Phys.*29(1958)378.
[4] M. Tanaka, T. Mizoguchi, Y. Aiyama, *J. Phys. Sot. Japan* 18(1963)1091.
[5] J. A. Kulkarni, V. S. Darshane, *Thermochim. Acta* 93(1985)473.
[6] T. Battault,R. Legros, A. J. Rousset, *European Ceram. Soc.* 15(1995)1141.

Session 13(T9) I-22

STUDIES ON SPINTRONICS-RELATED THIN FILMS USING SYNCHROTRON-RADIATION-BASED MÖSSBAUER SPECTROSCOPY

K. Mibu

Graduate School of Engineering, Nagoya Institute of Technology, Nagoya, Aichi 466-8555, Japan

Mössbauer spectroscopy, which can detect local electronic states around nuclei, has been used to study magnetism of thin films, including surface and interface magnetism, in these decades. The role of this experimental method becomes larger in phase with the recent development of "spintronics", where spins of electrons are actively used for electronic devices.

When Mössbauer spectroscopy is applied to thin films or nanostructures prepared on thick substrates, conversion electron Mössbauer spectroscopy with a radioactive source is usually used in laboratories. With this method, however, it is relatively difficult to perform measurements at special sample conditions, such as at very low temperatures and in magnetic fields. Besides, more and more sensitivity has been required for very thin films and patterned nanostructures prepared on substrates. Synchrotron-radiation-based Mössbauer spectroscopy is a promising method to overcome these problems and make Mössbauer spectroscopy more attractive for researchers in industrial applications of magnetic thin films and nanostructures.

When the synchrotron radiation, which is basically a "white" light source, is used for Mössbauer spectroscopy, special ideas and setups are required. The method which has mainly been used so far for thin film experiments is "time domain" measurements, where interference patterns of pulsed X-rays resonantly scattered by nuclei are detected as a function of time [1]. By analyzing the time spectra, the size and direction of magnetic hyperfine field can be obtained. This method is quite time-effective and the validity for the determination of the direction of magnetization in thin film systems has been well-demonstrated so far [2, 3]. However, magnetic materials for industrial use often have inhomogeneity in the nuclear environments, so that the analysis of time spectra becomes complicated [4]. Therefore, "energy domain" measurements are desirable for industrial applications.

In this presentation, examples of synchrotron-radiation-based Mössbauer spectroscopy in energy domain on thin films performed by our group are introduced. Two methods have been developed and optimized for experiments on magnetic thin films. One is to use a standard absorber to create an energy dip in neV order in the light source [5] (Fig. 1(a)). The other is to use a nuclear Bragg monochromater to monochromatize the light source into neV order [6] (Fig. 1(b)). The dip energy (in the former case) or the peak energy (in the latter case) is modulated by the Doppler shift. The X-rays resonantly scattered by the sample are detected synchronized with the Doppler velocity to obtain Mössbauer spectra in energy domain.

The measured samples are spintronics-related thin films, which include layered Fe/Cr films, where giant magnetoresistance effect was first observed [7, 8], Co_2MnSn Heusler alloy films, where high conduction-electron spin polarization is expected [9], Fe_4N films, where negative anisotropic magnetoresistance was observed [10], and layered Fe/Fe_3O_4 films, where strong antiparallel magnetic coupling is observed [11]. The validity and limitation of the energy-domain methods for industrial application will be discussed.

The synchrotron radiation experiments were performed as a part of Core Research for Evolutional Science and Technology (CREST) Project of Japan Science and Technology Agency in collaboration with Dr. M. Seto (Kyoto Univ.), Dr. Y. Yoda (JASRI/SPring-8), and Dr. T. Mitsui (JAEA) at the beam lines BL09XU and BL11XU, SPring-8. The samples were prepared under the collaborations with Dr. M. A. Tanaka (Nagoya Inst. Tech.), Dr. Tsunoda (Tohoku Univ.), Dr. H. Yanagihara and Dr. E. Kita (Univ. Tsukuba).

[1] E. Gerdau *et al.*, Phys. Rev. Lett. **57** (1986) 1141.
[2] R. Röhlsberger *et al.*, Phys. Rev. Lett. **89** (2002) 237210.
[3] C. L'abbé *et al.*, Phys. Rev. Lett. **93** (2004) 037201.
[4] Yu. V. Shvyd'ko *et al.*, Phys. Rev. B **57** (1998) 3552.
[5] M. Seto *et al.*, Phys. Rev. Lett. **102** (2009) 217602.
[6] T. Mitsui *et al.*, Jpn. J. Appl. Phys. **46** (2007) L930.
[7] M. N. Baibich *et al.*, Phys. Rev. Lett. **61** (1988) 2472.
[8] G. Binasch *et al.*, Phys. Rev. B **39** (1989) 4828.
[9] K. Mibu *et al.*, J. Phys.: Conf. Ser. **200** (2010) 062012.
[10] M. Tsunoda *et al.*, Appl. Phys. Exp. **3** (2010) 113003.
[11] H. Yanagihara *et al.*, Appl. Phys. Exp. **1** (2008) 111303.

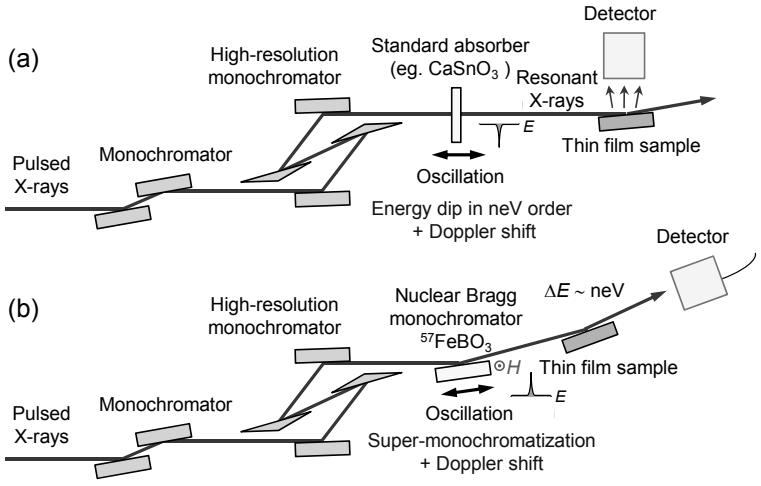

Fig. 1 Typical setups for synchrotron-radiation-based Mössbauer spectroscopy in energy domain for the investigations on thin-film magnetism.

Stability of the ferric state in ion implanted ZnO

K. Bharuth-Ram[1], H. P. Gunnlaugsson[2], H. Masenda[3], K. Johnston[4], G. Langouche[5], R. Mantovan[6], T. E. Mølholt[7], D. Naidoo[3], H. P. Gíslason[7], S. Ólafsson[7], M. B. Madsen[8], and G. Weyer[2]

[1]*School of Physics, University of KwaZulu-Natal, South Africa*
[2]*Department of Physics and Astronomy, Aarhus University, Aarhus, Denmark*
[3]*School of Physics, University of the Witwatersrand, South Africa*
[4]*PH Department, ISOLDE/CERN, Geneva, Switzerland*
[5]*Department of Physics, Katholieke Universiteit - Leuven, Leuven, Belgium;*
[6]*Laboratorio MDM IMM-CNR, Agrate Brianza (MB), Italy;*
[7]*Science Institute, University of Iceland, Reykjavík, Iceland*
[8]*Niels Bohr Institute, University of Copenhagen, Denmark;*

ZnO doped with dilute fractions of transition metal (TM) ions are predicted to be ferromagnetic above room temperature [1]. The potential spintronic applications of such systems have given impetus to considerable investigations on the magnetic properties of TM doped ZnO. While observation of magnetic effects in TM implanted substrates has been reported, the origin of the magnetism remains unclear.

Our Mössbauer emission spectroscopy (MES) measurements following implantation radioactive ^{57}Mn show that the magnetic effects observed at implantation fluences $<10^{12}$ cm^{-2} are due to paramagnetic Fe^{3+} with relatively long relaxation times (> 20 ns) [2]. In addition, recent results show that the Fe^{3+}/Fe^{2+} ratio depends strongly on the implantation fluence [3], and that the ZnO crystal, after low fluence implantation and annealing above 700K and/or long time storage, reverts to its virgin state [4]. We have further investigated this phenomenon in MES measurements on ZnO co-implanted with ^{57}Co and ^{57}Fe.

Two ZnO single crystal substrates were co-implanted with ^{57}Co* ($T_{1/2}$ = 272 d) and ^{57}Fe ions with 50 keV energy to total fluences of ~$1\cdot10^{15}$ ions/cm^2 and ~$3\cdot10^{14}$ ions/cm^2, respectively, at the RIB facility ISOLDE at CERN. MES data were collected, after storage of the samples for about a year, using a resonance detector equipped with stainless steel electrodes enriched in ^{57}Fe.

Spectra obtained with the lower fluence implantation are displayed in Fig 1, in which three components are identified: a crystalline fraction Fe_C (= Fe^{2+}_{Zn}) showing angular dependence and assigned to Fe^{2+} on substitutional Zn sites, a damage fraction Fe_D, most likely due to Co/Fe in implantation induced damaged environments, and a sextet-like distribution due to paramagnetic Fe^{3+}_{Zn} showing slow relaxations.

The MES data obtained at RT for the higher fluence ($1\cdot10^{15}$ ions/cm^2) implanted ZnO show that approx. 50% of the spectral area is due to probe atoms such as Fe_C and the remaining area fraction as Fe_D. After annealing at 400°C, part of the iron in the damage fraction disappears and instead a ~30% fraction occurs as high-spin Fe^{3+} showing fast spin-relaxations [4]

The area fractions of the components for the two samples are compared in Table 1. These results taken together with our earlier studies, show that the implantation at a fluence ~ 10^{14}/cm^2 apparently stabilises the Fe^{3+} charge state in ZnO.

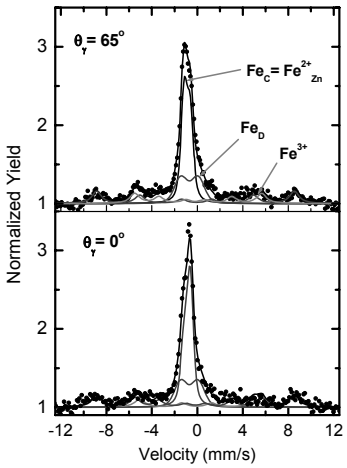

Figure 1: RT Mössbauer emission spectra of ZnO implanted with 3 x 10^{14} ^{57}Co/^{57}Fe, collected at the angles indicated.

Table 1: Areal fractions of components observed RT at the two implantation fluencies in ZnO

Spectral component	Fluence 1 x 10^{15}/cm^2	Fluence 3 x 10^{14}/cm^2
$Fe_C = Fe^{2+}_{Zn}$	52(5)%	44(5)%
Fe^{3+}_{Zn}	< 5%	34(4)%
Fe_D	48(5)%	22(4)%

[1] T. Dietl et al., Science 287 (2000) 1019
[2] H.P. Gunnlaugsson et al., App. Phys. Lett. 92 (2010) 142501
[3] T.E. Molholt et al., Physica B 404 (2009) 4820
[4] D. Naidoo et al. (to be published)
[5] H. P. Gunnlaugsson et al., Appl. Phys. Lett. 100(2012)042109

Session 13(T4) Oral-19

MÖSSBAUER STUDY OF GAMMA'''-IRON NITRIDE FILMS

Y. Yamada[1], R. Usui[1], and Y. Kobayashi[2]
[1]*Tokyo University of Science,* [2]*RIKEN*

Iron nitride has many phases and each phase has different magnetic characteristics. Iron nitride films or particles have been prepared by various methods [1]. FeN has been reported to have two phases, γ''-FeN (ZnS structure) and γ'''-FeN (NaCl structure), which generally form simultaneously so that it is difficult to produce a single phase [2-6]. We have previously reported that the yields of the two phases could be varied and pure γ''-FeN and γ'''-FeN could be obtained by varying the substrate temperature during pulsed laser deposition (PLD) [7]. In this study, Mössbauer spectra of a γ'''-FeN film were measured at the temperatures between 5 and 300 K to observe the temperature dependence of hyperfine field.

PLD was performed using a Nd:YAG laser (wavelength: 532 nm, pulse energy: 85 mJ, repetition rate: 10 Hz). A Fe metal sheet was employed as the target material. The focal point of the laser light was continually scanned across the flat surface of the Fe metal target to prevent droplets from forming. The vapor was deposited on an Al substrate and 1.1×10^5 pulses were irradiated. The pressure of the N_2 atmosphere was maintained at the desired pressure between 1 and 1300 Pa. The Al substrate was maintained at the desired temperature between 100 and 520 K. The film samples were measured by Mössbauer spectroscopy (Wiessel, MDU1200) in the temperature range between 5 and 300 K, and XRD (RINT2500, Rigaku; Cu-Kα) patterns were measured to confirm the assignments.

FeN films were produced by PLD in 70 Pa of N_2 atmosphere varying the temperature of the substrate between 100 and 520 K while deposition; γ''-FeN was dominant at low substrate temperatures, whereas γ'''-FeN was dominant at high substrate temperatures. The assignments were confirmed by XRD patterns of the samples. The film produced at 100 K was almost pure γ''-FeN showing a paramagnetic singlet in the temperature range between 5 and 300 K. The film produced at 520 K was pure γ'''-FeN, and the Mössbauer spectra of the sample were measured in the temperature range between 5 and 300 K (Fig. 1). The spectrum measured at 5 K showed two sets of sextets. Since the sextets had broad half widths, the spectra were fitted by assuming distributions of hyperfine magnetic fields. The abundant hyperfine magnetic fields were H = 300 kOe and 500 kOe. The spectrum measured at 300 K showed a combination of a singlet and a doublet. Comparison of the area intensities of the spectra reveals that the doublet corresponds the components with H = 300 kOe, and the singlet corresponds the component with H = 500 kOe. Ratio of the two components was 3:1. Pure γ'''-FeN was antiferromagnetic with H = 300 kOe at 5 K and the hyperfine magnetic field decreased with increasing the temperature: the Néel temperature was found to be 220 K. Another component show hyperfine magnetic field H = 500 kOe at 5 K and became a singlet at room temperature. This component did not show clear Néel temperature. The origin of the second component may be a defect of γ'''-FeN. We are currently performing density functional calculations to help clarify the structure and the defects of γ'''-FeN.

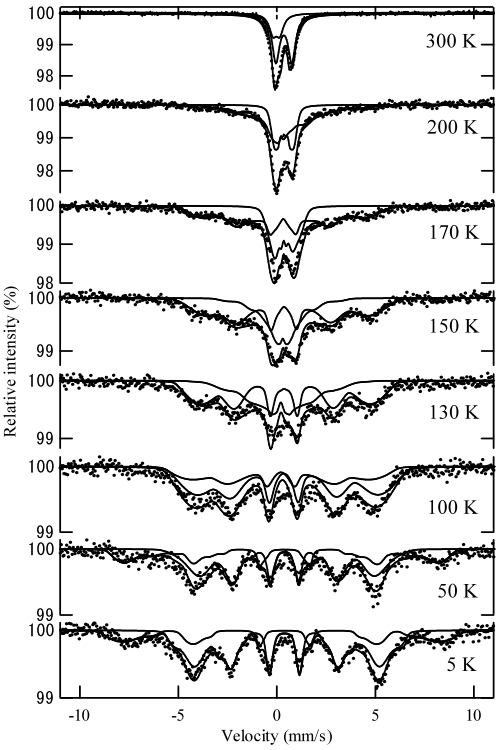

Figure 1. The Mössbauer spectra of the γ'''-FeN film measured at temperatures between 5 and 300 K

[1] P. Schaaf, *Progress in Materials Science* 47 (2002) 1
[2] T. Hinomura, S. Nasu, *Physica* B 237–238 (1997) 557
[3] I. Jouanny, P. Weisbecker, V. Demange, M. Grafouté, O. Peña, E. Bauer-Grosse, *Thin Solid Films* 518 (2010) 1883
[4] P. Schaaf, C. Illgner, M. Niederdrenk, K. P. Lieb, *Hyp. Int.* 95 (1995) 199
[5] P. Prieto, J. F. Macro, J. M. Sanz, *Surf. Interface Anal.* 40 (2008) 781
[6] H. Nakagawa, S. Nasu, H. Fuji, M. Takashi, and F. Kanamaru, *Hyp. Int.* 69 (1991) 455
[7] R. Usui, Y. Yamada and Y. Kobayashi, *Hyp. Int.* 205 (2012) 13

PROPERTIES OF INTERSTITIAL Fe IN α-Al_2O_3

H.P. Gunnlaugsson[1], K. Johnston[2], H. Masenda[3], G. Langouche[4], K. Bharuth-Ram[5,6], H.P. Gislason[7], M.B. Madsen[8], R. Mantovan[9], T.E. Mølholt[7], D. Naidoo[3], M. Ncube[3], S. Ólafsson[7], G. Weyer[1] and the ISOLDE collaboration[2]

[1]*Department of Physics and Astronomy, Aarhus University, DK-8000 Aarhus C, Denmark*
[2]*PH Dept, ISOLDE/CERN, 1211 Geneva 23, Switzerland*
[3]*Instituut voor Kern- en Stralingsfysica, University of Leuven, B-3001 Leuven, Belgium*
[4]*School of Physics, University of the Witwatersrand, WITS 2050, South Africa*
[5]*School of Physics, University of KwaZulu-Natal, Durban 4001, South Africa*
[6]*iThemba LABS, P.O. Box 722, Somerset West 7129, South Africa*
[7]*Science Institute, University of Iceland, Dunhaga 3, IS-107 Reykjavík, Iceland*
[8]*Niels Bohr Institute, University of Copenhagen, DK-2100 Copenhagen, Denmark*
[9]*Laboratorio MDM, IMM-CNR, Via Olivetti 2, 20864 Agrate Brianza (MB), Italy.*

Room temperature ^{57}Fe emission Mössbauer spectra of α-Al_2O_3 samples implanted with ^{57}Co ($T_{½}$ = 271 d) [1] or ^{57}Mn ($T_{½}$ = 1.5 min.) [2, 3] are dominated by lines originating from Fe^{2+} (Fe(II)) in implantation damage sites and Fe^{3+} (Fe(III)) showing slow paramagnetic relaxation, together with a single line (SL) of disputed origin [1-3].

Here we present new experimental data obtained on ^{57}Co and ^{57}Mn implanted single crystalline α-Al_2O_3 samples. These new data show evidence that the intensity of this single line exhibits a distinct angular dependence.

There are (at least) two possible explanations for the angular dependence of the intensity of the SL: (1) due to an anisotropic recoilless fraction [4] and/or (2) due to fast localised diffusion of Fe in an interstitial cage [5]. Both models can explain the observed angular dependence. However, the SL is found to have a negligible quadrupole interaction ($|\Delta E_Q| < 0.05$ mm/s), which seems inconsistent with a non-cubic surrounding lattice configuration and instead suggests an interpretation of this line as due to interstitial cage motion.

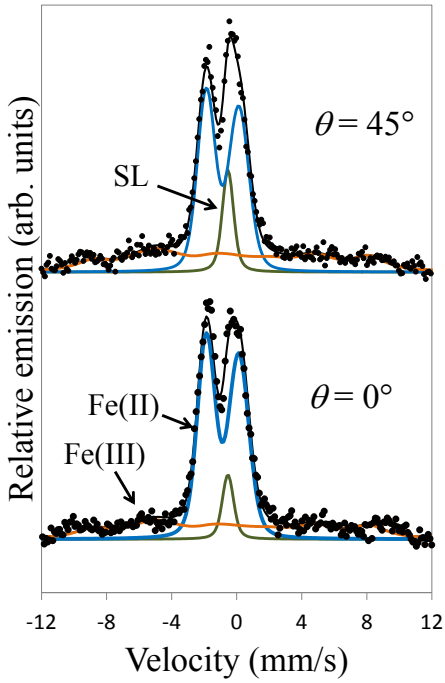

Fig. 1: Room temperature ^{57}Fe emission Mössbauer spectra obtained on an α-Al_2O_3 sample implanted with ~3×10^{12} cm^{-2} ^{57}Co and ~5×10^{14} cm^{-2} ^{57}Fe under the emission angles indicated.

[1] I. Dézsi *et al.*, *J. Phys.: Condens. Matter* **12** (2000) 2291.
[2] H.P. Gunnlaugsson *et al.*, *Hyp. Int.* **198** (2010) 5.
[3] Y. Kobayashi *et al.*, *Hyp. Int.* **198** (2010) 173.
[4] V.I. Goldanskii and E.F. Makarov, Fundamentals of gamma-resonance spectroscopy. In Chemical applications of Mössbauer spectroscopy, V.I. Goldanskii and R.H. Herber (Eds.) pp. 1-113 (Academic Press, New York, 1968).
[5] W. Petry and G. Vogl, *Z. Phys. B - Cond. Mat.* **45** (1982) 207.

Corresponding author: guido.langouche@kuleuven.be

Session 13(T4) Oral-21

^{57}Fe Mössbauer spectroscopy study of superconducting $Sm_{0.85}Ba_{0.15}FeAsO$ doped with fluorine

V. O. Pelenovich, Y. L. Chen*, R. Z. Xiao, S. Y. Liu, D. J. Fu **

Key Laboratory of Artificial Micro- and Nano-Materials of Ministry of Education and Accelerator Laboratory, School of Physics and Technology, Wuhan University, 430072 Wuhan, China

Recent discovery of high-T_c superconductivity in iron arsenide oxides ReFeAsO (Re–rare earth element) doped with fluorine excited interest in the research into superconductors beyond hight-T_c superconducting cuprates. The highest T_c in $SmFeAsO_{1-x}F_x$ has reached 56K [1]. Without fluorine doping SmFeAsO does not show superconductivity, but has antiferromagnetic ordering below 130K. The magnetic order may be suppressed by fluoride doping and superconductivity appears [2]. In the present work we investigate Mossbauer spectra of new superconductor $Sm_{0.85}Ba_{0.15}FeAsO_{0.70}O_{0.30}$ (T_c~37K) in the temperature range 20-290K. The Mossbauer spectra were recorded using a conventional spectrometer in transmission geometry. ^{57}Co in Rh matrix was used as a gamma ray source. The spectra appeared to be a singlet pattern throughout the temperature range, except a doublet corresponding to small amount of foreign phase (Fig. a). Hyperfine parameters of the singlet at room temperature: δ_{CS} =0.40 mm/s, Γ = 0.28 mm/s. For the doublet, the parameteres are δ_{CS} =0.42 mm/s, QS=0.55 mm/s, corresponding to FeAs. Below 80K the doublet changed into a sextet. This changing is conformed to the magnetic order transition in FeAs with a Neel temperature of 77K. Within the Debye model framework the Debye temperature of the superconductor is obtained (θ_D ~390K). An anomaly near T_c is observed on the temperature dependence of central shift (Fig. b). Similar behavior of temperature dependence had been found in $Ba_2EuCu_3O_{9-x}$ near T_c [3]. The anomaly is explained by the change of electron density at the iron nuclei. Phonon softening near T_c has not yet been observed within the experimental uncertainty.

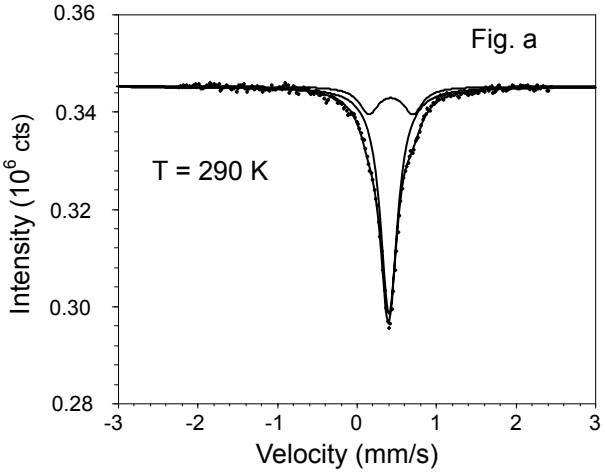

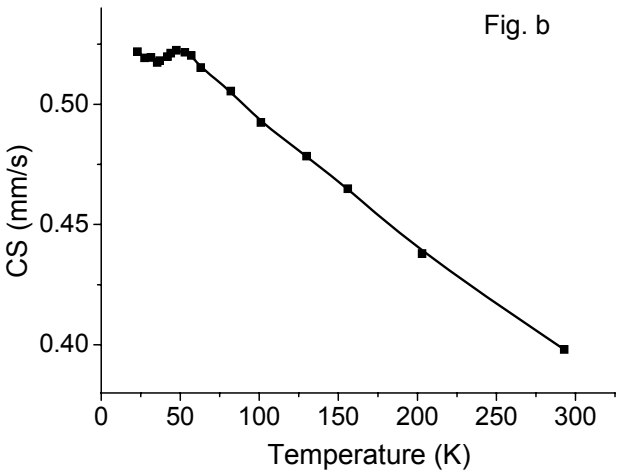

[1] Ren Z-A et al., Chinese Phys. Lett. 25, 2215 (2008).
[2] Ding L et al., Phys. Rev. B 77, 180510 (R) (2008).
[3] Liu R. et al., Chinese Phys. Lett. 5 (5), 213 (1988).

* ylchen@whu.edu.cn; ** djfu@whu.edu.cn

MÖSSBAUER EFFECT STUDY ON THE ENHANCED MICROWAVE PERMEABILITY OF Fe-Si-Al ALLOY

Mangui Han, Longjiang Deng

State Key Laboratory of Electronic Thin Films and Integrated Devices, University of Electronic Science and Technology of China, Chengdu, 610054,China.

The ternay Fe-Si-Al magnetic alloys (also known as "Sendust") with the compositions of $Fe_{(88\text{-}81\%)}Si_{(8\text{-}11\%)}Al_{(4\text{-}8\%)}$ is well known for their excellent soft magnetic properties. Recently, there is increasing interests in them due to their promising applications in suppressing the unwanted electromagnetic radiations from electronic devices working in the quasi-microwave band [1]. In this contribution, we present the shape effect of FeSiAl particles on their microwave permeability using the ^{57}Co(Rh) source Mössbauer spectroscopy. The starting powder material of $Fe_{84.94}Si_{9.68}Al_{5.38}$ alloy with irregualar particle shape has been milled into the flake shape by ball milling of 30 hours. The high frequency measurements show that the particles with flake shape exhibit significant enhancement in microwave permeability, see Fig. 1(a) and (b). The Mössbauer spectra are shown in Fig. 2. It is found that the unmilled powder exhibit 8 obvious absorption peaks, while only 6 absorption peaks can be found in the Fe-Si-Al sample with flaky particles. According to the well-established theory: $I_{2,5}/I_{3,4} = (4\sin^2\theta)/(1+\cos^2\theta)$, where θ is the angle between the magnetic moment and the γ-ray, I is the relative intensity of absorption peak, it can be inferre from Fig. 2(a) and (b) that the magnetic moments in umilled particles align randomly, while they strongly tend to align in the plane of a flaky particle which is believed beneficial to increase the microwave permeability. The measured Mössbauer spectra have been fitted based on the fact that Fe atoms in the Fe-Si-Al alloy system have many different surrounding environments in the disorder α-Fe(Si,Al) crystal structure[2]. The distributions of hyperfine magnetic field (Bhf) and isomer shift are shown different and are helpful to understand the observed shape effects on the microwave permeability on the atomic scale.

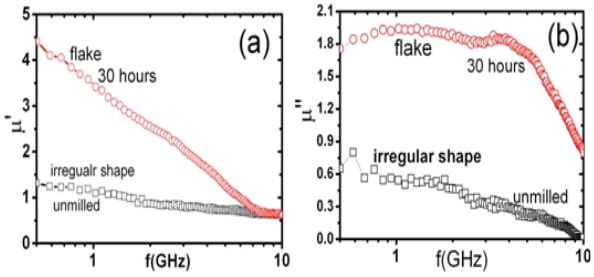

Fig.1. Effect of particle shapes on the microwave permeability

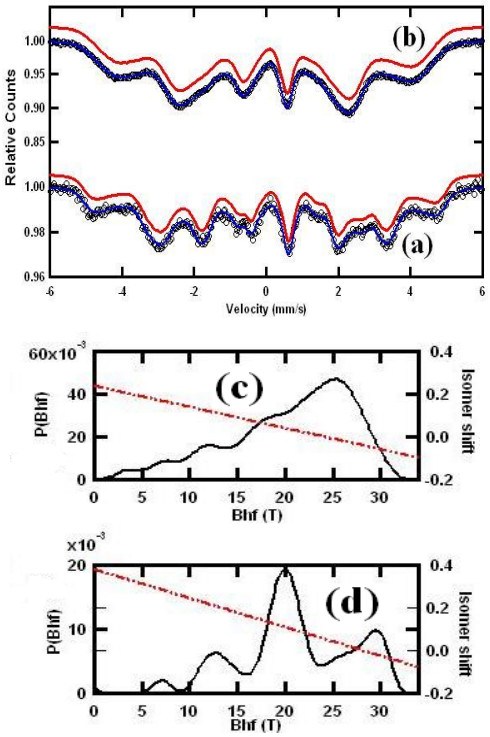

Fig. 2. Transmission Mössbauer spectra of Fe-Si-Al powder with different shape and the distributions of hyperfine interaction parameters. (a) and (d) are for irregualr shape particles; (b) and (c) are for flaky particles.

[1] M. Han, D. Liang, J. Xie, L. Deng, J. Appl. Phys. 111(2012)07A317.

[2] O. Ikeda, I. Ohnuma, et al, Intermetallics, 9(2001)755.

Session 14(T11) Oral-23

WHAT CAN WE LEARN ABOUT Fe-Cr ALLOYS WITH MÖSSBAUER SPECTROSCOPY?

S.M. Dubiel

Faculty of Physics and Applied Computer Science, AGH University of Science and Technology, 30-059 Kraków, Poland

Fe-Cr alloys have been of industrial interest since a century or so, since they are the basis for a production of a large class of important engineering materials known as stainless steels (SS). SS possess excellent mechanical properties connected with good corrosion resistance, also at elevated temperatures. For these reasons they have been used as construction materials in various branches of industry including (nuclear) power plants, oil refinery and others. Recently, an interest in these materials has significantly increased as they are considered as good candidate for new generation of reactors and for other technologically important plants [1-8].

However, these materials also have some drawbacks. The ferrite in ferritic, martensitic and duplex SS is susceptible to the "475°C embrittlement", which is harmful to the mechanical properties. The embrittlement stems from a phase separation into regions rich in iron (α) or those rich in chromium (α'). The detrimental effect has also the formation of the σ phase as well as an irradiative environment to which devices constructed from SS are often exposed at service.

The primary goal of the renewed interest in the Fe-Cr alloys is to improve their useful properties through a better i.e. more profound understanding of the phenomena responsible for their properties.

In this contribution it will be shown that the Mössbauer Spectroscopy (MS) is likely the most suitable techniques to quantitatively study various aspects of scientific and industrial interests in the Fe-Cr alloys. The emphasis will be put on the latter. In particular, applications of MS in the investigation of the phase separation into α and α', kinetics of the σ phase precipitation, determination of the σ phase properties (Curie and Debye temperatures), distribution of atoms over neighbouring coordination shells (short-range order), and the effect of irradiation on these phenomenta will be illustrated and discussed.

[1] L. K. Mansu et al., J. Nucl. Mater., **329** (2004) 166
[2] L. Malerba et al., J. Nucl. Mater., **382** (2008) 112
[3] A. V. Ruban et al., Phys. Rev. B, **77** (2008) 094436
[4] K. H. Lo et al., Mater. Sci. Eng. R, **65** (2009) 39
[5] I. Mirebeau and G. Parette, Phys. Rev. B, **82** (2010) 104203
[6] W. Xiong et al., Crit. Rev. Sol. State Mater. Sci., **35** (2010) 125
[7] S. M. Dubiel and J. Cieślak, Phys. Rev. B, **83** (2011) 180202(R)
[8] S. M. Dubiel and J. Cieślak, Crit. Rev. Sol. State Mater. Sci., **36** (2011) 192

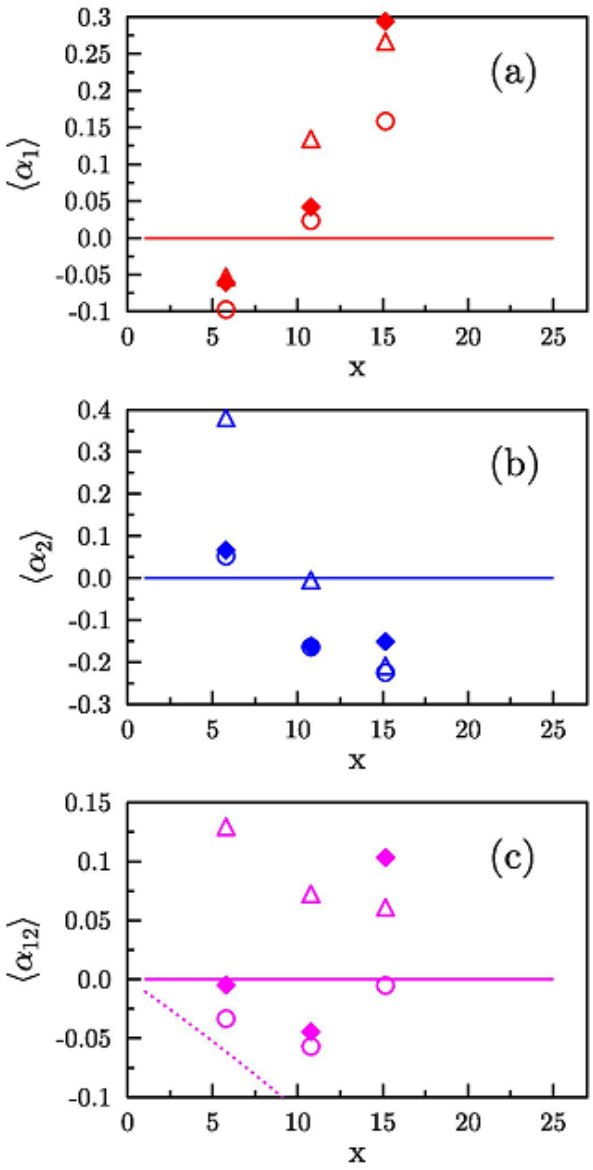

Fig. 1 Cowley average short-range order parameters as found for $Fe_{100-x}Cr_x$ alloys in three different metallurgical states : quenched (△), cold-rolled (○) and equilibrium (◆) for (a) the first-neighbour shell, (b) the second-neighbour shell (b) and (c) both neighbour shells. The dashed-line in (c) indicates the minimum allowed value of $<\alpha_{12}>$.

STUDY OF PHASE SEPARATION IN Fe-Cr ALLOYS*

S.M.Dubiel, and J.Żukrowski

AGH University of Science and Technology, Faculty of Physics and Applied Computer Science, 30-059 Kraków, Poland

Despite Fe-Cr alloys have been the subject of numerous studies, a knowledge of their properties is not yet complete. In particular, data relevant to a miscibility gap (MG), the pecularity of the phase diagram of the system, are not known with enough precision. The MG and underlying mechanism(s) are of interest not only *per se* as a scientific curosity but also because the MG is responsible for an enhanced embritlement, the so called "475°C embrittlement", which is detrimental to mechanical properties of industrially important construction materials produced from the Fe-Cr alloys viz. stainless steels (SS). SS possess exceptionally good mechanical properties combined with a good corrosion resistance at elevated temperatures. For these reasons they have been used as construction materials in various branches of industry including (nuclear) power plants, oil refineries and others. Recent interest in these materials stems from the fact that they are considered as good candidate for a new generation (IV) of reactors and for other technologically important plants [1-4].

Concerning the industrially important aspect of the MG, a precise knowledge of its Fe-rich border is of relevance. Classical [5,6] and freshly published theoretical calculations [7,8] show significant differences that are especially meaningful at temperatures T < ~700 K. A lack of a suitable experimental data available in the literature does not allow to verify the calculations.

Here we report on the Mössbauer spectroscopic study of two issues pertinent to the MG viz. determination of: (1) its Fe-rich border, and (2) activation energy, E, for the phase decomposition. As samples, a $Fe_{100-x}Cr_x$ alloy with x = 15 in form of ~0.2 mm plates, obtained by a cold-rolling, in two different states were used: (a) non-irradiated and (b) irradiated with 25 keV He-ions to a final dose of 7.5 dpa. ^{57}Fe spectra were recorded in CEMS mode at 300 K. The phase decomposition into Fe-rich (α) and Cr-rich (α') phases was done by a vacuum isothermal annealing at T_1 = 688 K, and T_2 = 723 K for different periods of time, t. The spectra were analysed in terms of a superposition method described in detail elsewhere [9]. Based on spectral parameters obtained, an average hyperfine field, $<B>$, a quantity pertinent for determining the composition of the α-phase, was calculated as described in Ref. [9]. The x-values found with this procedure are displayed in Fig. 1 together with theoretically calculated lines. It is clear that our data, for the non-irradiated sample, is in disaccord with C, D and E lines. Also it is evident that for the irradiated sample the concentration of Cr in the α-phase is significantly higher (the MG is narrower). The activation energy was found using the Arrhenius law and the knowledge of the rate constant, k, for T_1 and T_2. The k-values were derived from the time dependence of $<B>$, as shown in Fig. 2.

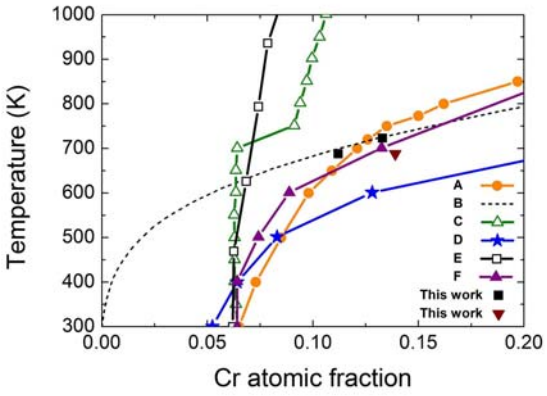

Fig. 1 Fe-rich borders of the miscibility gap in Fe-Cr as calculated A-F [8], and, as determined in this work: squares are for the non-irradiated sample, the triangle for the irradiated one.

In this way, the activation energy of the phase decomposition in the temperature interval of 688-723 K for the non-irradiated sample was estimated as 2.24 eV or 216 kJ/mol. This value is very close to the activation energy of the σ-phase formation in the Fe-Cr system. Finally, the difference in E between irradiated and non-irradiated sample, ΔE = 0.03 eV (2.9 kJ/mol) was found.

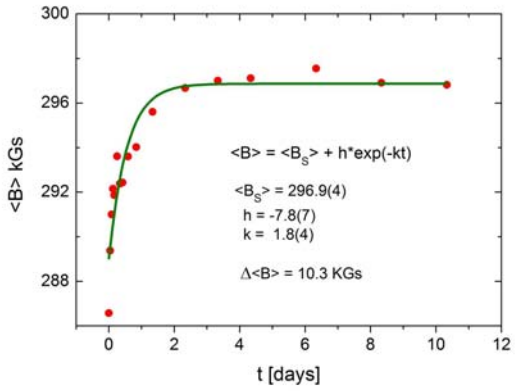

Fig. 2 Average hyperfine field, $<B>$, vs. annealing time, t, for the non-irradiated sample vaccum annealed at 723 K.

* Supported by Association EURATOM-IPPLM and Ministry of Science and Higher Education, Warsaw, Poland.

[1] L. K. Mansu et al., J. Nucl. Mater., **329** (2004) 166
[2] L. Malerba et al., J. Nucl. Mater., **382** (2008) 112
[3] A. V. Ruban et al., Phys. Rev. B, **77** (2008) 094436
[4] K. H. Lo et al., Mater. Sci. Eng. R, **65** (2009) 39
[5] O. Kubaschewski, Iron-binary phase diagrams, Springer Verlag, Ber (1982)
[6] J.-O. Andersson and B. Sundman, Calphad, **11** (1987) 83
[7] W. Xiong et al., Crit. Rev. Sol. State Mater. Sci., **35** (2010) 125
[8] M. Levesque et al., Phys. Rev. B, **84** (2011) 184205
[9] S. M. Dubiel and G. Inden, Z. Metallkde, **78** (1987) 544

Session 14(T11) Oral-25

MAGNETIC HYPERFINE FIELDS ON ^{119}Sn PROBE NUCLEI AND THE FEATURES OF MAGNETIC EXCHANGE IN 3d-, 4f-, AND URANIUM-BASED INTERMETALLIC COMPOUNDS

V.I. Krylov
Institute of Nuclear Physics, Moscow State University, 119992 Moscow, Russia
vkrylovmag@gmail.com

The results of Mössbauer spectroscopy (MS) investigation of the magnetic hyperfine fields (HFs) on ^{119}Sn probe nuclei for the different groups of the intermetallic compounds based on the 3d-, 4f-elements and uranium are presented in this work. The observed regularities of the spin density formation on the nuclei of nonmagnetic tin atoms reflect the specific features of the magnetic 3d-3d, 4f-4f, 3d-4f, and 5f-5f exchange interactions. It has been shown that the mechanisms of electron polarization on ^{119}Sn nuclei are significantly different for the following groups of the compounds.

1. The compounds TFe_2 (T=Sc, Ti, Y, Zr, Lu, Hf, U) with cubic $MgCu_2$-type and hexagonal $MgZn_2$-type Laves structures are ferromagnets (FM) except for $TiFe_2$ that is an antiferromagnetic (AFM). The Fe-Fe magnetic exchange interaction is responsible for magnetic ordering of the TFe_2 compounds. In the FM compounds TFe_2, the HFs for ^{119}Sn atoms localized on T-sites (B_1) are positive and proportional to the Fe magnetic moments: $B_1=A_1\times\mu_{Fe}$, where $A_1=28$ T/μ_B is the hyperfine coupling constant. The HF B_1 reaches the value of about 50 T for ^{119}Sn in $ZrFe_2$ [1]. The HFs for ^{119}Sn atoms localized on Fe-sites (B_2) are negative: $B_2=A_2\times\mu_{Fe}$, where $A_2=-3.8$ T/μ_B.

2. In the ordered alloys of rare earth metals (RE) with p-metals, the HFs for ^{119}Sn atoms occur due to 4f-4f indirect magnetic interaction and reach the values of 40 T. Systematics of the HFs for ^{119}Sn in the FM and AFM binary Gd - X compounds (X is a p-metal) of different compositions and crystalline structures are presented in this work. The HFs on ^{119}Sn nuclei are induced by the nearest neighboring Gd magnetic moments. The HF values on ^{119}Sn nuclei in $REAl_2$ и REGa ferromagnetic compounds are proportional to the spin magnetic moment of RE ions [2, 3].

3. The HFs for ^{119}Sn probe atoms in the Gd -Ni, Gd –Rh, GdT_2 (T=Ni, Ru, Rh, Os, Ir, Pd, Pt), GdT_5 (T=Cu, Ni, Rh, Pt), $RERu_2$ (RE= Pr, Nd, Gd, Tb, Dy, Ho) compounds have been investigated. It was shown that transition d-metals have a significant influence on ^{119}Sn HF values despite the absence of the localized magnetic moment of d-metals. The values of the HFs for ^{119}Sn in this group of the compounds are much smaller than corresponding ones for ^{119}Sn in the isostructural compounds of RE metals with p-metals.

4. Huge HFs reaching to 56 T have been found for ^{119}Sn atoms localized on RE-sites of RE-3d compounds (3d are Fe, Co and Mn atoms with the localized magnetic moments) [1]. This value is the maximum of the known HF values for ^{119}Sn atoms in the metallic magnets. It has been shown that the HFs are formed due to two additive contributions of RE- and 3d-magnetic sublattices [4]. The temperature dependencies of the HFs for ^{119}Sn atoms localized on RE- and 3d-sites of $REFe_2$, $RECo_2$, $RECo_5$ compounds, are directly related to the temperature changes of 4f-4f, 3d-4f and 3d-3d exchange interactions.

5. The selectivity of the magnetic hyperfine interaction for ^{119}Sn atoms to the certain 3d-3d or 4f-4f magnetic exchange interactions of the ternary RE-based intermetallic compounds has been observed. The HFs on ^{119}Sn nuclei localized in Si sites of GdMnSi and GdCoSi ferrimagnetic compounds are induced only by Gd magnetic moments. The contributions of Mn and Co magnetic moments to the HF are equal to zero [5]. On the contrary, the HFs for ^{119}Sn atoms localized in Ge-positions of $REMn_2Ge_2$ compounds are formed only by the Mn-magnetic moments.

6. The HFs on ^{119}Sn nuclei in UTM (T is a d-metal, M is a p-metal) compounds with ZrNiAl-type crystal structure are proportional to the full magnetic moment of U-ions: $B = A \times \mu_U$, where A= 6.5(4) T/μ_B. The HFs are formed by the nearest U-ions and reach of 10 T [6]. The results of ^{119}Sn MS study on UPdSn, UCuSn, UAuSn, UNiSn, UCuGe [7], UGa_3, UIn_3, UPb_3, UGa_2, UGe_2, USn_2 [8] compounds indicate a strong anisotropy of the magnetic hyperfine interaction and magnetic exchange interaction caused by the significant nonsphericity of 5f-electron shell of uranium ion.

Among the 3d-, 4f-, and U-magnetic moments, the ability to create an spin polarization on the ^{119}Sn nuclei is the largest for 3d-moments (in equivalent of the unit magnetic moment) and this one is the smallest for the unit magnetic moment of RE-ions.

[1] V.I. Krylov, N.N. Delyagin. J. Magn. Magn. Mater. 305 (2006) 1
[2] N.N. Delyagin, V.I. Krylov, I.N. Rozantsev. J. Magn. Magn. Mater. 308 (2007) 74
[3] N.N. Delyagin, V.I. Krylov. Sol. State Commun. 126 (2003) 401
[4] N.N. Delyagin, V.I. Krylov. J. Phys.: Condens. Matter. 19 (2007) 086205
[5] N.N. Delyagin, V.I. Krylov, G.T. Mujiri, V.I. Nesterov, S.I. Reiman. Phys. Stat. Sol. (b), 131 (1985) 555
[6] V.I. Krylov. J. Appl. Phys.109 (2011) 07E140
[7] V.I. Krylov, N.N. Delyagin, S.I. Reiman, I.N. Rozantsev, A.V. Andreev, V. Sechovský. J. Alloys. Comp. 347 (2002) 36
[8] V.I. Krylov, N.N. Delyagin, S.I. Reiman, I.N. Rozantsev, A.V. Andreev, V. Sechovský. J. Alloys. Comp. 343 (2002) 33

STUDY ON THE STRUCTURE AND ELECTRONIC STATE OF THIOLATE-PROTECTED GOLD CLUSTERS BY MEANS OF ^{197}Au MOSSBAUER SPECTROSCOPY

N. Kojima[1*], Y. Kobayashi[2], T. Tsukuda[3], Y. Negishi[4], G. Harada[1], T. Sugawara[1] and M. Seto[2]

[1]Graduate School of Arts and Sciences, The University of Tokyo, Tokyo 153-8902, Japan, [2]Research Reactor Institute, Kyoto University, Osaka 590-0949, Japan, [3]Graduate School of Science, The University of Tokyo, Tokyo 113-0033, Japan, [4]Department of Chemistry, Graduate School of Science, Tokyo University of Science, Tokyo 162-8601, Japan. *e-mail:cnori@mail.ecc.u-tokyo.ac.jp, phone/fax:+81-3-5454-6741

In the last decade, small Au clusters composed of less than 100 atoms protected by organic ligands have attracted much attention as a prototypical system for fundamental studies on quantum size and as a building block of nano-scale devices [1]. Among small Au clusters, the Au-thiolate compound composed of 25 Au atoms and 18 thiolates ($Au_{25}(SR)_{18}$) has been studied most extensively as a prototype system of stable $Au_n(SR)_m$ clusters [2]. According to the structural analysis, $Au_{25}(SC_2H_4Ph)_{18}$ is composed of an icosahedral Au_{13} core whose surface is protected by six staples, –S(R)–Au–S(R)–, which is shown in Fig. 1 [3]. Based on the geometrical structure of $Au_{25}(SC_2H_4Ph)_{18}$, we have successfully analyzed the ^{197}Au Mössbauer spectra of $Au_n(SG)_m$ (n = 10 – ~55) and dodecanethiolate-protected Au clusters with the average diameters of 2 – 4 nm [4].

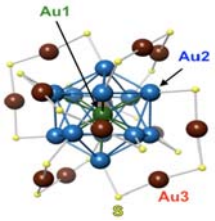

Figure 1. Core structure of $Au_{25}(SC_2H_4Ph)_{18}$ [3],

The $Au_n(SG)_m$ samples with (n, m) = (10, 10) - (~55, m) were fractionated using polyacrylamide gel electrophoresis (PAGE) [5]. In order to obtain the ^{197}Au Mössbauer spectra with sufficient S/N ratio, each cluster was accumulated up to 50 - 100 mg by repeating the elaborative PAGE procedure [6]. The dodecanethiolate-protected Au clusters with the average diameters of 2 nm and 4 nm were prepared by the direct chemisorption method and the ligand-exchange method, respectively [7]. ^{197}Au Mössbauer measurement was carried out at Research Reactor Institute of Kyoto University. The γ-ray source (77.3 keV), ^{197}Pt, was generated by the neutron irradiation to 98 % - enriched ^{196}Pt metal foil. The γ-ray source and samples were cooled down to 16 K. The isomer shift of Au foil was referenced to 0 mm/s.

The ^{197}Au Mössbauer spectra of $Au_n(SG)_m$ are shown in Fig. 2. These spectra were analyzed based on the structure of $Au_{25}(SR)_{18}$ (SR = SC_2H_4Ph). The Mössbauer spectra of a series of $Au_n(SG)_m$ evolve drastically as a function of the core size. Asymmetric doublet profile of the $Au_{10}(SG)_{10}$ spectrum can be fitted by a superposition of two sets of doublets, which correspond to the Au(I) atoms directly coordinated by two SG ligands.

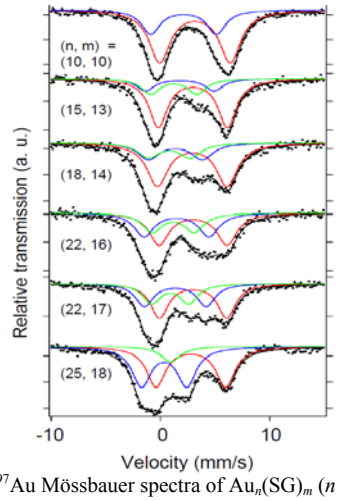

Figure 2. ^{197}Au Mössbauer spectra of $Au_n(SG)_m$ (n = 10 – 25) [4].

The spectra of $Au_n(SG)_m$ ($15 \leq n \leq 22$) can be fitted by three sets of doublets. Two components are assigned to the Au(I) atoms coordinated by two SG ligands since the *IS* and *QS* values are smoothly correlated to those of $Au_{10}(SG)_{10}$. The third component having the smallest *IS* and *QS* values is assigned to the Au(I) atoms coordinated by single SG ligand which is smoothly correlated to those of the Au(I) atoms coordinated by single SG ligand in $Au_{25}(SR)_{18}$. The spectral profile abruptly changes on going from $Au_{22}(SG)_{16}$ to $Au_{25}(SG)_{18}$, where a core Au atom free from SG appears for the first time, then it smoothly changes to that of $Au_{\sim 55}(SG)_m$.

In this paper, we will review the molecular structures and the Au electronic states of small Au clusters composed of less than 100 Au atoms protected by organic ligands by means of ^{197}Au Mössbauer spectroscopy.

[1] M.-C. Daniel, D. Astruc, Chem. Rev. 104 (2004) 293.
[2] (a) T. G. Schaff, R. L. Whetten, J. Phys. Chem. B104 (2009) 2630, (b) R. C.Price, R. L. Whetten, J. Am. Chem. Soc., 127 (2005) 13750, (c) H. Tsunoyama, Y. Negishi, T. Tsukuda, J. Am. Chem. Soc., 128 (2006) 6036.
[3] (a) M. W Heaven, A. Dass, P. S. White, K. M. Holt, R. W. Murray, J. Am. Chem. Soc., 130 (2008) 3754, (b) M. Zhu, E. Lanni, N. Garg, M. E. Bier, R. Jin, J. Am. Chem. Soc., 130 (2008) 1138.
[4] N. Kojima, K. Ikeda, Y. Kobayashi, T. Tsukuda, Y. Negishi, G. Harada, T. Sugawara, M. Seto, Hyperfine Interactions, (2012) in press.
[5] Y. Negishi, K. Nobusada, T. Tsukuda, J. Am. Chem. Soc. 127 (2005) 5261.
[6] K. Ikeda, Y. Kobayashi, Y. Negishi, M. Seto, T. Iwasa, K. Nobusada, T. Tsukuda, N. Kojima, J. Am. Chem. Soc., 129 (2007) 7230.
[7] O. Nagao, G. Harada, T. Sugawara, A. Sasaki, Y. Ito, Jpn. J. Appl. Phys., 43 (2004) 7742.

Session 15(T10) Oral-26

MÖSSBAUER AND MAGNETIZATION STUDIES OF NICKEL FERRITE NANOPARTICLES SYNTHESIZED BY THE MICROWAVE-COMBUSION METHOD

M. H. Mahmoud[1], A. M. Elshahawy[1*], Salah A. Makhlouf[1], and H. H. Hamdeh[2]

[1]*Department of Physics, Assiut University, Assiut, Egypt 71516*
[2]*Department of Physics, Whichita State University, Whichita, KS USA*

Recently, various methods have been developed to synthesize nanocrystalline $NiFe_2O_4$. In the present study, Nanocrystalline Nickel ferrite were synthesize from a stoichiometric mixture of corresponding metal nitrates and urea powders, using microwave assisted combustion method. The process was a convenient, inexpensive and efficient preparation method for the $NiFe_2O_4$ nanomaterial. It takes only a few minutes to obtain as-received Ni-ferrite powders. The metallic nitrates and urea were heated in microwave oven using the power of 800W. Significant effect of the ratio between urea and nitrates on the physical parameters like crystalline phase, lattice constant and magnetic properties of the nanoparticles has been investigated. The structural and magnetic properties of the samples were determined by X-ray powder diffraction (XRD), transmission electron microscopy (TEM), vibrating sample magnetometer (VSM) and Mössbauer spectroscopy. Investigations of XRD (Fig.1) showed that the material was spinel structure and the particle size of the samples change with change of the Urea ratio (table I). Mössbauer spectra of the samples (Fig.2) show that a combination of ordered and super-paramagnetic behavior were obtained. Two magnetic subpatterns were analyzed and attributed to Fe3+ ions at the tetrahedral A-sites and octahedral B-sites. Room temperature magnetization results showed that the magnetic properties of $NiFe_2O_4$ strongly depend on the ratio between urea and nitrates (table I). The coercivity of the $NiFe_2O_4$ nano-powders changed from 152 to 172 Oe according to the change in the ratio between urea and nitrates.

Table I: XRD parameters of Ni–Ferrites at different metal nitrates and urea ratios, the average crystallite size (C), lattice constant (a) , the XRD density (d_{XRD}) saturation magnetization (Ms) and remnant magnetization (Mr)

Urea Ratio	C (nm)	a (nm)	d_{XRD} (gm/cc)	M_s (emu/g)	M_r (emu/g)
1	---	0.8395	5.27	2.5399	0.21172
1.5	15	0.8442	5.18	---	---
1.7	25	0.8423	5.21	33.003	6.8553
2	38	0.8343	5.36	42.703	8.6612
3	69	0.8324	5.401	---	---

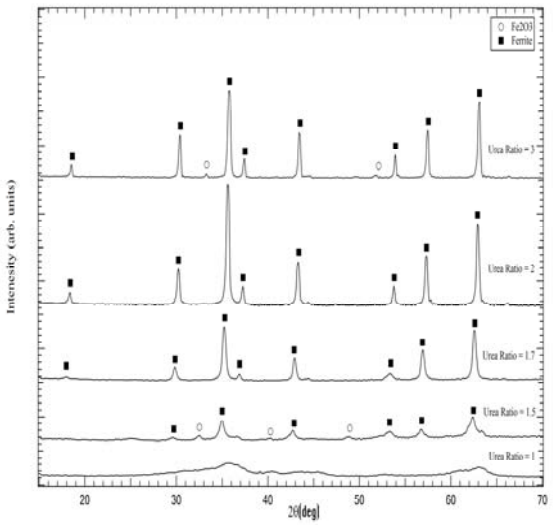

Figure1. XRD patterns of Ni–Ferrites at different metal nitrates and urea ratios synthesized by microwave combustion method

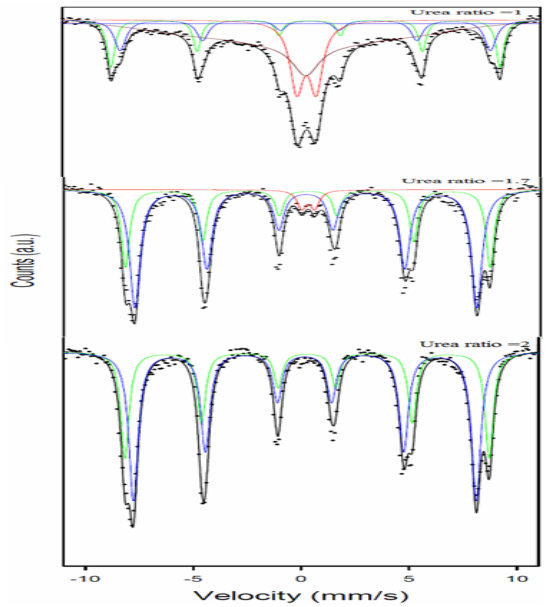

Figure2. Rome temperature mössbauer spectra for Ni-ferrites at different metal nitrates and urea ratios synthesized by microwave combustion method.

*Corresponding author. Tel. (02) (088) 412195; fax: (02) (088) 312564 (central office)

E-mail: abdelnaby.elshahawy@yahoo.commailto:Mohom63@yahoo.com

BIODEGRADATION OF MAGNETIC NANOPARTICLES EVALUATED FROM MÖSSBAUER AND MAGNETIZATION MEASUREMENTS

I.Mischenko[1], M.Chuev[1], V.Cherepanov[2], M.Polikarpov[2], and V.Panchenko[2]
[1]*Russian Institute of Physics and Technology, Russian Academy of Sciences, 117218 Moscow, Russia*
[2]*National Research Centre "Kurchatov Institute", 123182 Moscow, Russia*

Mössbauer spectroscopy is well known sensitive method for study of structural, magnetic and thermodynamic properties of magnetic nanomaterials. Even more widely uses technique for research such systems is magnetization measurements. In fact, the combination of those two methods can supply full set of practically important characteristics inherent to the magnetic nanoparticles, in particular those delivered in a body [1, 2]. So, there is a great interest in elaboration models which provide description both Mössbauer and magnetization experiments.

Recently we have developed a stochastic model accounting the relaxation effects in the system of homogeneously magnetized single-domain particles [3-6], which is enough to analyze large amount of Mössbauer and magnetization information, including biological data.

Investigation of mice organs at different times after nanoparticles injection by Mössbauer spectroscopy obviously demonstrates along with erosion of iron-contain particles accumulation of ferritin-like protein in living tissues. A conventional analysis of such spectra and their decomposition into partial components is based on a formal consideration of continuous hyperfine field distributions at iron nucleus. But it results in only qualitative treatment of the spectra. In order to extract quantitative information about characteristics of the studied samples we used self-consistent fitting procedure based on the relaxation model of the magnetic dynamics. Thus, we managed to match the large set of the experimental data, particularly, the evolution of Mössbauer spectral form with temperature and external magnetic field as well as the magnetization curves.

The method allowed us to reliably evaluate changes in the nanoparticles parameters and numerically characterized the conversion of the iron to paramagnetic ferritin-like forms in animals' organs in the course of time. In particular, we have estimated iron concentrations in both chemical phases and sizes of the residual particles at different stages of biodegradation. Actually, the approach allows one to quantitatively characterize biodistribution and metabolism of magnetic nanoparticles injected into a body.

Improvement of the stated method consists in development more detailed models for describing nanoparticles of various magnetic natures (ferro-, antiferro- and ferrimagnetism) [7]. Though Mössbauer spectral shapes for particles of different magnetic types often are similar the mechanisms of their formation are essentially different and the precise spectrum calculation requires specific schemes for each sort of magnetic structure. Implementation of this program shall result in data analysis procedure for ^{57}Fe Mössbauer spectroscopy of single-domain particles of almost every kind.

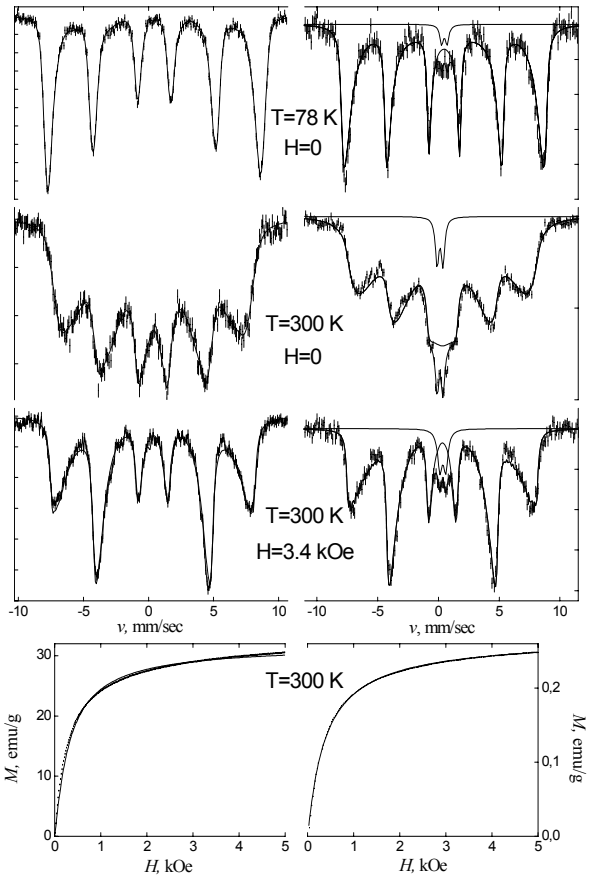

Figure 1. ^{57}Fe Mössbauer spectra and magnetization curves of initial nanoparticles (left panel) and a mouse liver 2 days after nanoparticles injection (right panel). The results of simultanious treating are represented by solid lines. These are partial spectra of nanoparticles, ferritin-like contribution as well as the resulting spectra and magnetization curves.

Support by Russian Foundation for Basic Research is acknowledged.

[1] M.A.Chuev et al., AIP Conf. Proc., 1311 (2010) 322
[2] I.Mischenko, M.Chuev, J. Phys.: Conf. Ser. 345 (2012) 012026
[3] M.A.Chuev, J.Hesse, in 'Magnetic Properties of Solids' (Ed. K.B. Tamayo), Nova Science Publ., New York, 2009, 1-104
[4] M.A.Chuev, JETP, 108 (2009) 249
[5] M.A.Chuev, J. Phys.: Condens. Matter 23 (2011) 426003
[6] M.A.Chuev, JETP, 114 (2012) 609
[7] M.A.Chuev, Pis'ma v ZhETF, 95 (2012) 323 (in Russian)

Session 15(T10) Oral-28

SYNTHESIS AND SPECTROSCOPIC CHARACTERIZATION OF SOME NEW HYDROPHOSPHONATO, PHOSPHATO AND HYDROGENOPHOSPHATO DERIVATIVES

Libasse Diop[1*], Waly Diallo[1], and José Domingos Ardisson[2]

1 Laboratoire de Chimie Minérale et Analytique (LA.CHI.M.A)-Département de Chimie- Faculté des Sciences et Techniques-Université Cheikh Anta Diop-Dakar.
2 Centro de Desenvolvimento da Tecnologia Nuclear – CDTN/CNEN-, Serviço de Nanotecnologia - SENAN, Laboratorio de Fisica Aplicada, Av. Antonio Carlos 6.627, Campus da UFMG, Pampulha, 31270-901 Belo Horizonte, MG, Brazil

Abstract: Four new hydrophosphonato, phosphato and hydrogenophosphato derivatives have been synthesized and studied by infrared and Mossbauer spectroscopies. Discrete, infinite chain or oligomeric structures have been suggested, the anion behaving as a tetra- and a bidentate ligand. Supramolecular architectures are obtained when secondary interactions are considered.

$H_2enPO_4SnPh_3$: δ=1.27, Δ=3.99, Γ=0.96

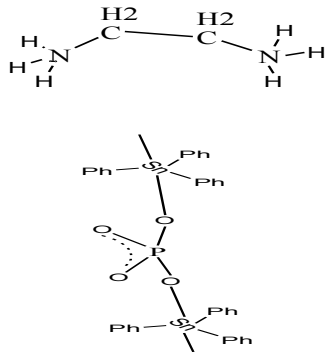

Scheme1a

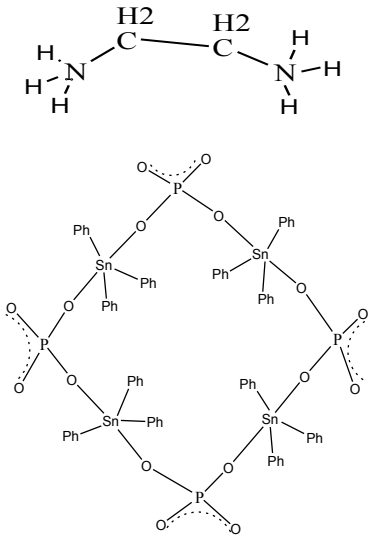

Scheme1b

(B) $HenPO_4(SnPh_3)_2.2H_2O$: δ=1.19, Δ=2.96, Γ=0.98

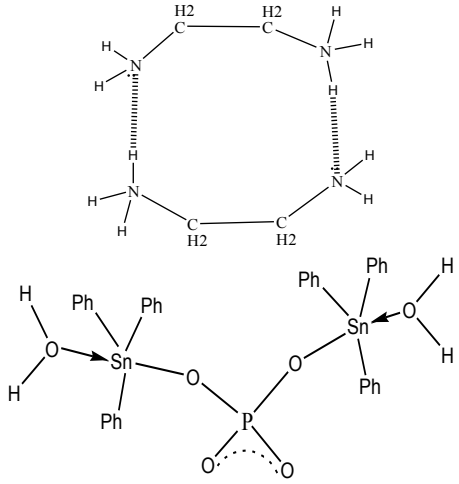

Scheme 2

(C) $Et_4NHPO_4SnPh_3.1/2H_2O$: δ=1.23, Δ=2.93, Γ:0.92 A complex-anion an infinite chain or an oligomer as above (schemes 1a and b).

(D) $HPO_3(SnMe_3)_2.H_2O$: δ=1.30 Δ=3.73, Γ=0.84

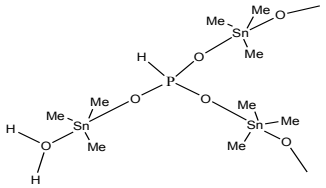

Scheme 3

COMBINED *OPERANDO* STUDIES OF NEW ELECTRODE MATERIALS FOR Li-ION BATTERIES

J.-C. Jumas

Institut Charles Gerhardt (UMR 5253) , Université Montpellier 2, Place E. Bataillon, CC 1502 34095 Montpellier Cedex 5 (France)

The development of high energy and power Li-ion batteries for portable power tools applications, automotive electric transportation (hybrid and electrical vehicles), electrical storage of renewable energies (small and medium size outfits), leads to intensive world-wide research on new electrode materials and electrolytes [1]. The performances of Li-ion batteries depend on many factors amongst which the important ones are the electrode materials and their structural and electronic evolution upon cycling. Fundamental studies are necessary for a better understanding of lithium reactivity mechanism by means of experimental techniques providing both structural and electronic information during the electrochemical cycles as X-Ray Powder Diffraction (XRPD) and Transmission Mössbauer Spectroscopy (TMS). A specific test cell [2], derived from a conventional Swagelok (Figure 1) cell was designed to allow measurements both in reflection mode (XRPD) or transmission mode (TMS) (Figure 2). Thanks to these two complementary techniques it is now possible to follow *in situ* and from *operando* mode the electrochemical behaviour of promising new Sn or Fe-based electrode materials.

XRPD spectra provide valuable information about the structural change behaviour and different contributions of each individual crystallized component during the charge/discharge process.

From TMS spectra the hyperfine parameters, δ (isomer shift) and Δ (quadrupole splitting), respectively proportional to the *s electronic density* at the nucleus and to the *electric field gradient*, make it possible to characterize the oxidation state and coordination of the probed element. The *f* recoil-free fraction which governs the intensity of the Mössbauer absorption gives information about the network rigidity and bonding and allows us to determine the relative proportions of each individuals species (crystallized, amorphized, nanosized).

Several examples will be presented to illustrate the greatness of combining XRPD and TMS for the study of Fe or Fe,Mn-based phosphates [3] as positive electrodes and Sn-based intermetallics [4] or composites [5] as negative electrodes. Different kind of reactions have been identified (insertion, phase transition, conversion) and in all cases understanding of such mechanisms is essential to optimize existing materials or to create new materials.

With the massive arrival of Sn-based nanocomposite electrodes joined with the advent of new Fe-based electrodes, the combination of XRPD and TMS has a bright future within the field of Li-ion batteries.

Acknowledgements

The Mössbauer platform has been implemented at the University of Montpellier with supports from the EC (NoE ALISTORE SES6-CT-2003-503532), Région Languedoc Roussillon (Contracts n° 2006-Q086 and 2008-094192). The author is grateful to these institutions and to CNES (Toulouse, France), SAFT (Bordeaux, France) and UMICORE (Olen, Belgium) for financial supports.

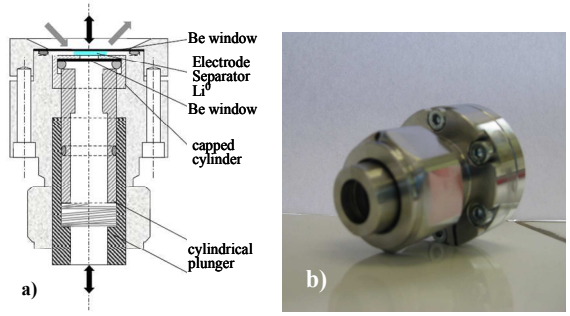

Figure 1. Electrochemical cell for *operando* measurements: a) schema from [2], b) photo

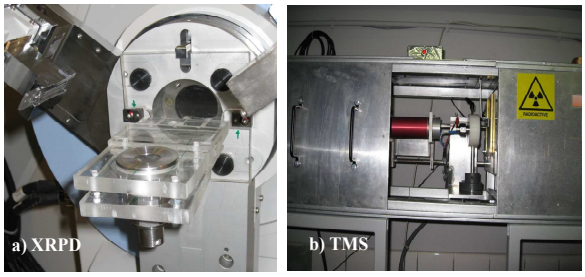

Figure 2. Experimental setup : a) XRPD, b) TMS

[1] 16th International Meeting On Lithium Batteries, IMLB-16, Jeju, Korea, June 17th– 22th, 2012.
[2] J.B. Leriche et al., J. Electrochem. Soc., 157 (2010) A606.
[3] A. Perea et al., RSC Advances 2 (2012) 2080.
[4] M. Chamas et al., J. Power Sources, 196 (2011) 7011.
[5] D.E. Conte et al., J. Power Sources, 196 (2011) 6644.

Session 17(T12) I-25

The Miniaturized Mössbauer Spectrometers MIMOS II & MIMOS IIA: Instrument Development and Applications

G.Klingelhöfer
University Mainz, Inst. Inorganic and Analytical Chemistry, Mainz, Germany

The Miniaturized Mössbauer Spectrometer MIMOS II has been developed for extraterrestrial applications and has contributed significantly to the success of NASA's Mars Exploration Rover mission [1]. MIMOS II is part of the science payload onboard NASA's twin Mars Exploration Rovers "Spirit" and "Opportunity" (see Fig.1) . In January 2004, the first in situ extraterrestrial Mössbauer spectrum was received from the Martian surface.

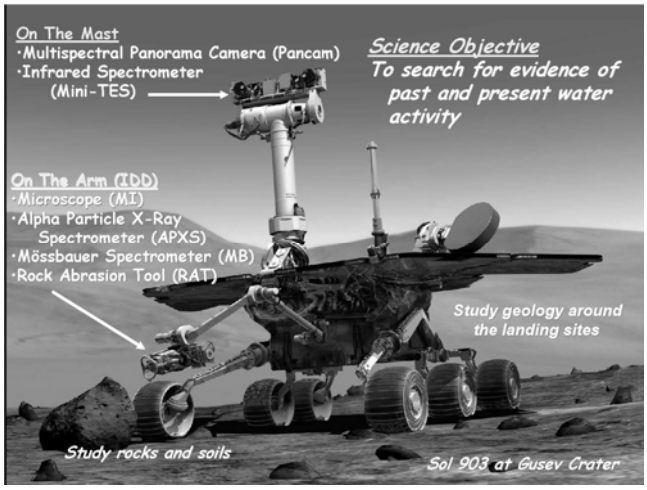

Fig.1 : Artist view of the Mars Exploration Rovers. Size of the rover is about 1m x 1m (length and width) by ~1.6m hight (position of the Panorama Camera).
The Mössbauer spectrometer is mounted on the robotic arm (IDD), together with a microscope (~30 micron resolution per pixel), the APXS for chemical analysis (XRF), and a grinder and drilling tool (RAT).

An improved version of the instrument was part of the scientific payload of the Russian Phobos-Soil mission in 2011 [3]. Because MIMOS II works in back-scattering geometry, no sample preparation is needed. In addition to 14.4 keV γ-rays, 6.4 keV X–rays can be detected simultaneously. The sampling depth of a photon is energy dependent, so that 6.4 keV X-rays are more sensitive to the surface part of a sample. In stainless steel, the sampling depth is on the order of ~50 μm. [2].
We have developed a new instrument MIMOS IIA with XRF capability for future missions to Mars, Venus, Martian moons, asteroids and the Earth moon. This instrument also has high potential for new terrestrial applications. MIMOS IIA uses newly designed Si-Drift detectors [4] with circular geometry (SDDs) allowing high resolution X-ray fluorescence spectroscopy simultaneously to Mössbauer measurements. The main goal of the new detector system design is to combine high energy resolution at high counting rates and large detector area while making maximum use of the area close to the collimator of the ^{57}Co Mössbauer source. The energy resolution at 5.9 keV is 136 eV FWHM at –20^{o}C, increasing the signal to noise ratio (SNR) and reducing the integration time of a Mössbauer measurement by a factor of up to 10 compared with the MER instrument MIMOS II.
Due to its miniaturization and back scattering geometry **MIMOS II / MIMOS IIA** are portable and can be used in a wide range of Fe-Mössbauer applications, especially where no sample preparation is possible (**non-destructive measurement**). The system operates autonomously without any time limitations. **MIMOS II/IIA can also be used for transmission measurements** in standard lab applications.

References

[1] Klingelhöfer, G., et al., JGR, 108(E12) (2003) 8067 .
[2] Fleischer, I., et al., JGR 113, E06S21 (2008*)*
[3] D. Rodionov, G. Klingelhöfer et al, *Solar System Research*, Vol. 44, No. 5 (2010) pp. 362–370
[4] M. Blumers, G. Klingelhöfer et al. *Nucl. Instr. and Meth.* A 624 (2010) 277-281

MossWinn - Methodological Advances in the Field of Mössbauer Data Analysis

Z. Klencsár
Budapest, Hungary

In the last decade advance in the field of computer technology has again opened up new opportunities for further developments in the field of scientific data handling and analysis. One of the advances relevant from this point of view is the significant influence of the internet on various aspects of the scientific work, which was further enhanced in the 21st century by the wide-spreading broad-band internet services and the online availability of high-capacity data storage devices. Another relevant development of recent years is that parallel computers became the mainstream when computer chip manufacturers turned to the development of multi-core processors with the aim to enhance computing performance without the need to raise clock speeds further above ~ 3-4 GHz that would raise problems related to economical cooling [1].

The MossWinn program, developed by the present author for the purposes of Mossbauer spectral analysis and data handling since 1995, was recently ported to the modern Delphi programming environment (version 2007) [2], and thereby became a native 32 bit MS Windows executable in the form of the MossWinn 4.0 series. The utilization of an up-to-date compiler also opened up ways to exploit the above-mentioned computer-technological developments in order to advance the field of Mössbauer data handling and analysis.

In the work to be presented it will be focused upon two of the main areas on which progress has been made via further developments of the MossWinn program in the last few years.

The first area concerns database systems developed for Mössbauer spectroscopy and the corresponding utilization of the internet and its resources. Whereas most of the experimental fields of science can benefit from the systematic collection and sharing of experimental observations and/or associated data, the straightforward and rather precise inherent reproducibility of Mössbauer spectroscopy measurements renders them especially well suited to become synthesized and utilized in the form of a database. It must have been the great potential usefulness of databases in this field that has already motivated enormous and still ongoing work put into the compilation of existing large-scale Mössbauer databases [3-8]. Whereas in general database systems can be seen as consisting of a collection of data and a corresponding database management system (DBMS) handling the data and providing the functionality of the database system, it appears that a common feature of existing large-scale Mössbauer database systems [3-8] is that they put emphasis mainly on the collection of database data as opposed to emphasis on the DBMS.

Due to the worldwide availability of broad-band internet services, however, today the establishment of a database system can proceed more efficiently by developing first a database management system that—beside providing access to database data—furthermore also handles the collection of the data itself. Such a database management system has been developed and put into operation as an integral part of the MossWinn program. The corresponding database system has been named accordingly as the MossWinn Internet Database (MIDB) [9]. The seamless combination of data analysis and database manager functionalities in a single application software made it possible to implement program features that present an advance in the field of Mössbauer spectral analysis as well as in the field of Mössbauer database systems. At the same time, the approach that was adopted for the design and development of the MIDB database is very different from that characteristic to other existing Mössbauer databases. This approach is going to be introduced along with relevant operational details of the MIDB system.

The second area of developments to be presented concerns the utilization of the computing potential of recent multi-core processors in the field of Mössbauer data handling and analysis. This requires the development of new, parallel counterparts of existing sequential algorithms for which parallelism is potentially beneficial. The identification of such algorithms of the MossWinn program and the implementation of the corresponding parallel procedures has recently begun, and for some of the algorithms it has been already successfully completed. The benefits and limits of applying parallel computing techniques in the field of Mössbauer data handling and analysis is going to be presented on the basis of experience gained during this work.

References

[1] J. Larus, D. Gannon: *Multicore Computing and Scientific Discovery*, in T. Hey, S. Tansley, K. Tolle (eds.): The Fourth Paradigm: Data Intensive Scientific Discovery (Microsoft Research, Redmond, Washington, 2009).

[2] http://en.wikipedia.org/wiki/Embarcadero_Delphi

[3] J.G. Stevens: *Comput. Phys. Commun.* **33** (1984) 105.

[4] J.G. Stevens, A. Khasanov, J.W. Miller, H. Pollak, Z. Li: *Hyp. Int.* **117** (1998) 71.

[5] Mössbauer Effect Data Center, at the University of North Carolina at Asheville (1969-2010), at the Dalian Institute of Chemical Physics, Chinese Academy of Science (2010-) http://www.medc.dicp.ac.cn/

[6] Mars Mineral Spectroscopy Database, at Mount Holyoke College, http://www.mtholyoke.edu/courses/mdyar/marsmins/

[7] M.D. Dyar, M.W. Schaefer: *Earth Planet. Sci. Lett.* **218** (2004) 243.

[8] J. Wang, C.Z. Jin, X. Liu, D.R. Liu, H. Sun, F.F. Wei, T. Zhang, J.G. Stevens, A. Khasanov, I. Khasanova: *Hyp. Int.* **204** (2012) 111.

[9] http://www.mosswinn.hu

Session 17(T9) I-27

INVESTIGATIONS OF THERMOELECTIC MATERIALS USING SYNCHROTRON RADIATION

R. P. Hermann[1,2]
[1]*Jülich Centre for Neutron Science JCNS-2 and Peter Grünberg Institute PGI-4, JARA FIT Forschungszentrum Juelich GmbH, Germany*
[2]*Faculty of Science, University of Liège, Belgium*

Our society has increasing requirements in terms of energy and information processing. Meeting these needs in a sustainable why is among the most important current challenges. Two-third of the used energy is lost in the form of waste heat. Technologies for recovering part of this thermal waste are a priority. The direct conversion of thermal to electric current via thermoelectric devices is such a recovery technology which is promising for several niche applications but also, potentially for the automotive industry or for autonomous sensors.

In order to optimize thermoelectric properties of a material, simultaneous tuning of the electric conductivity and thermopower is required, in combination with a reduction of the thermal conductivity. There has been extensive research on the lattice dynamics of thermoelectric materials in the past ten years, aiming at unraveling the mechanisms that lower the thermal transport. Open framework structures with guest atoms and the influence of these guests on the thermal transport have been investigated, as well as materials with a large unit cell, in which a low relative amount of vibrational modes participate to heat transport. In addition to selecting and tuning the material's crystal structure, further tuning is possible by controlling the dimensions of the material in nanostructures. An efficiency enhancement through improved electronic properties and through reduction of the phononic heat transport can be achieved by tuning the size of nanoobjects. Characterizing the lattice dynamics in these nanoobjects is a challenging task that nuclear inelastic scattering can tackle elegantly.

Measurements of the partial density of phonon states with inelastic nuclear resonance scattering have recently passed the 15th anniversary[1]. Monochromatization in the meV range is required in order to properly resolve the phonon spectrum. Obtaining such resolution becomes very challenging for nuclear resonances above 30 keV, as an energy resolution $\Delta E/E$ better than 3.10^{-8} is required. With the use of a single crystal sapphire backscattering monochromator we have been successful in carrying out measurements with the antimony-121 37.2 keV[2], tellurium-125 35.4 keV[3] and xenon-129 39.9 keV[4] nuclear resonances. Nuclear inelastic scattering measurements on several compounds with ~1 meV resolution will be presented.

A review of the phonon properties obtained mostly in in thermoelectric bulk antimonides and tellurides as well as in similar compounds with confined geometry such as nanowires and thin films will be reviewed. In bulk thermoelectric materials, the specific dominating mechanisms that limit the thermal conductivity have been identified for several antimonide Zintl phases such as $Yb_{14}MnSb_{11}$ and Zn_4Sb_3 [5]. For skutterudite compounds, for the first time, the study of the unfilled $FeSb_3$ [6] was possible and direct comparison with the lattice dynamics in filled skutterudites reveals that besides the presence of rattling modes, an overall very soft framework might also contribute to the low thermal conductivity *e.g.* in $YbFe_4Sb_{12}$ [7]. In $A_8Ga_{16}Ge_{30}$ clathrates the combination of nuclear resonance scattering, inelastic neutron scattering and Mössbauer spectroscopy reveal unique phenomena, such as Eu-guest tunneling [8], but an in-depth investigation also reveals that a quantitative understanding of thermal transport is still lacking [9]. First experimental insights in the specificity of lattice dynamics in nanoscaled thermoelectrics obtained both by inelastic neutron and nuclear inelastic scattering will conclude our review[10], notably in $(Sb,Bi)_2Te_3$ nanowires, in $FeSb_2$, ZnSb, and NiSb nanopowders, and in LAST-*m*, $Pb_mAgSbTe_{2+m}$, phases, with $6<m<18$.

The Helmholtz Gemeinschaft Deutscher Forschungszentren is acknowledged for funding VH NG-407 “Lattice dynamics in emerging functional materials”. The European Synchrotron Radiation Facility and the Advanced Photon Source are acknowledged for provision of synchrotron radiation at ID18 and ID22N, and at 6IDD respectively. The JCNS, ILL, SINQ-PSI, and the SNS are acknowledged for provision of neutron scattering beam time. The DFG is acknowledged for funding SPP1386 'Nanostructured thermoelectrics' and SFB915 'Nanoswitches'. The BMBF is acknowledged for funding project 'NanoKoCh' number 03X3540B. I am greatly indebted to I. Sergeev, A. Chumakov, R. Rüffer, H.-C. Wille, Yu. Shvyd'ko, B. Klobes, A. Möchel, D. Bessas, P. Bauer Pereira, J. Gallus, T. Claudio Weber, R. Simon, and M. Herlitschke for the fruitful collaboration.

[1] Seto M. *et al., Phys. Rev. Lett.* **74**, 3828 (1995); Sturhahn W. *et al.*, *Phys. Rev. Lett.* **74**, 3832 (1995); Chumakov A. *et al.*, *Europhys. Lett.* **30**, 427 (1995).
[2] Wille H.-C. *et al.*, *Phys. Rev. B* **76**, 140301(R) (2007).
[3] Wille H.-C. *et al.*, *Europhys. Lett.* **91**, 62001 (2010).
[4] Klobes B. *et al.*, *in prep.* (2012).
[5] Moechel A. *et al.*, *Phys. Rev B* **84**, 184303 (2011).
[7] Moechel A. *et al.*, *Phys. Rev B* **84**, 064302 (2011).
[7] Moechel A. *et al.*, *Phys. Rev B* **84**, 184306 (2011).
[8] Hermann R. P. *et al., Phys. Rev. B* **72**, 174301 (2005); Hermann R. P. *et al., Phys. Rev. Lett.* **97**, 017401 (2006).
[9] Moechel A., *Lattice dynamics in thermoelectric Zintl phases,* Ph.D. Dissertation, Univ. Liège (2011).
[10] D. Bessas *et al.* ; T. Claudio *et al.* ; P. Bauer Pereira *et al.*, submitted (2012).

RESONANT X-RAY ABSORPTION BY ^{57}FE: A SITE-SELECTIVE PROBE OF PROTEIN STRUCTURE AND ELASTICITY

J. T. Sage[1,2]

[1]*Department of Physics, Northeastern University, Boston (USA)*

[2]*Center for Interdisciplinary Research on Complex Systems, Northeastern University, Boston (USA)*

Iron-containing proteins are indispensable to the life, regulation, aging, and death of the cell. Cellular metabolism depends on enzymes containing Fe and other metals and contributes to global biogeochemical cycles that exchange atmospheric pools of oxygen and nitrogen with biologically useable forms of these elements.

Measurements of resonant nuclear absorption by ^{57}Fe at synchrotron facilities selectively reveal vibrational motion of individual iron atoms within proteins containing thousands of other atoms. Quantitative comparison of the resulting information on vibrational amplitudes and directions, as well as frequencies, with quantum chemical predictions identifies vibrations of all Fe-ligand bonds and also provides a detailed test of the predicted electronic structure. I will present recent applications to enzymes that contain iron within a planar heme group.

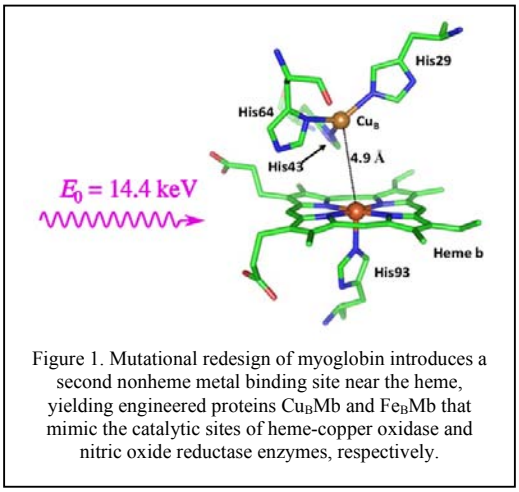

Figure 1. Mutational redesign of myoglobin introduces a second nonheme metal binding site near the heme, yielding engineered proteins Cu_BMb and Fe_BMb that mimic the catalytic sites of heme-copper oxidase and nitric oxide reductase enzymes, respectively.

One question of current interest is how a nearby nonheme metal site controls the reaction of the heme with nitric oxide (NO). NO inhibits the heme-copper site that consumes oxygen in cellular respiration, but is metabolized to produce the greenhouse gas nitrous oxide (N_2O) in closely related bacterial enzymes with iron in the nonheme site. Protein engineering mimics the catalytic site (Fig. 1) and enables selective metal replacement at either heme or nonheme site, opening the door to detailed spectroscopic investigation of reaction intermediates that are too unstable to characterize in the natural enzyme. In addition, recent results demonstrate that vibrational dynamics of heme and nonheme irons can be probed independently (Fig. 2).

Finally, averaged force constants, derived directly from the experimentally determined vibrational density of states (VDOS), quantify important aspects of structure and elasticity even when individual vibrational modes cannot be resolved and identified. Fe-ligand vibrations make the primary contribution to the *stiffness*, an effective force constant which measures the average strength of nearest neighbor interactions, while low frequency oscillations of the protein determine the *resilience*, a distinct force constant that probes the elasticity of the iron environment.

Table I: The stiffness and resilience, averaged force constants derived from vibrational measurements, quantitatively measure distinct elastic properties of heme and nonheme sites.

	force constant (pN/pm)	
	stiffness	**resilience**
Mb(II)	189 ± 20	21.2 ± 1.3
$Fe(II)_B$*Mb(II)	182 ± 9	20.3
*$Fe(II)_B$Mb(II)	155.± 6	20.1

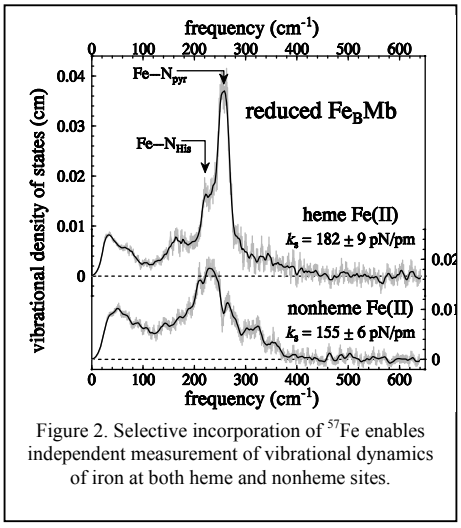

Figure 2. Selective incorporation of ^{57}Fe enables independent measurement of vibrational dynamics of iron at both heme and nonheme sites.